ASSESSMENT OF VARIABLE EFFECTS OF SYSTEMS WITH DEMAND RESPONSE RESOURCES

BY

ANUPAMA SUNIL KOWLI

B.Eng., University of Mumbai, India, 2006

THESIS

Submitted in partial fulfillment of the requirements
for the degree of Master of Science in Electrical and Computer Engineering
in the Graduate College of the
University of Illinois at Urbana-Champaign, 2009

Urbana, Illinois

Adviser:

Professor George Gross

ABSTRACT

The push toward sustainability and the impacts of high electricity prices are the key drivers behind the efforts to harness active participation of consumers in electricity markets. In particular, there is a new class of consumers - called *demand response resources* (DRRs) - whose role has become increasingly important in ensuring that the supply-demand balance is efficiently attained. In addition to purchasing electricity from the electricity markets, DRRs can sell load curtailment services to these markets by reducing their loads during certain hours. For these hours, the DRRs compete to provide the load curtailment services directly against the sales of the supply-side resources. DRR deployments affect both the market outcomes and the utilization of the generation and transmission resources. In fact, DRRs impact and, in turn, are impacted by the planning activities on the generation and transmission side and the regulatory/legislative developments. Consequently, appropriate tools for quantifying the impacts of DRRs on market performance, generation and transmission resource utilization and other variable effects are required. One particularly important need is that of a simulation tool and we focus on addressing this need. We present in this report the development of a comprehensive methodology that provides the basis for such a simulation tool. We illustrate its application to the quantification of various variable effects of large-scale power systems incorporating DRRs.

The principal challenge in the development of our simulation methodology is to integrate the effective representation of the time-dependent transmission-

constrained markets and that of the supply and demand resources so as to construct a practical approach that can be computationally tractable when implemented for simulating large-scale systems over longer-term periods. To meet this challenge, we incorporate the representation of DRRs into the snapshot-based transmission-constrained market model. In this way, the DRR curtailment offers appear as controllable resources in attaining the supply-demand equilibrium. For a specified simulation period, we adopt the assumptions of the probabilistic production simulation approach for both the load and the generation units, so we can explicitly represent the various sources of uncertainty in planning studies. We reformulate the load model of the probabilistic simulation approach to allow the representation of DRRs in the time-dependent transmission-constrained markets. The modified probabilistic load and available generation capacity models imply that the bids and the offers in the electricity markets are uncertain and, consequently, so are the market outcomes. We construct a simulation engine to compute approximations of the probability distributions of these market outcomes and to evaluate the expected values of system variable effects for the simulation period. To capture the seasonal effects, changes in the resource mix and the transmission grid, maintenance schedules of generators as well as policy and legislative developments, the study period is partitioned into appropriate simulation periods to which we apply the engine.

In the implementation of the proposed methodology, we take advantage of the similar load and resource patterns to select representative simulation periods so as to reduce the simulation workload. Furthermore, for the simulation of each such period, we use the *Latin hypercube* technique to judiciously sample across the distributions of the load and the available generation capacities and, therefore, lessen the number of snapshots used to approximate the probability distributions of the market outcomes. These efficiency improvements in the implementation

bring about computational tractability in the application of the methodology to the simulation of large-scale systems over longer-term periods.

We illustrate the application of the proposed methodology to the assessment of the range of benefits the integration of DRRs can provide to a realistic large-scale test system and discuss some representative simulation results. The simulations indicate that DRR deployments can result in substantial savings in the total cost of electricity in comparison to a reference scenario without DRRs. We observe that the annual savings range from 8 to 15% with DRR penetration no more than 10% of the annual peak load. Furthermore, as the penetration of DRRs deepens, the savings become more pronounced. We observe similar impacts on the congestion rents and the CO_2 emissions for the system. As DRRs can prevent *loss of load* events by curtailing the load, they provide tangible reliability benefits in addition to the reductions in the loading of the generation units and in their emissions. The report also discusses the wide range of questions – including the analysis of the impacts of new policies, alternative market designs and investment in transmission assets and generation and demand resources – that can be addressed using the proposed methodology.

To Aai and Baba

ACKNOWLEDGMENTS

I am deeply indebted to my adviser, Prof. George Gross, for his guidance and support. His patience despite my many mistakes and doubts is greatly appreciated. His faith in me has greatly boosted my confidence and inspired me to strive harder and set higher goals for myself.

I would like to thank Matias, Gui and other students in my research group for their valuable input, support and friendship during these years. I am grateful to the students, faculty and staff of the Power and Energy System Group for making me a part of this wonderful extended family.

I would also like to express my deepest gratitude to Alan, Jim, Walt, Ralph and other KEMA consultants for a wonderful internship experience. This work would have been possible without support and help from all these wonderful people at KEMA, Inc.

These acknowledgments would be incomplete without thanking my fiancé, Ankur, for his love and support. His patience and kindness during my rants and raves has helped me get through many tough times. His clear thinking has kept me grounded. We make a great team and I am looking forward to our life together.

Finally, I would like to thank my family for their immense faith, unwavering support, and unconditional love. I would never have had this opportunity had it not been for the vision and the foresight of my parents. I am who I am because of them.

TABLE OF CONTENTS

LIST OF TABLES

LIST OF FIGURES

CHAPTER 1

INTRODUCTION

In this chapter, we set the stage for the work presented in this thesis. Our research interests lie in the integration of the so-called demand response resources into the operations of the power systems and electricity markets. We start by discussing the motivation and the background behind our research so as to allow the reader to better understand the nature of the problem discussed and the solution we have developed in this thesis. We also provide a brief description of the current state-of-the-art in the field of demand response resources. We then discuss the scope and the contribution of this thesis and provide an outline of the contents.

1.1 Motivation and Background

The electricity system in the United States is operated in such a way so as to ensure that the electricity demands of the consumers are met in a reliable and economic manner. The assurance of electricity delivery to the loads of the consumers requires a careful matching of the generation with the demand for electricity. Specifically, the system operators and planners need to carefully consider and address the growing electricity demand needs of the future, because of the long lead times associated with the building of new generation. Now, the stationarity of the power generation and the fact that a large fraction of the electricity demand is met using thermal generators makes electricity generation one of the most visible sources of pollution. With increased awareness of the global warming

issues and the need for energy independence, efforts have been directed towards the the exploration and development of cleaner resource alternatives. In view of these challenges, considerable investment has been made in wind and solar energy generation. However, the intermittency effects associated with these renewable generation technologies and the lack of transmission support for the delivery of the energy from the generators to the loads are the key barriers impeding the reliable integration of renewables into the power system. Consequently, the renewable generation has not grown at a pace commensurate with the electricity demand growth rate and has not able to replace the thermal generation. As a result, investors, policy makers and system operators are turning towards the demand-side to preserve the supply-demand balance necessary for the operation of the electricity systems.

Since a large fraction of the electricity demand is met using the thermal generators, high fuel prices such as those observed during 2005-2007 cause significant spikes in the electricity prices thereby increasing the overall payments received from the demand-side buyers. The economic pressures of high electricity prices coupled with the drive for sustainability have led to growing interest in the harnessing of the so-called *demand response* of the consumers. Demand response activities broadly encompass mechanisms and programs which allow consumers to respond to electricity prices or load reduction requests from the Independent System Operator (ISO) or the Regional Transmission Organization (RTO). In this way, the demand-side actively participates in maintaining the supply-demand balance. The responsive consumers get paid for curtailing their electricity usage every time they deliver the specified cuts in their demands. The curtailment in the electricity demand of such responsive consumers reduces the aggregate system demand, thereby lessening the reliance on the generation in the system. The decreased generation lowers the emission of harmful greenhouse gases (GHGs) and

the production costs to meet the demand.

Increasing participation of the consumers in the demand response activities has created a new class of loads known as *demand response resources* (DRRs). The DRRs modify their electricity consumption in response to signals from the *independent grid operator*[1] (IGO) who operates the wholesale electricity markets. Generally, the term "DRRs" is used to broadly encompass all such loads who have the capability of modifying their energy consumption in the event of the high electricity prices or when system reliability is jeopardized. However, we use the term DRRs to specifically refer to those consumer loads which *actively* participate in the IGO-run electricity markets and modify their consumption based on the price signals generated in these markets. We note that the deployment of DRRs is different from the traditional price responsive demand or loads enrolled in *dynamic pricing* schemes.[2] The consumers involved in the latter two mechanisms may be viewed as *passive* participants in the electricity markets, in the sense that their participation is limited by their willingness to pay. The DRRs, however, play a more active role by offering load curtailments in the electricity markets and competing with the supply-side sellers to maintain the supply-demand balance. The integration of the DRRs into the operations of the power system and the electricity markets and the associated impacts on, and benefits for, the system and the individual players are the key issues investigated in this report.

Prior to the restructuring of the electricity industry, load curtailments by end-use consumers fell under the umbrella of the so-called *demand-side management* (DSM) activities. DSM refers to the deliberate intervention by the monopoly utility so as to influence the customer use of electricity. DSM includes any in-

[1]We use the generic term, IGO, to encompass the organizations such as ISOs and RTOs who are responsible for the operation of the transmission grid and the electricity markets.

[2]We use the term dynamic pricing to refer to electricity rates of the end-use consumers that vary with real-time supply and demand conditions. Typical examples include schemes that implement real-time pricing or critical peak pricing.

tentional activities on the customer side of the meter that bring about desired changes in the utilitys load shape. A broad definition of the concept of DSM and its categorization into six load shaping objectives – peak clipping, valley filling, load shifting, strategic conservation, strategic load growth and flexible load shape – was provided in [1]. DSM activities were primarily driven by the additional resource and reliability needs for the vertically integrated utilities. However, with the advent of competition, the focus of the utility companies changed and DSM was relegated to a less prominent position.

The restructuring of the electricity industry introduced many new players, including the IGO. The IGO was created to ensure competition in the functioning of the electricity markets and to oversee the reliable operation of the transmission grid. In the restructured industry, the smaller consumers purchase electricity from the energy service providers (ESPs), while the ESPs, in turn, procure the electricity demands of all their consumers from the spot markets organized by the IGO. However, the ESPs charge the consumers at flat electricity rates, while themselves purchasing energy at more volatile spot prices. The lack of dynamic pricing schemes for the end-use consumers creates a disconnect between the competitive wholesale side and the regulated retail side of the electricity industry. Due to the lack of signals from the spot markets, the consumers have no incentives for reducing their electricity consumption when the electricity prices or the demands in the spot markets are high. Consequently, the participation of the demand-side in the electricity markets has been rather passive, as compared to the supply-side.

However, it is widely acknowledged that an actively participating demand-side encourages competition and has several benefits. In particular, it is understood that consumers can reap benefits from shifting their electricity consumption from the high price hours to low price hours. The load curtailment by the responsive consumers reduces the system demand, which may induce lower electricity

prices and make more effective use of the existing system resources. As a result, many IGOs and ESPs are rolling out demand response programs to facilitate the communication of the spot prices to the consumers and to enable the consumers to offer load curtailments in the electricity markets. Although the load curtailment service is a *capacity*-related product, it is often traded in the MWh market. Actual implementations of such markets include the day-ahead energy markets of ISO New England (ISO-NE), Pennsylvania-New Jersey-Maryland ISO (PJM-ISO), and New York ISO (NY-ISO). In such markets, a consumer with a successful load curtailment offer reduces his load for the entire duration of the period for which the curtailment was successful. The load curtailment is achieved by turning down the air conditioning, water heaters and/or water pumps or industrial processes. Such curtailment in the consumption decreases the system demand, thereby reducing the generation in the system. The reduced generation, overall improvement in the utilization of the system resources and the lower electricity prices benefit the whole system. Hence, in many markets, the responsive consumer gets compensated for curtailing the specified MWh amount on a $/MWh basis, as if he were generating the specified MWh amount [2] - [4]. Thus, not only do the responsive consumers, a.k.a. DRRs, benefit from avoiding consumption when prices are high, but they may also receive compensation from the IGO for their services.

The economic benefits and incentives available to the loads with demand response capabilities have attracted a large number of consumers to the demand response programs run by the IGOs. Aggregation of the smaller loads capable of providing load curtailments is fast becoming a norm, because most individual consumers do not have the expertise or the financial incentives for directly participating in the wholesale electricity markets. Several companies like EnerNOC and Comverge are successfully aggregating loads of smaller consumers to provide load

curtailment services in the wholesale electricity markets [5], [6]. The companies involved in the business of DRR aggregation work with the ESPs to facilitate the implementation of the demand response programs and provide the necessary platform in terms of the control/communications/metering equipment needed for the same. With the necessary equipment in place, the ESP can effectively harness the load curtailment capabilities of the responsive consumers so as to be able to provide load curtailment services in the IGO run markets.

The wholesale consumers as well as ESPs receive compensatory payments from the IGO for the provision of DRR services. The ESPs may then distribute these compensatory payments among the consumers enrolled in the demand response programs. Clearly, an ESP with a DRR aggregation acts as a load as well as a resource. Hence, in concept, the ESP interacts with the IGO in two possible ways:

- as a load: procure its electricity demand from the IGO which is then made available to all its consumers
- as a resource: provide load curtailment services in the electricity markets operated by the IGO by utilizing the demand response capabilities of its consumers

Thus, the ESP itself is a DRR from the point of view of the IGO. Throughout this report, we focus on the wholesale markets and we adopt a "system" point of view. Henceforth, we use the term DRRs to specifically refer to those ESPs and wholesale customers with the capability of providing load curtailments in the electricity markets.

The participation of the DRRs in the electricity market and power system operations provides the IGO additional degrees of freedom in maintaining balance between the demand-side consumption and the supply-side generation. Since the IGO operates the system in the most economic and reliable manner, the deploy-

ment of DRRs is often restricted to those hours when the load demand or the prices are high. In addition to the lowering of the electricity prices, there are other key benefits associated with the deployment of the DRRs. Load reduction at such critical peak hours results in a decrease in the electricity generation for those hours. Thus, lowering the electricity demand during the critical peak hours defers the operation of peaking units. In some instances, cycling load may be curtailed due to high prices or constraints on the system operations. Reduced loads throughout the system impact the transmission usage and may effect a possible congestion relief. In general, the deployment of the DRRs results in a more effective utilization of the existing resources and lowers the emissions of harmful GHGs. Reduced peaking generation may also defer the need for additional peaking generation in the future.

Recognizing the importance of the DRRs in achieving economic as well as environmental benefits has resulted in several legislative and regulatory initiatives in the United States. These policy changes have been aimed at encouraging consumers to be more active participants in the electricity business. In particular, the Energy Policy Act of 2005 (EPAct) prescribed provisions for the assessment of demand response potential on a nation-wide basis [7]. EPAct directed the Federal Energy Regulatory Commission (FERC) to formulate steps needed to encourage recognition of DRRs as reliable resources in electricity market operations. Many legislative and regulatory policies, on the federal as well as the state level, were formulated in the aftermath of the EPAct to promote demand response in wholesale and retail electricity markets. Of particular interest is the Energy Independence and Security Act of 2007 which instructs FERC to develop a national action plan for demand response while estimating on a nation-wide basis the demand response potential for the next 5- and 10-year horizons [8]. Annual assessments conducted by FERC have indicated a significant increase in the demand response participa-

tion since the EPAct [9]. The recent policy initiative at FERC [10] has reaffirmed the positive impacts of demand response on electricity prices in the organized wholesale electric markets leading FERC to strongly advocate the removal of all the barriers to demand response.

The policy initiatives since 2005 have made DRRs an extremely attractive option for system operators as well as potential investors. With DRRs emerging as key market players, there is a need to understand their role and impacts in the electricity markets in order to quantify the benefits associated with their deployment. Several studies have analyzed the impacts and the benefits of DRRs for short- and medium-term periods [11] - [14]. But the deployment of DRRs may negatively impact the supply-side, eating into the profits of the generating companies and affecting the addition of new generation units. Similarly, the load curtailments provided by the DRRs affect the usage of the transmission grid and the possible congestion situations, thereby influencing transmission asset additions. Such impacts of the DRRs bring about the need to analyze the effects of DRR integration into the power system over longer-term periods. While the nature of such impacts is well understood on a qualitative basis, the systematic quantification of the DRR impacts over the longer term is yet to be accomplished. In this report, we present the modeling and the analysis required to develop the simulation methodology for the evaluation of the DRR impacts over longer-term study periods. The application of the proposed methodology to simulation studies of systems with DRRs allows the assessment of the variable effects such as total energy consumption, GHG emissions, and production costs as well as reliability metrics. The variable effects serve as key metrics for the analysis of the impacts of DRR integration in to the power grid.

The EPAct of 2005 has renewed interest in the demand-side and successful demand response programs implemented by the IGOs have attracted several con-

sumers. Although the total demand response potential still remains less than 10 % of the peak load capacity for the United States, FERC predicts that the demand response related activities will further increase due to continued promotion at the state level and increased interest on behalf of consumers and ESPs [9]. In fact, a recent report prepared by FERC and some leading consultants in the electricity industry has concluded that the potential for peak load reductions across the country is between 38 GW and 188 GW, which roughly constitutes about 20% of the nation-wide peak demand [15]. Extensive promotion of demand response enabling technologies is needed to tap into the unrealized demand response potential of the consumers. Deployment of the DRRs in such large quantities can reduce the need to operate a large number of power plants during peak hours. Hence, a simulation methodology useable in the assessment of the DRR impacts on the market and the power system over longer term horizons is timely and may even be useful for shaping policies geared at eliciting more demand-side participation.

1.2 Survey of the State of the Art

DRRs are emerging as important players in the electricity industry. Several industry developments, regulatory initiatives and academic research and reports are instrumental in furthering the DRR participation into the electricity industry. We present in this section a brief summary of the state of the art and of the developments in the electricity industry related with the DRRs and their use.

The DRR integration into the power system is often viewed as an evolution of the DSM practices. However, unlike DRR deployment, DSM programs have been driven primarily by the monopoly utility's resource planning and system reliability requirements rather than the competitive market pressures and the interests of individual consumers [16]. In fact, regulatory driven DSM was initially introduced

to maximize the utilization of the existing resources and to defer the addition of new generating units. DSM activities were aimed at modifying the utility's load shape. Several studies in the literature provide models for the quantification of the impacts of the DSM activities on the utility's load shape and total demand. Since demand is a key driver in power system planning and operations, DSM was integrated into the planning activities [17]. DSM was a fundamental component of the widely used integrated planning technique, which determines the "least-cost" supply- and demand-side alternatives needed to meet the existing and future load demand requirements. As the electricity industry underwent restructuring, DSM activities became less prominent. In the restructured environment, the demand-side played a fairly passive role in the electricity markets during the late 1990s and the early 2000s.

Several studies and reports available in the literature highlight the imbalance in the competitive electricity markets due to the passive demand-side. The ESPs procure the electricity from the spot markets which are subject to volatility in the prices but provide energy to the consumers at flat prices. As a result, there are no incentives for the consumers to reduce their loads during the hours when the spot prices of electricity reach very high levels. The lack of demand response to the high price during critical hours when there is a shortage of supply or when the system is stressed can have disastrous effects in the electricity markets, as evident from the famous California crisis of 2001 [18]. The absence of price-responsiveness among the demand-side in the organized electricity markets has received considerable attention [19]. Many academicians believed that the introduction of dynamic pricing schemes would be the panacea for this problem [20], [21]. However, the implementation of such schemes has been hindered by the regulation and the lack of advanced metering equipment [22], [23].

The IGOs in the United States are following the example of the England and

Wales market, which adopted the *demand-side bidding* scheme in the mid-1990s. The scheme allows large industrial consumers to offer load curtailment services in the competitive pool and receive a payment for the same. Analysis of the scheme and its implications on scheduling and pricing of electricity is available in [11] and [12]. Both analyses not only incorporate load curtailments during high price periods, but also take into account the impacts of demand recovery by the corresponding customers in the low price periods. The explicit consideration of the demand recovery process is important because the customers cannot reduce their demand on a regular basis without demand recovery; otherwise, their profits could suffer. In effect, the successful load curtailment from the demand-side bidders contributes to the redistribution of the demand and a possible leveling of the load curve. Similar mechanisms have been adopted in the NY-ISO, PJM-ISO and ISO-NE in the early 2000s. The specific program details for each ISO are available on the respective web sites and the program manuals [2] - [4].

The demand response programs offered by the IGOs have created significant opportunities for the technologies and the businesses that allow ESPs and other wholesale customers to control and manage the loads their end-user consumers. We refer to all the wholesale customers with responsive loads as the DRRs. When the fuel prices escalated during 2005-2007, the IGOs found that deploying the DRRs and reducing the load was cheaper than dispatching the peaking units. Around this time, the EPAct of 2005 directed FERC to identify steps that need to be taken to ensure that the DRRs are provided equitable treatment as a quantifiable, reliable resource by the ESPs and the IGOs. The confluence of the high electricity prices and the regulartory initiatives from FERC and state governments resulted in growing interest in the aggregation of responsive consumers, thereby increasing the DRR capacity in the power systems. Record reductions in electricity prices to the tune of several hundred dollars per MWh in the PJM

and Midwest ISO systems gave further evidence of the substantial benefits of the DRRs.

The demand response programs of the IGOs identify potential curtailment in the consumption of the customer and treat the curtailment as a service provided. The practice of compensating the customers for such load curtailment services has received considerable criticism from the academic community. Specific comments include the following:

- If customers are paid for curtailing their loads, then they receive double benefits – they avoid consumption at high prices *and* receive a payment for not consuming. As a result, Ruff claims that paying a customer for demand that it would have purchased but did not, is essentially paying twice for the same thing [24].

- A program design that pays customers to not consume suffers from the drawback that the IGO does not know precisely what the customer would have consumed in the absence of the compensatory payments [25]. Even the best statistical or economic models used by the IGOs provide, at best, rough estimates of the so-called baseline of the customers against which the curtailments are measured. Since it is impossible to verify the accuracy of the estimated baseline, it is impossible to determine accurately the consumption of the customer without compensation from the IGO.

- The last critique is related to the procedure used for determining the baseline. Baseline prediction schemes and models typically use the past behavior of the customer to estimate the baseline consumption levels against which load curtailments are measured [26], [27]. Clearly, a customer enrolled as a DRR profits by having a higher baseline level and hence has a strong incentive to inflate the baseline level. This situation is further aggravated

in instances where the customers can consume all that they want at fixed retail rates and sell their load curtailments at spot prices [28].

However, the proponents of DRRs and IGO demand response programs justify the compensatory payments by citing the various benefits accrued to the system due to the DRR deployment. Specific justifications are listed below:

- The load curtailments by the DRRs often lead to a decrease in the electricity prices. The lower prices benefit customers who do not curtail any demand and continue to consume their usual amount of electricity consumption. In fact, the benefits to the non-responsive customers are significantly larger than those to the responsive customers in the case of the PJM system [13]. The compensatory payments provide incentives to the responsive customers and aid in correcting this disparity.

- The program designs adopted by the IGOs treat the load curtailment offers from the DRRs on par with the generation offers from the supply-side sellers, as directed by EPAct [7]. In fact, the DRR offers provide the IGO with additional controllable resources which may be dispatched so as to maintain reliable and economic operation for the entire system.

The increasing popularity of the IGO demand response programs and the economic benefits associated with their use have created several business opportunities. According to the FERC, in the year 2008, the potential for load reduction during peak load periods increased by 26 % as compared to that of 2006; the majority of this increase is observed in the industrial sector [9].

Several reports showcase the capability of the consumers with demand response capabilities to be a reliable, quantifiable and usable resource in the power system and electricity market operations [29] - [31]. Most reports are qualitative in nature. Efforts have also been made to evaluate the impacts of DRRs

on the power system, the electricity market outcomes and the individual players using quantitative metrics. Borghetti et al. demonstrate the ability of DRRs to mitigate the market power on the supply-side [12]. Analysis of PJM's demand response program indicates that the program structure provides a net benefit to the system [13]. Su et al. present a market clearing mechanism that has the capability to take into consideration the load shifting behavior of consumers who submit price-sensitive demand bids [14]. The analysis indicates that the load shifting improves the economic efficiency of the day-ahead market. The problem of formulating the bidding strategies for the demand-side buyers in the competitive environment has also received considerable attention [32], [33]. Although the above mentioned studies strongly justify the benefits of the DRR integration to the entire system as well as to individual players, the methodologies some limitations. In particular, these methodologies are only applicable to short-term study periods. Consequently, the analysis is deterministic in nature and the uncertainty with respect to the demand, the generator availability and the behavior of the market participants is not taken into consideration. Also, the models presented in the aforementioned references fail to take into account the impacts of transmission constraints. Ignoring the interactions of the DRRs and other resources with the transmission network ignores the possible congestion relief due to the load curtailment and hence, it may undervalue the benefits of DRRs.

A study conducted by Faruqui et al. claims that even a 5 % drop in the peak demand can yield substantial savings in the electricity costs; the reduction in the peak demand is sufficient to eliminate the need for installing generation capacity that would be dispatched for less than 100 hours in a year [34]. An analysis of the different demand response programs indicates that the DRRs successfully reduce the peak load demand of the system [9]. Clearly, the deployment of the DRRs impacts the need for additional peaking generation. Similarly, the use

of DRRs may impact transmission congestion and the potential asset additions. To capture such consequences of the DRR deployment, we need to study the operation of the electricity markets and power system over longer term periods due to long lead times associated with the asset additions. Unfortunately, the current methodologies for evaluating DRR impacts are applicable only to short-term periods, with the transmission considerations and uncertainty effects ignored. Furthermore, the methodologies are unable to accommodate long-term effects such as changes in the resource mix, the transmission grid and the policies which impact the power system and market operations. Consequently, the current state of the art cannot be applied to analyze the impacts of DRRs in the context of resource investment, transmission planning and policy developments. Such analysis requires a systematic quantification of the long-term impacts of the DRRs on the generation dispatch and the transmission usage. This report presents the modeling, the analysis and the methodology needed to simulate the operations of the power system and the electricity markets with DRR players over longer-term periods so as to comprehensively assess the impacts of DRRs.

1.3 Scope and Nature of the Contributions

The literature review presented in the previous section highlights the benefits that may be achieved from the integration of the DRRs into the operations of the power system and the electricity markets. The review also pinpoints the specific needs for a comprehensive assessment of the impacts of DRRs. In particular, we realize the inability of the current state of the art to incorporate the effects of transmission constraints, uncertainty and long-term changes. Consequently, the existing methodologies are not suitable for analyzing the impacts of DRRs on the potential generation and transmission asset additions in the system. We

focus on the development of a methodology which comprehensively evaluates the performance of the DRRs over longer-term periods.

The development of the proposed methodology necessitates the modeling of the DRRs and their impacts on the integrated market and system operations of the IGO. Throughout the report, we adopt the point of view of the IGO. We use our knowledge of the power system operations and electricity markets to model the decision making problem of the IGO for transmission-constrained markets with DRR players. We model the problem so as to take into consideration the characteristics of the DRRs, the economics of the electricity markets and the physical constraints on the generators and the transmission grid. The analysis of the problem solution provides a comprehensive set of metrics which quantify the variable effects of the system including total DRR curtailment, net cleared demand, total dispatched generation, GHG emissions, electricity prices, production costs and congestion rents. The model also captures the variable effects for the individual players such as electricity sold (purchased) by a seller (buyer) and the corresponding revenues (payments).

A key requirement for the proposed methodology is the explicit representation of the various sources of uncertainty for the longer-term simulations of the power system behavior. The widely used probabilistic production simulation techniques cannot be directly applied to the systems with DRRs due to the inability of such techniques to accommodate the time-dependent phenomena associated with the DRR deployments and transmission usage. We overcome this challenge by suitably modifying the probabilistic models so as to incorporate temporal information in the modified probabilistic representations. We develop a simulation engine based on the extended probabilistic simulation approach which incorporates the transmission-constraint market impacts. The simulation engine allows the consideration of the various sources of uncertainty along with the transmis-

sion capacity constraints and competitive market outcomes. The application of the engine to the simulation of the system with DRRs for longer-term periods provides quantification of the variable effects of the system, including the expected generation, the revenues and the emissions for each generation unit as well as the system and the key reliability metrics.

The application of the proposed engine to longer-term study period simulations requires careful consideration of the assumptions introduced in the extended probabilistic simulation approach. We propose a simulation methodology, based on the extensive use of the simulation engine, to apply to a long-term study period. Furthermore, we exploit the structural characteristics of the power system and electricity market models to reduce the computing in the implementation of the proposed methodology for studies of practical interest. We also employ Latin hypercube sampling to improve the computational tractability of the simulation engine which is the main constituent of the proposed methodology.

We demonstrate the comprehensiveness and versatility of the proposed simulation methodology through various application studies. The application studies presented in the report serve to illustrate how the proposed methodology may be used to address several *what if* questions in the context of policy analysis, transmission planning and resource investment analysis. We examine the system-wide benefits as well as individual player benefits due to use of DRRs. The results of the simulation studies provide quantification of such benefits, including reductions in net energy consumption, total energy payments, CO_2 emissions and congestion rents. We investigate the impacts of DRRs on transmission/generation investments; our analysis indicates that the curtailment in the peak demand does indeed defer the need for additional transmission capability as well as generation capacity. We also compare the DRR integration with two related demand-side activities – implementation of energy conservation measures and deployment of

the advanced metering infrastructure (AMI) – and highlight the similarities as well as the differences between all three activities.

1.4 Thesis Outline

This thesis consists of five additional chapters and two appendices. In Chapter 2, we discuss the explicit representation of the DRRs in electricity markets in transmission-constrained networks. We extend the basic electricity market model to incorporate the impacts of DRR curtailments. The analysis of the transmission-constrained electricity market model with DRRs allows the assessment of the key variable effects of interest. We also consider the shift of the demands from high price periods to low price periods and discuss its implications for long-term analysis. The DRR modeling work is used extensively in the simulation methodology development.

In Chapter 3, we develop the simulation engine which emulates the behavior of the systems with DRRs. The principal challenge in the development of the proposed engine is to mesh the time-abstracted framework of the probabilistic production simulation technique with the time-dependent framework of the transmission-constrained IGO markets with DRRs. Such an effort entails modifications to the probabilistic simulation techniques to accommodate the time-varying phenomena associated with DRR deployment. We describe a two-step synchronization process for the development of the simulation engine. We first develop a representation of the load that is compatible with the representation of the DRR capacities. Next, we use the realizations of the random variables (rv's) characterizing the load and the available generation capacities to construct the distributions of the outcomes of the transmission-constrained markets with DRR players. The expectations of the rv's representing the outcomes of the

transmission-constrained markets are then used to evaluate the variable effects of the system for the period.

In Chapter 4, we describe the proposed simulation methodology for the emulation the operations of the electricity markets and power system during longer-term study periods which may include long-term changes to the system. The proposed methodology makes extensive use of the simulation engine developed in Chapter 3. We also focus on the computational tractability issues in the long-term simulations of large-scale systems. We discuss in detail the implementational aspects of the proposed simulation methodology. We introduce appropriate mechanisms into the implementation embodying the proposed methodology so as to make it useable for simulation studies of practical interest. We highlight the wide range of applications of the methodology for power system planning and analysis studies.

In Chapter 5, we go further than the conceptual modeling approach and provide simulation results for some representative applications of the proposed methodology. The studies serve to illustrate the nature of the results, and provide valuable insights on the deployment of DRRs. We present a set of simulation studies which investigates the impacts of DRR curtailments on the system. We pay special attention to the level of penetration of DRRs in the resource mix as well as to payback effects. Another set of simulation studies evaluates the benefits to an ESP for implementing DRR aggregation of varying size. We also show how DRR deployments defer the need for additional transmission and generation resources. We compare the deployment of the DRRs with implementation of energy conservation measures and the use of AMI.

Chapter 6 summarizes the key results of our studies and points out directions for future work. In Appendix A, we summarize the notation and the acronyms used in the report. In Appendix B, we present the supplementary details of the Latin hypercube sampling technique discussed in Chapter 4.

CHAPTER 2

MODELING AND ANALYSIS OF TRANSMISSION CONSTRAINED MARKETS WITH DRRs

The quantification of the impacts of the DRR integration into power systems requires the explicit representation of DRRs in the models of electricity markets. The analysis of the models which represent DRRs in the integrated market and transmission grid operations of the IGO allows the assessment of variable effects of the system such as total energy consumption, production costs and GHG emissions as well as key reliability metrics. We devote this chapter to review the modeling of electricity market and system operations and to introduce the required modifications in the models so as to allow the incorporation of DRRs. The chapter contains three sections. In Section 2.1, we review of the basics of electricity market modeling and present the market clearing model for the systems without DRRs. In Section 2.2, we extend the basic market clearing model to explicitly represent impacts of DRR curtailments in the market outcomes and grid operations. We conclude, in Section 2.3, with a discussion on the impacts of DRRs on the system over longer-term study periods.

2.1 Review of the Electricity Market Model for Transmission Constrained Systems

Electricity markets for systems without DRRs have been widely discussed in the literature [35] - [37]. In this section, we review the modeling of electricity markets. In particular, we discuss the basics of the modeling and the problem formulation

for the market clearing.

In this work, we consider the MWh commodity markets. We define a subperiod to be the smallest indecomposable unit of time. There exist different markets for each subperiod in the study period, differentiated by the time at which the market decisions are taken. In Fig. 2.1, we use a simple illustration to indicate the sequence of electricity markets that are used for buying and selling electricity for a subperiod h of the study period. We focus on the single subperiod h day-

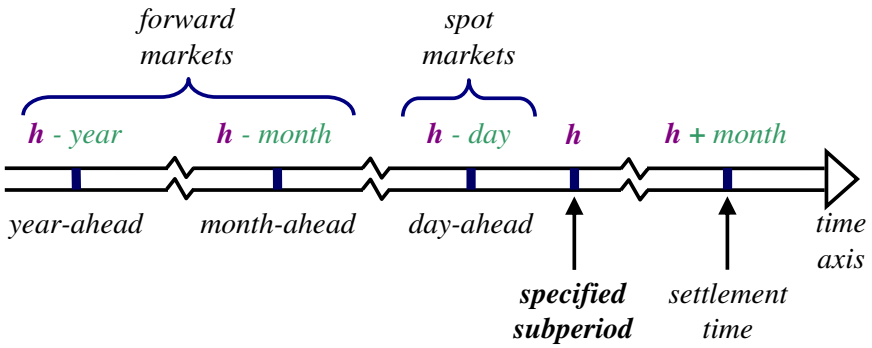

Figure 2.1: Time frame for electricity markets

ahead market (DAM), one of K such markets operated by the IGO – one for each subperiod of the next day.[1]

We assume that the DAM has the centralized pool market structure widely adopted in the North America. The IGO is the operator of the pool market. The sellers indicate, to the IGO, their willingness to sell electricity, by submitting sealed offers specifying the sale quantities and prices. At the same time, the pool buyers submit sealed bids to the IGO to indicate their willingness to buy electricity. Note that the offers and bids may not reflect the actual costs and benefits of the sellers and buyers, respectively, since true costs and benefits constitute private information. The IGO determines the outcomes for the day-ahead pool market so

[1]In the case of hourly markets, there exist 24 separate energy markets for each hour of the day, so $K = 24$.

that demand requirements are met in the most economic manner, and it provides transmission service for the successful sellers and buyers. The IGO determines the successful sellers (buyers) based on the willingness to sell (buy) as indicated by the submitted offers (bids). In doing so, the IGO also determines the quantity sold by each seller and the quantity bought by each buyer. We depict the basic structure of the single DAM for the subperiod h in Fig. 2.2. The figure also indicates the direction of the electricity and money flows.

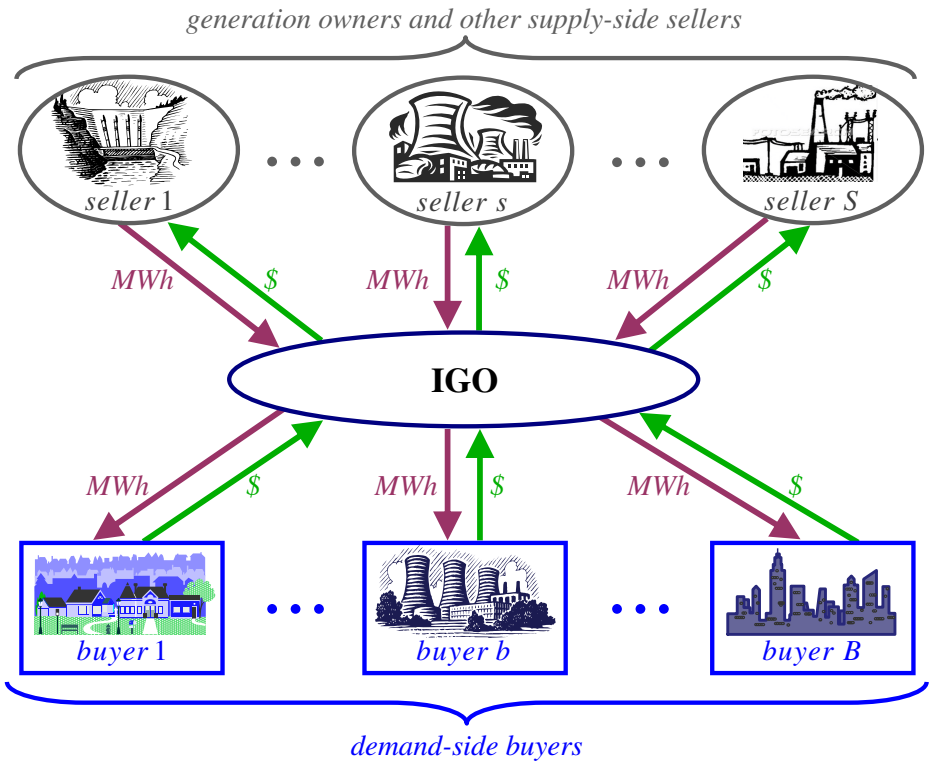

Figure 2.2: Structure of a single DAM for a specified subperiod

We now discuss the modeling of the DAM for the subperiod h in terms of the offers and bids of the sellers and the buyers. We consider the DAM consisting of a set of S sellers, denoted by $\mathcal{S}$, and a set of B buyers, denoted by $\mathcal{B}$. We denote by $\mathscr{C}^s(p^s)$ the integral of the seller s's marginal offer price as a function of the real power supply p^s MWh/h. Similarly, we denote by $\mathscr{B}^b(p^b)$ the integral of

the buyer b's marginal bid price as a function of the real power consumption $p^{\,b}$ MWh/h. We denote by $\alpha^{\,s}$ the capacity offered by the seller s and by $\ell^{\,b}$ the load demand requested by the buyer b.

While there exist many market schemes for the pool market, we consider only the uniform-price auction mechanism. The IGO determines the outcomes of the DAM by maximizing the auction surplus.[2] To explain the process, we first ignore the transmission capacity constraints. In effect, we assume that there exists ample transmission capacity to accommodate all the transactions as scheduled by the IGO. We note that the outcomes of the DAM must satisfy the supply-demand balance. In order to determine the outcomes of the DAM, the IGO formulates and solves the following optimization problem:

$$\left\{\begin{array}{ll} \max & \displaystyle\sum_{b\,\in\,\mathcal{B}} \mathscr{B}^{\,b}\left(p^{\,b}\right) \;-\; \sum_{s\,\in\,\mathcal{S}} \mathscr{C}^{\,s}\left(p^{\,s}\right) \\ \text{subject to} & \\ \displaystyle\sum_{s\,\in\,\mathcal{S}} p^{\,s} \;=\; \sum_{b\,\in\,\mathcal{B}} p^{\,b} & \longleftrightarrow \qquad \bar{\lambda} \end{array}\right. . \tag{2.1}$$

$\bar{\lambda}$ denotes the dual variable associated with the supply-demand balance constraint. Since the transmission constraints are ignored in this problem, it is referred to as the *transmission unconstrained market clearing problem* [38], [39]. The optimal solution of (2.1) determines the sales and purchases of the pool players. Each seller s sells $\left[\,p^{\,s}\,\right]^*$ MWh/h electricity to the IGO and each buyer b buys $\left[\,p^{\,b}\,\right]^*$ MWh/h electricity from the IGO. The optimal value of the dual variable associated with the supply-demand balance constraint, $\left[\,\bar{\lambda}\,\right]^*$, determines the uniform *market clearing price* (MCP). Each seller (buyer) sells (buys) at the MCP.

The solution of (2.1) corresponds to the solution obtained by the so-called

[2]We use the terminology auction surplus instead of social welfare because the bid/offer data for the buyers/sellers may not reflect true benefits/costs. Auction surplus may be viewed as the "perceived" social welfare based on the submitted offers and bids.

merit order dispatch technique [35]. For this, the IGO constructs the *supply curve* by sorting the pool sellers' offers according to their marginal offer prices. Similarly, the *demand curve* is constructed by sorting the pool buyers' bids according to their marginal bid prices. The intersection of the supply and demand curves determines the market equilibrium $\left(\left[\,\bar{\lambda}\,\right]^*, \left[\,\bar{\ell}\,\right]^*\right)$ which satisfies the equality constraint of (2.1) and maximizes the auction surplus. $\left[\,\bar{\ell}\,\right]^*$ is the total cleared demand and given as

$$\left[\,\bar{\ell}\,\right]^* \;=\; \sum_{b\,\in\,\mathcal{B}} \left[\,p^b\,\right]^* \;. \tag{2.2}$$

We provide in Fig. 2.3 the graphical illustration of the equilibrium of a specified hourly DAM.

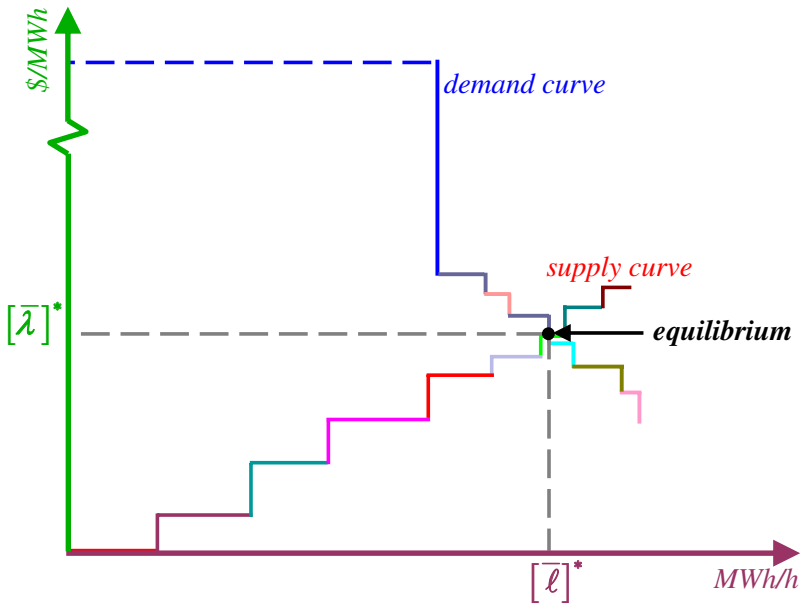

Figure 2.3: Equilibrium of the DAM with supply-side offers and demand-side bids

The physical capacity limits on the transmission, along with the operational and security constraints for the operation of the power system, impact the outcomes of the DAM. Hence, the IGO's decision making problem for the market

clearing needs to explicitly incorporate such constraints in the problem formulation. The incorporation of the constraints in the problem formulation necessitates the integration of the electricity market model with the modeling of the physical transmission grid and the associated operational and security constraints. We now discuss the modeling of the physical grid for the subperiod h for which the DAM is operated. We assume that the parameters of the generation and transmission along with the network topology do not vary within the subperiod h and we represent the power system by a system snapshot during the subperiod h. We model the transmission network using the network topology and the parameters observed during this snapshot.

We consider a transmission network with $(N+1)$ buses and J lines. We use

$$\mathcal{N} = \{n \,:\, n = 0, 1, \,\ldots\, , N\}$$

to denote the index set of the buses in the network, with bus 0 being the slack bus. We denote by p_n^g the real power generation at the node n and by p_n^d the real power demand at the node n. Since the total generation and demand at a node depend on the sellers and buyers present at the node, we define the total generation at node n as

$$p_n^g \;=\; \sum_{\substack{s \,\in\, \mathcal{S} \; is \\ at \; the \; node \; n}} p^{\,s} \tag{2.3}$$

and the total demand at the node n as

$$p_n^d \;=\; \sum_{\substack{b \,\in\, \mathcal{B} \; is \\ at \; the \; node \; n}} p^{\,b} \;. \tag{2.4}$$

To explain this concept, we use a simple illustration provided in Fig. 2.4 to

indicate the impacts of the sales and purchases at node n on the generation and demand at that node.

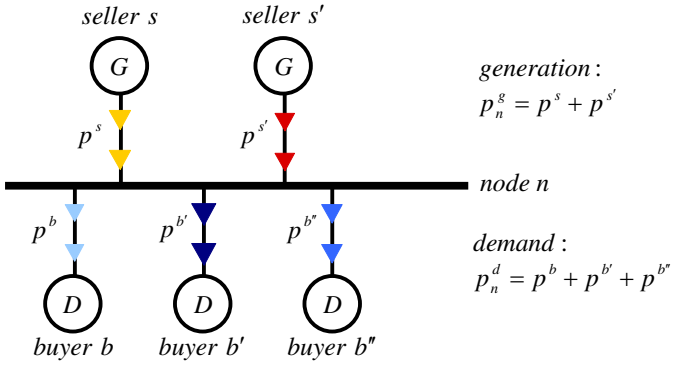

Figure 2.4: The generation and demand at the node n

We denote the index set of the lines and the transformers which connect the buses by

$$\mathcal{J} = \{j \ : \ j = 1, 2, \ \ldots \ , J\} \ .$$

We associate with each line $j \in \mathcal{J}$ the *ordered* pair $j = (n_1, n_2)$, with the convention that the direction of the flow, f_j, on line j is *from* the node n_1 *to* the node n_2, with $n_1, n_2 \in \mathcal{N}$, so that $f_j \geq 0$. We denote by $\underline{\boldsymbol{B}}_d$ the *diagonal branch susceptance matrix* with

$$\underline{\boldsymbol{B}}_d \triangleq diag\,\{b_j : \ j \in \mathcal{J}\} \in \ \mathbb{R}^{L \times L} \ ,$$

where, b_j is the susceptance of the line j. We use the *augmented branch-to-node incidence matrix* $\underline{\hat{\boldsymbol{A}}}$ with

$$\underline{\hat{\boldsymbol{A}}} \ = \ \begin{bmatrix} a_{1,0} & a_{1,1} & \ldots & a_{1,N} \\ a_{2,0} & a_{2,1} & \ldots & a_{2,N} \\ \vdots & \vdots & \ddots & \vdots \\ a_{J,0} & a_{J,1} & \ldots & a_{J,N} \end{bmatrix} \in \mathbb{R}^{J \times (N+1)} \ , \tag{2.5}$$

where,

$$a_{j,n} = \begin{cases} 1 & \text{if } n = n_1 \\ -1 & \text{if } n = n_2 \\ 0 & \text{otherwise} \end{cases} \tag{2.6}$$

for $j = (n_1, n_2)$, to construct the *augmented nodal susceptance matrix* $\hat{\underline{\boldsymbol{B}}}$ with

$$\hat{\underline{\boldsymbol{B}}} = \hat{\underline{\boldsymbol{A}}}^T \underline{\boldsymbol{B}}_d \hat{\underline{\boldsymbol{A}}} = \begin{bmatrix} b_{0,0} & b_{0,1} & \dots & b_{0,N} \\ b_{1,0} & b_{1,1} & \dots & b_{1,N} \\ \vdots & \vdots & \ddots & \vdots \\ b_{N,0} & b_{N,1} & \dots & b_{N,N} \end{bmatrix} \in \mathbb{R}^{(N+1)\times(N+1)} . \tag{2.7}$$

Note that $\hat{\underline{\boldsymbol{B}}}$ is symmetric and singular. Next, we obtain the *reduced branch-to-node incidence matrix* $\underline{\boldsymbol{A}}$ from $\hat{\underline{\boldsymbol{A}}}$ by removing the column corresponding to the slack node, so that

$$\underline{\boldsymbol{A}} = \begin{bmatrix} a_{1,1} & \dots & a_{1,N} \\ \vdots & \ddots & \vdots \\ a_{J,1} & \dots & a_{J,N} \end{bmatrix} \in \mathbb{R}^{J\times N} \tag{2.8}$$

and $\underline{\boldsymbol{A}}$ is full rank [36, p. 134]. Analogously, we partition the matrix $\hat{\underline{\boldsymbol{B}}}$ as

$$\hat{\underline{\boldsymbol{B}}} = \begin{bmatrix} b_{0,0} & \underline{\boldsymbol{b}}_0^T \\ \underline{\boldsymbol{b}}_0 & \underline{\boldsymbol{B}} \end{bmatrix} , \tag{2.9}$$

where,

$$\underline{\boldsymbol{b}}_0 = [b_{0,1}, b_{0,2}, \dots, b_{0,N}]^T$$

and $\underline{\boldsymbol{B}}$ is the *reduced nodal susceptance matrix*. Note that

$$\underline{\boldsymbol{B}} \;=\; \underline{\boldsymbol{A}}^T\, \underline{\boldsymbol{B}}_d\, \underline{\boldsymbol{A}} \;=\; \begin{bmatrix} b_{1,1} & \dots & b_{1,N} \\ \vdots & \ddots & \vdots \\ b_{N,1} & \dots & b_{N,N} \end{bmatrix} \in \mathbb{R}^{N\times N} \tag{2.10}$$

and $\underline{\boldsymbol{B}}$ is symmetric and nonsingular.

The key characteristics of the transmission network may be described by the power flow equations and the various constraints. Under the assumptions that the power system is lossless and that the DC power flow conditions hold [36], the power flow equations have the form

$$\underline{\boldsymbol{p}}^{\,g} \;-\; \underline{\boldsymbol{p}}^{\,d} = \underline{\boldsymbol{B}}\,\underline{\boldsymbol{\theta}} \tag{2.11a}$$

$$p_0^{\,g} \;-\; p_0^{\,d} = \underline{\boldsymbol{b}}_0^{\,T}\,\underline{\boldsymbol{\theta}} \tag{2.11b}$$

where

$$\underline{\boldsymbol{p}}^{\,g} \triangleq [\, p_1^{\,g}, p_2^{\,g}, \,\dots\, , p_N^{\,g}\,]^{\,T} \in \mathbb{R}^{\,N}$$

is the generation vector,

$$\underline{\boldsymbol{p}}^{\,d} \triangleq \left[\, p_1^{\,d}, p_2^{\,d}, \,\dots\, , p_N^{\,d}\,\right]^{\,T} \in \mathbb{R}^{\,N}$$

is the withdrawal vector and

$$\underline{\boldsymbol{\theta}} \triangleq [\, \theta_1, \theta_2, \,\dots\, , \theta_N\,]^{\,T} \in \mathbb{R}^{\,N}$$

is the vector of nodal voltage phase angles θ_n of the network nodes. The scarcity of the transmission capability is represented by the capacity limits under both the base case and the contingency cases. For simplicity, in this work, we only

represent the active power line flow limits under the base case. We define the line flow vector as

$$\underline{\boldsymbol{f}} \triangleq [\, f_1, f_2, \, \ldots \, , f_J \,]^T \in \mathbb{R}^J \, .$$

Then we have

$$\underline{\boldsymbol{f}} \;\; = \;\; \underline{\boldsymbol{B}}_d \, \underline{\boldsymbol{A}} \, \underline{\boldsymbol{\theta}} \, . \tag{2.12}$$

The constraints on the real power flows on the lines of the network are modeled using the inequality

$$\underline{\boldsymbol{f}} \;\; \leq \;\; \underline{\boldsymbol{f}}^{\,max} \, , \tag{2.13}$$

where,

$$\underline{\boldsymbol{f}}^{\,max} \triangleq [\, f_1^{\,max}, f_2^{\,max}, \, \ldots \, , f_J^{\,max} \,]^T \;\; ,$$

with $f_j^{\,max}$ representing the active power flow limit of the line j. We call a line j *congested* if $f_j = f_j^{\,max}$. We call a transmission network *congested* if there are one or more congested lines in the network.

The problem formulation of (2.1) may be modified to incorporate the transmission constraints described by Equations (2.11)-(2.13). The modified problem formulation is stated here:

$$\left\{ \begin{array}{l} \max \;\; \displaystyle\sum_{b \, \in \, \mathcal{B}} \mathscr{B}^{\,b} \left(p^{\,b} \right) \; - \; \sum_{s \, \in \, \mathcal{S}} \mathscr{C}^{\,s} \left(p^{\,s} \right) \\ \text{subject to} \\ \quad \begin{array}{lcll} \underline{\boldsymbol{p}}^{\,g} \; - \; \underline{\boldsymbol{p}}^{\,d} & = & \underline{\boldsymbol{B}} \, \underline{\boldsymbol{\theta}} & \longleftrightarrow \quad \underline{\bar{\boldsymbol{\lambda}}} \\ p_0^{\,g} \; - \; p_0^{\,d} & = & \underline{\boldsymbol{b}}_0^{\,T} \underline{\boldsymbol{\theta}} & \longleftrightarrow \quad \bar{\lambda}_0 \\ \underline{\boldsymbol{B}}_d \, \underline{\boldsymbol{A}} \, \underline{\boldsymbol{\theta}} & \leq & \underline{\boldsymbol{f}}^{\,max} & \longleftrightarrow \quad \underline{\bar{\boldsymbol{\rho}}} \end{array} \end{array} \right. \; . \tag{2.14}$$

We denote the modified problem by $\mathscr{M}(\mathcal{S}, \mathcal{B})$. The vectors and the scalar associated with the right-hand sides of the constraints are the dual variables for the corresponding constraints. The problem formulation provides solutions for the integrated market and network operations performed by the IGO.

The DAM is settled on the basis of the optimal solutions of $\mathscr{M}(\mathcal{S}, \mathcal{B})$. With the transmission constraints considered, the market may no longer have a single uniform clearing price. Such a situation arises because we explicitly consider the supply-demand balance at each node of the system in the equality constraints of $\mathscr{M}(\mathcal{S}, \mathcal{B})$. The optimum value of the dual variable associated with the power balance constraints at the node $n \in \mathcal{N}$, $\left[\, \bar{\lambda}_n \,\right]^*$, is the location marginal price (LMP) at that node n. Each seller (buyer) sells (buys) electricity at the LMP of the node where he is connected. The optimal values of the decision variables $[\, p^s \,]^*$ and $\left[\, p^b \,\right]^*$ determine the sales and purchases by the sellers and buyers, respectively.

In the event of congestion, the LMPs at each node may become different. Consequently, the nonzero LMP differences are an indication of the impacts of system operational constraints. The LMP differences yield nonnegative revenue for the IGO; such revenues are commonly referred to as the *congestion rents* [39]. The IGO collects these revenues, which are given by

$$\bar{\kappa} \;=\; \sum_{n \in \mathcal{N}} \left[\, \bar{\lambda}_n \,\right]^* \cdot \left[\, p_n^d \,\right]^* \;-\; \sum_{n \in \mathcal{N}} \left[\, \bar{\lambda}_n \,\right]^* \cdot [\, p_n^g \,]^* \;, \tag{2.15}$$

where, $\left[\, p_n^d \,\right]^*$ is the cleared demand at the node n while $[\, p_n^g \,]^*$ is the generation at the node n. The congestion rents, the LMPs, and the sale and purchase amounts serve as key metrics to assess performance of the DAM and the power system. These may be used to develop additional metrics such as the total supply-side

revenues $\bar{w}^{\mathcal{S}}$

$$\bar{w}^{\mathcal{S}} = \sum_{n \in \mathcal{N}} \left[\bar{\lambda}_n \right]^* \cdot \left[p_n^g \right]^* , \tag{2.16}$$

the total demand-side payments $\bar{w}^{\mathcal{B}}$

$$\bar{w}^{\mathcal{B}} = \sum_{n \in \mathcal{N}} \left[\bar{\lambda}_n \right]^* \cdot \left[p_n^d \right]^* \tag{2.17}$$

and the total cleared demand $\left[\bar{\ell} \right]^*$

$$\left[\bar{\ell} \right]^* = \sum_{n \in \mathcal{N}} \left[p_n^d \right]^* . \tag{2.18}$$

Conceptually, we assess the performance of the integrated market and network operations of the IGO for each subperiod in the study period. In effect, we model the electricity market and the physical network for each subperiod in the study period. The analysis of all the DAMs during the study period entails the formulation of the $\mathscr{M}(\mathcal{S}, \mathcal{B})$ for each subperiod in the study period. The solutions of the $\mathscr{M}(\mathcal{S}, \mathcal{B})$ are used to evaluate the performance metrics for that subperiod and the subperiodic values are aggregated to compute the performance metrics for the entire study period. The aggregated metrics may then be used to quantify the variable effects of the power system for the study period.

2.2 Representation of DRRs in the Transmission Constrained Electricity Market Model

In this section, we extend the models of the electricity market and the physical grid presented in the previous section to explicitly incorporate the impacts of the

DRR players. Again, we focus on a single DAM for a specified subperiod h, and represent the system by its snapshot during the subperiod h under consideration. We modify the existing models of the DAM and the grid to accommodate the effects of DRR curtailments.

By definition, a DRR player must be a buyer. Consequently, we partition the set of buyers $\mathcal{B}$ into two non-overlapping subsets – buyers without demand response capability, $\bar{\mathcal{B}}$ and buyers with demand response capability, $\widehat{\mathcal{B}}$, also known as the DRRs. A buyer $\bar{b} \in \bar{\mathcal{B}}$ acts as *pure* buyer only purchasing electricity from the IGO. On the other hand, a DRR $\hat{b} \in \widehat{\mathcal{B}}$ interacts with the IGO as both a buyer purchasing electricity from the IGO and as a seller selling DRR curtailment services to the IGO. The DRR player acts as a *net* buyer – after all, he cannot sell more load than he can consume – and purchases only the net MWh amount for the load remaining as a result of the DRR curtailment. We emphasize the interactions of this seller-cum-buyer in Fig. 2.5 using the two-sided arrows to indicate the two types of interactions with the IGO.

The IGO collects the offers and bids of all the players and determines the outcomes of the DAM, to meet the demand requirements in the most economic and reliable manner. To discuss the impacts of DRRs on the market outcomes, we first consider the DAM with unconstrained transmission services. To include DRRs in the DAM model, we model the demand bid and the curtailment offer of a DRR player as two separate transactions with the IGO. Thus, each DRR player $\hat{b} \in \widehat{\mathcal{B}}$ is represented as a buyer of electricity and a seller of DRR curtailment services. We denote by $\mathscr{B}^{\hat{b}}\left(p^{\hat{b}}\right)$ the integral of the marginal bid function of $\hat{b}$ as a buyer, for the purchase of $p^{\hat{b}}$ MWh/h. Similarly, we denote by $\mathscr{C}^{\hat{b}}\left(\hat{p}^{\hat{b}}\right)$ the integral of the marginal offer function of $\hat{b}$ as a DRR seller, for the sale of $\hat{p}^{\hat{b}}$ MW/h of DRR curtailment. To avoid gaming by DRR players and to circumvent the *free*

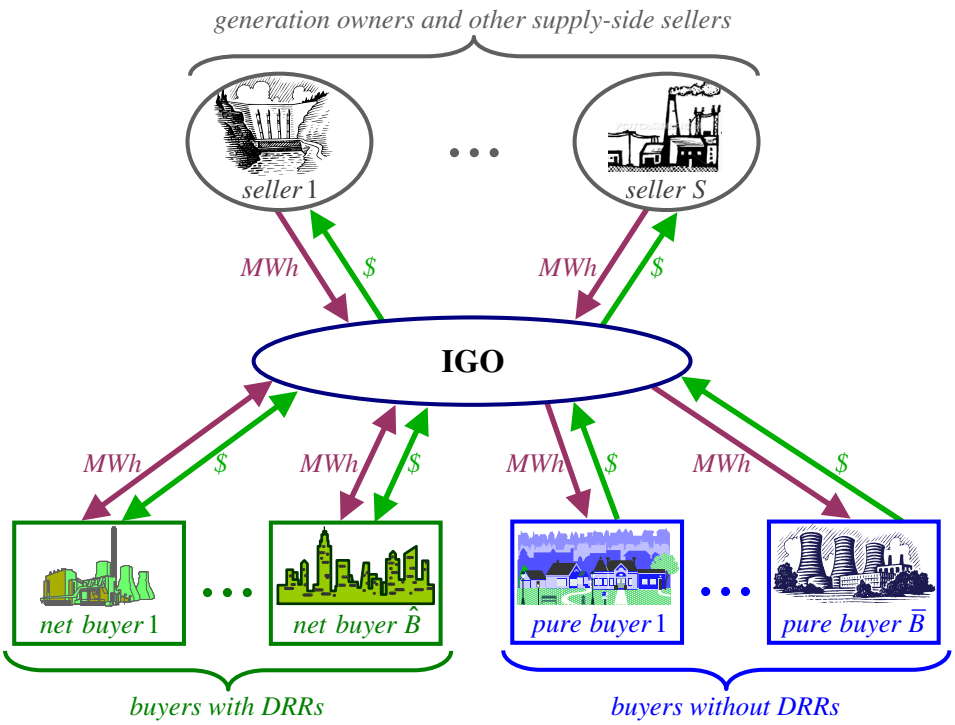

Figure 2.5: Structure of the DAM with DRR players

rider problem,[3] we impose the restriction $\hat{p}^{\hat{b}} \leq p^{\hat{b}}$. This condition ensures that the DRR player $\hat{b}$ may sell an amount of DRR curtailment that cannot exceed his demand. Therefore, the demand of the DRR $\hat{b}$ as a net buyer is the non-negative term $\left(p^{\hat{b}} - \hat{p}^{\hat{b}}\right)$ MW.

Now, if the offer for load curtailment of a DRR player is successful, then that player has the obligation to reduce his demand by the "cleared" load curtailment amount for that subperiod. In concept, we may view the load curtailment amount cleared in the DAM as a supply of electricity. However, treating DRR load curtailment services as an addition to the electricity supply "leads to confusion, errors and inefficiencies" [24, pp. 24-27]. Instead, we view the load curtailment as a reduction in the demand of the DRR player. Then, the extended problem for-

[3]The free riders are consumers who claim to have performed load reductions in a specified time frame, when they actually had no intention of using electricity in that time frame. In essence, a successful curtailment offer for such players does not actually result in any modification to the system demand.

mulation for the transmission unconstrained market with DRRs may be stated as follows:

$$\begin{cases} \max \sum\limits_{\bar{b} \in \bar{\mathcal{B}}} \mathscr{B}^{\bar{b}}\left(p^{\bar{b}}\right) + \sum\limits_{\hat{b} \in \hat{\mathcal{B}}} \mathscr{B}^{\hat{b}}\left(p^{\hat{b}}\right) - \sum\limits_{s \in \mathcal{S}} \mathscr{C}^{s}\left(p^{s}\right) - \sum\limits_{\hat{b} \in \hat{\mathcal{B}}} \mathscr{C}^{\hat{b}}\left(\hat{p}^{\hat{b}}\right) \\ \text{subject to} \\ \quad \sum\limits_{s \in \mathcal{S}} p^{s} = \sum\limits_{\bar{b} \in \bar{\mathcal{B}}} p^{b} + \sum\limits_{\hat{b} \in \hat{\mathcal{B}}} \left(p^{\hat{b}} - \hat{p}^{\hat{b}}\right) \qquad \longleftrightarrow \qquad \lambda \end{cases} . \tag{2.19}$$

λ denotes the dual variable associated with the supply-demand balance constraint. As in the case of DAM without DRRs, the optimal solution of (2.19) determines the sales and purchases by the pool players and $[\,\lambda\,]^*$ determines the MCP of the market. The net demand of each DRR player is given as $\left(\left[\,p^{\hat{b}}\,\right]^* - \left[\,\hat{p}^{\hat{b}}\,\right]^*\right)$ MWh/h.

The load curtailment by DRR players leads to a decrease in the system load demand. Thus, the impacts of the curtailments by DRRs may be represented by modifying the demand curve by the curtailed load amounts and causing the demand curve to shift to the left. Thus, the market equilibrium in the event of DRR curtailments is determined by the intersection of the shifted demand curve with the supply curve and denoted as $([\,\lambda\,]^*, [\,\ell\,]^*)$. We note that $[\,\ell\,]^*$ is the total cleared net demand for the market, given by

$$[\,\ell\,]^* = \sum_{\bar{b} \in \bar{\mathcal{B}}} \left[\,p^{\bar{b}}\,\right]^* + \sum_{\hat{b} \in \hat{\mathcal{B}}} \left(\left[\,p^{\hat{b}}\,\right]^* - \left[\,\hat{p}^{\hat{b}}\,\right]^*\right) , \tag{2.20}$$

and it explicitly takes into account the total load curtailment of all the successful DRR players. Hence, the cleared demand of the DAM with successful DRRs is less than that of the DAM with only supply-side offers. This decrease in the cleared demand may induce a reduction in the MCP. We illustrate in Fig. 2.6 the impacts of the DRR curtailments on the equilibrium for a specified hourly DAM.

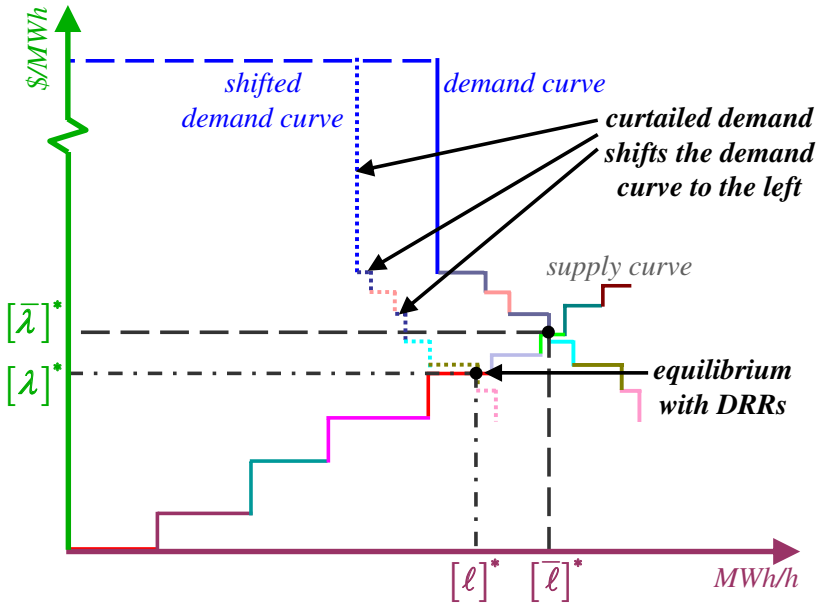

Figure 2.6: Impacts of DRR curtailments on the market equilibrium

We summarize the market outcomes with and without DRRs and indicate the nature of the resulting equilibria in the Table 2.1. As in the case of the DAM

Table 2.1: Comparison of market equilibria with and without DRRs

parameter	no DRRs	with DRRs	relationship
MCP	$[\,\bar{\lambda}\,]^*$	$[\,\lambda\,]^*$	$[\,\bar{\lambda}\,]^* \geq [\,\lambda\,]^*$
cleared demand	$[\,\bar{\ell}\,]^*$	$[\,\ell\,]^*$	$[\,\bar{\ell}\,]^* > [\,\ell\,]^*$

without DRRs, the sellers (buyers) sell (buy) at the MCP $[\,\lambda\,]^*$. The DRR players only pay for the net load purchased in the market, and hence benefit by avoiding consumption when electricity prices are high. In addition to this, the DRR players may be compensated by the IGO for providing load curtailment services. The IGO recovers these compensation payments by imposing *DRR curtailment service*

payments[4] on the buyers on a pro-rated basis; the additional per unit charge as seen by the buyers, υ, is given as

$$\upsilon \;=\; \frac{[\,\lambda\,]^* \cdot \left[\,\hat{p}^{\,\widehat{\mathcal{B}}}\,\right]^*}{[\,\ell\,]^*}\;, \tag{2.21}$$

where, $\left[\,\hat{p}^{\,\widehat{\mathcal{B}}}\,\right]^*$ is the total curtailment from all the DRRs, so that the product in the numerator is the total compensation received by the successful DRR sellers. We note that the determination of υ using Equation (2.21) assumes that the DRRs are compensated at the MCP. Appropriate changes need to be made to (2.21) if the IGO employs an alternate compensation scheme for the DRRs.

To incorporate the DRRs in transmission constrained market model, we extend the physical grid model to take into account the DRR load curtailment. The expression for the nodal withdrawal amount in Equation (2.4) may be restated to explicitly represent the demand requests of the DRRs and the pure buyers so that

$$p^{\,d}_{\,n} = \sum_{\substack{\hat{b}\,\in\,\widehat{\mathcal{B}}\;is\\ at\;the\;node\;n}} p^{\,\hat{b}} \;+\; \sum_{\substack{\bar{b}\,\in\,\bar{\mathcal{B}}\;is\\ at\;the\;node\;n}} p^{\,\bar{b}}. \tag{2.22}$$

To represent the impacts of the DRR curtailments on the physical grid, we introduce the variable $\hat{p}^{\,d}_{\,n}$ which represents the total DRR curtailment at the node n so that

$$\hat{p}^{\,d}_{\,n} = \sum_{\substack{\hat{b}\,\in\,\widehat{\mathcal{B}}\;is\\ at\;the\;node\;n}} \hat{p}^{\,\hat{b}}\;. \tag{2.23}$$

The net demand at any node n is given by the non-negative term $(p^{\,d}_{\,n} - \hat{p}^{\,d}_{\,n})$. The

[4]The DRR curtailment service payments may be treated similarly to those credited as uplift payments: they are the charges levied on the buyers in addition to energy payments. The DRRs receive these payments as a compensation for providing the load curtailments to the IGO.

illustration in Fig. 2.7 indicates the impacts of the DRRs at the node n. We use

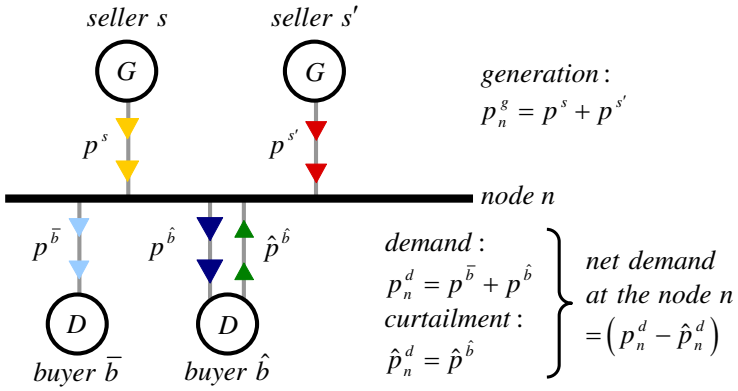

Figure 2.7: The impacts of the DRRs at the node n

$\hat{p}_n^d$ to construct the DRR curtailment vector $\underline{\hat{\boldsymbol{p}}}^d$, where,

$$\underline{\hat{\boldsymbol{p}}}^d \triangleq \left[\, \hat{p}_1^d, \hat{p}_2^d, \ \ldots\ , \hat{p}_N^d \,\right]^T \in \mathbb{R}^N \ .$$

Then, the DC power flow Equations are modified as follows:

$$\underline{\boldsymbol{p}}^g \ - \ \left(\underline{\boldsymbol{p}}^d - \underline{\hat{\boldsymbol{p}}}^d\right) = \underline{\boldsymbol{B}}\,\underline{\boldsymbol{\theta}} \ , \tag{2.24a}$$

$$p_0^g - \left(p_0^d - \hat{p}_0^d\right) = \underline{\boldsymbol{b}}_0^T\,\underline{\boldsymbol{\theta}} \ . \tag{2.24b}$$

The problem formulation for the DAM with DRRs may be obtained through careful modifications to the problem $\mathcal{M}\left(\mathcal{S}, \mathcal{B}\right)$ given in Equation (2.14). We replace the equality constraints of $\mathcal{M}\left(\mathcal{S}, \mathcal{B}\right)$ with the modified DC power flow Equations (2.24). Further, we restate the objective to incorporate the benefits and the costs of the DRR players. The modified problem formulation is denoted by $\mathcal{M}\left(\mathcal{S}, \widehat{\mathcal{B}}, \bar{\mathcal{B}}\right)$ to explicitly represent the two classes of buyers – $\widehat{\mathcal{B}}$, and $\bar{\mathcal{B}}$. We state the modified

formulation as follows:

$$\begin{cases} \max \sum_{\bar{b}\,\in\,\bar{\mathcal{B}}} \mathscr{B}^{\,b}\left(p^{\,b}\right) \;+\; \sum_{\hat{b}\,\in\,\widehat{\mathcal{B}}} \mathscr{B}^{\,\hat{b}}\left(p^{\,\hat{b}}\right) \;-\; \sum_{s\,\in\,\mathcal{S}} \mathscr{C}^{\,s}\left(p^{\,s}\right) \;-\; \sum_{\hat{b}\,\in\,\widehat{\mathcal{B}}} \mathscr{C}^{\,\hat{b}}\left(\hat{p}^{\,\hat{b}}\right) \\ \text{subject to} \\ \quad \underline{\boldsymbol{p}}^{\,g} \;-\; \left(\underline{\boldsymbol{p}}^{\,d} - \underline{\hat{\boldsymbol{p}}}^{\,d}\right) \;=\; \underline{\boldsymbol{B}}\,\underline{\boldsymbol{\theta}} \qquad \longleftrightarrow \qquad \underline{\boldsymbol{\lambda}} \\ \quad p_{\,0}^{\,g} - \left(p_{\,0}^{\,d} - \hat{p}_{\,0}^{\,d}\right) \;=\; \underline{\boldsymbol{b}}_{\,0}^{\,T}\underline{\boldsymbol{\theta}} \qquad \longleftrightarrow \qquad \lambda_{\,0} \\ \quad \underline{\boldsymbol{B}}_{\,d}\,\underline{\boldsymbol{A}}\,\underline{\boldsymbol{\theta}} \;\leq\; \underline{\boldsymbol{f}}^{\,max} \qquad \longleftrightarrow \qquad \underline{\boldsymbol{\rho}} \end{cases} . \tag{2.25}$$

The vectors and the scalar associated with the right-hand sides of the constraints are the dual variables for the corresponding constraints.

The DAM with the DRR players is settled based on the optimal solutions of $\mathscr{M}\left(\mathcal{S}, \widehat{\mathcal{B}}, \bar{\mathcal{B}}\right)$. The sales and the purchases of all the players are determined from the optimal values of the decision variables $\left[\, p^{\,s} \,\right]^*$, $\left[\, \hat{p}^{\,\hat{b}} \,\right]^*$, $\left[\, p^{\,b} \,\right]^*$ and $\left[\, p^{\,\hat{b}} \,\right]^*$. The optimum values of the dual variables associated with the nodal power balance constraints, $\left[\, \lambda_{\,n} \,\right]^*$, are the location marginal prices (LMPs) for each node $n \in \mathcal{N}$. Each player sells (buys) electricity at the LMP of the node where he is connected. The additional per unit charge, υ, for the buyers is given by

$$\upsilon \;=\; \frac{\sum_{n\,\in\,\mathcal{N}} \left[\, \lambda_{\,n} \,\right]^* \cdot \left[\, \hat{p}_{\,n}^{\,d} \,\right]^*}{\sum_{n\,\in\,\mathcal{N}} \left(\left[\, p_{\,n}^{\,d} \,\right]^* \;-\; \left[\, \hat{p}_{\,n}^{\,d} \,\right]^* \right)} \;, \tag{2.26}$$

where, $\left[\, \hat{p}_{\,n}^{\,d} \,\right]^*$ is the total cleared DRR curtailment at the node n and the quantity $\left(\left[\, p_{\,n}^{\,d} \,\right]^* \;-\; \left[\, \hat{p}_{\,n}^{\,d} \,\right]^* \right)$ is the net cleared demand at the node n. In effect, a buyer at the node n pays $\left(\left[\, \lambda_{\,n} \,\right]^* \;+\; \upsilon\right)$ \$/MWh for electricity. The congestion rents for

the DAM are given as

$$\kappa = \sum_{n \in \mathcal{N}} ([\,\lambda_n\,]^* + [\,\upsilon\,]^*) \cdot \left([\,p_n^d\,]^* - [\,\hat{p}_n^d\,]^* \right) - \sum_{n \in \mathcal{N}} [\,\lambda_n\,]^* \cdot [\,p_n^g\,]^* - \sum_{n \in \mathcal{N}} [\,\lambda_n\,]^* \cdot [\,\hat{p}_n^d\,]^* \quad (2.27)$$

The first summation gives the total payments by all the buyers, the second summation gives the the total revenues of all the supply-side sellers and the third summation gives the total compensation payments received by the DRR players. We use the LMPs and the sales/purchases of electricity to develop additional metrics such as the total supply-side revenues $w^{\mathcal{S}}$

$$w^{\mathcal{S}} = \sum_{n \in \mathcal{N}} [\,\lambda_n\,]^* \cdot [\,p_n^g\,]^* \ , \quad (2.28)$$

the total demand-side payments $w^{\mathcal{B}}$, taking into account the compensation received by the DRRs,

$$w^{\mathcal{B}} = \sum_{n \in \mathcal{N}} ([\,\lambda_n\,]^* + [\,\upsilon\,]^*) \cdot \left([\,p_n^d\,]^* - [\,\hat{p}_n^d\,]^* \right) - \sum_{n \in \mathcal{N}} [\,\lambda_n\,]^* \cdot [\,\hat{p}_n^d\,]^* \quad (2.29)$$

and the total cleared demand $[\,\ell\,]^*$,

$$[\,\ell\,]^* = \sum_{n \in \mathcal{N}} \left([\,p_n^d\,]^* - [\,\hat{p}_n^d\,]^* \right) . \quad (2.30)$$

The metrics listed above quantify the variable effects of the systems with DRRs. The metrics may be used to evaluate the benefits associated with integration of the DRRs into the power system. This may be accomplished by comparative assessments between scenarios with and without the deployment of the DRRs.

2.3 Impacts of DRRs over Longer-Term Periods

The extension of the analysis for a single subperiod to multiple subperiods over a longer term requires careful consideration of the impacts of DRR curtailments and the associated load recovery effects over the longer term. In this section, we discuss these issues.

The load curtailment by the successful DRR players in subperiod h may induce a deferred use of energy in the subsequent subperiods [11], [12]. The load recovery is typically a function of the weather, the economic conditions, the total number of subperiods for which the load demand is reduced and the amount of load reduced in each subperiod. We refer to the deferred energy due to the load recovery actions as the *load payback effect*. In this report, we assume that the load payback effects for each DRR player are exogenously specified.

The successful deployment of DRRs contributes to the redistribution of the demand and not necessarily to energy reduction, because the load curtailment subperiods may be followed by the load recovery subperiods. The resulting increase in the system demand is supplied by the system resources and this may result in additional costs during the demand recovery subperiods. The IGO deploys the DRRs in such a way as to ensure that the overall economics for all the subperiods in the scheduling horizon are optimized. The analysis of the impacts of DRRs on the outcomes of the DAMs associated with the K subperiods of a day requires the modeling of the electricity market for each subperiod k, where $k = 1, 2, \ldots, K$. In concept, we apply the market clearing problem formulation, $\mathscr{M}(\mathcal{S}, \widehat{\mathcal{B}}, \bar{\mathcal{B}})$, for each subperiod k. The deployment of DRRs may vary across different subperiods, because the IGO determines the outcomes of the K DAMs so that the system is operated in the most economic manner throughout the day.

Figure 2.8 illustrates the demand reduction in the peak load hours and the demand increase in the off-peak hours for a typical day, with hourly subperiods (so that $K = 24$).

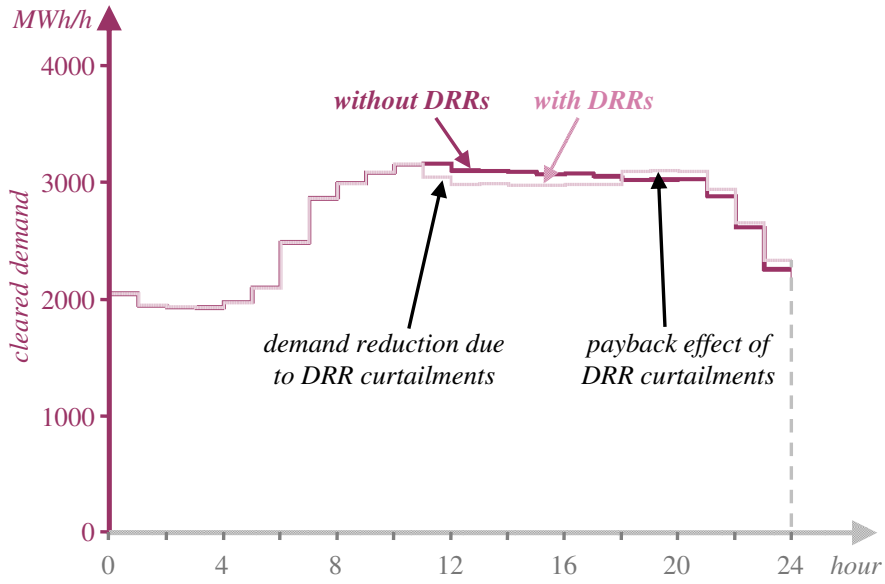

Figure 2.8: Impacts of the DRR curtailments on the cleared hourly demands for a typical day

Clearly, the maximum DRR curtailment in any subperiod is restricted by the total DRR curtailments offered in the subperiod. The DRR curtailment capacity offered in each of the K DAMs may be different. The DRR curtailment capacity offered by $\hat{b}$ in each of the K DAMs depends on the demand of $\hat{b}$ for the corresponding subperiods and the market rules of the IGO which may allow DRR participation in only a subset of the K subperiods. We assume that the capacity offered by the DRRs in the market is known *a priori*, and exogenously specified for each daily subperiod k, where $k = 1, 2, \ldots, K$.

In theory, the DRR deployment is most beneficial in those subperiods for which either the demand is high or the electricity prices are high. The deployment of the DRRs in such critical subperiods decreases the amount of dispatched generation, thereby reducing GHG emissions. When the prices are high, the DRR players

benefit from deferring the load consumption to those subperiods for which the prices are lower. The resulting reduction in the demand in the curtailment subperiods may induce lower prices in these subperiods, thereby benefitting all the buyers in the system. However, the load payback effects may lead to increased prices in the recovery subperiods, which may adversely impact the other buyers in the system. The procedure to analyze the DAMs corresponding to the subperiods of a single day may be extended to analyze DAMs over longer-term periods. In effect, the procedure outlined above is performed for each day in the period of interest. Figure 2.9 illustrates the impacts of DRRs over the days in a typical week.

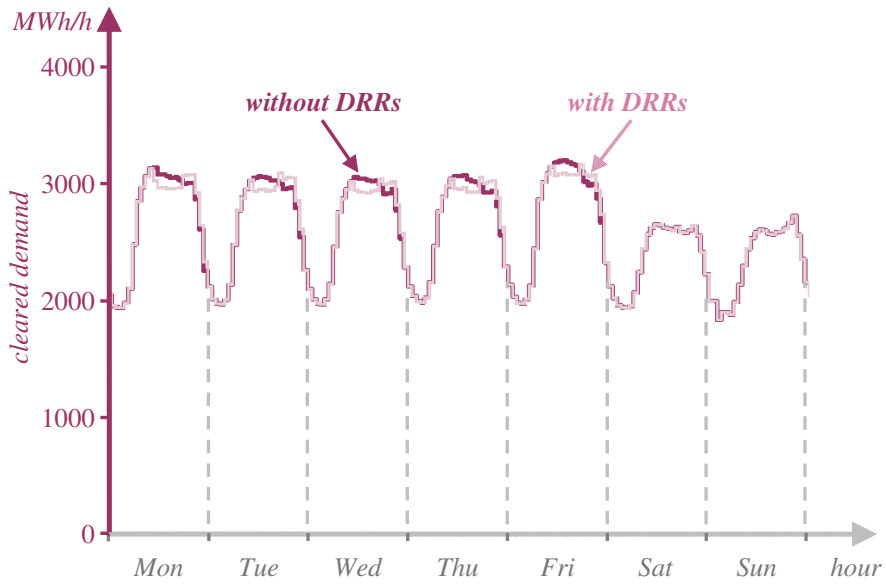

Figure 2.9: Impacts of the DRR curtailments on the cleared hourly demands for a typical week

We note that the DRR curtailment capacity offered in the subperiod k for a typical weekday and a typical weekend day may be different because the electricity consumption during the week is significantly different from the electricity consumption on the weekends. Hence, we specify the curtailment capacity offered by each DRR for each daily subperiod k, $k = 1, 2, \ldots, K$, for a typical weekday

and a typical weekend day.

2.4 Summary

In this chapter, we explicitly considered the impacts of DRRs on the market outcomes and the transmission usage. We discussed the extension of the existing models of electricity markets to incorporate DRR players as sellers as well as buyers in the market. We discussed the modifications to the problem formulation which represents the market clearing problem of the IGO to take into account the impacts of the DRR load curtailments. The analysis of the DAM model and the resulting market outcomes was used to develop metrics for the quantification of the variable effects for the systems with DRRs.

The participation of the demand-side buyers in the electricity markets as providers of load curtailment services results in additional degrees of freedom for the IGO, since the IGO now has control over more resources – the generation resources and the additional DRRs. The IGO uses these controllable resources to maintain reliable grid operations. The set of generators and DRRs serving the demand are chosen by the IGO so that the resulting dispatch is economically beneficial to the whole system. The problem formulation discussed in this chapter models the decision process of the IGO. Analysis of this problem formulation provides the metrics needed to quantify impacts of DRRs.

CHAPTER 3

DEVELOPMENT OF THE PROPOSED SIMULATION ENGINE

Probabilistic simulation realistically emulates the operations of the power system over longer periods of study. The availability of the generation resources, the demand, the fuel prices, the market outcomes, the transmission congestion and the nature of the policies in effect constitute examples of various sources of uncertainty. The effects of uncertainty need to be reflected in the simulation of the power system behavior over longer-term periods so as to appropriately evaluate the variable effects. The explicit representation of the uncertainty is a salient feature of the probabilistic simulation approach. Using this approach, we can evaluate the expected generation, the production costs and the emissions for each generation unit as well as the system, along with the reliability metrics and other figures of merit to obtain the entire set of variable effects of the system over a specified period of time. However, a major drawback of this approach is the inability to represent any time-dependent phenomenon such as the transmission network scheduling and the deployment of the DRRs. Hence, we modify the probabilistic simulation approach to accommodate the time-varying phenomena associated with the system with integrated DRRs.

In this chapter, we focus on the development of the simulation engine, which embodies the extended approach for simulating systems with DRRs with the various sources of uncertainty and the transmission congestion impacts explicitly taken into account. This chapter contains three sections. We review in Section 3.1 the basics of the probabilistic simulation approach. We discuss in Section

3.2 the modification to the probabilistic representation of the load to make it compatible with the representation of the DRRs. We present in Section 3.3 the proposed simulation engine which integrates the modified probabilistic simulation models with the time-dependent transmission-constrained market model described in Chapter 2 and allows the assessment of the variable effects for systems with DRRs.

3.1 Review of Probabilistic Simulation Basics

The probabilistic simulation approach is widely used to assess the behavior of a system over longer-term periods. In this section, we focus on the basics of the probabilistic simulation approach for the systems with dispatchable generation units.

The probabilistic production simulation is used to emulate the electricity system with the capability to mimic the operations of all the resources used to meet the demand. Such an emulation is performed over a specified simulation period. The simulation period is defined in such a way that there are no changes to the system in terms of additions/retirements in the resource mix, variations in the resource characteristics, investment decisions, the maintenance of the resources, the changes in the policy and the seasonality effects. The specific assumptions for the simulation period include the following:

A1. Any change in the policy environment due to regulatory or legislative initiatives persists for the entire duration of the simulation period.

A2. The seasonal effects do not vary during the simulation period.

A3. Any modification to the resource mix due to resource investment, equipment upgrade or unit retirement takes place at the beginning of the simulation

period and remains intact over that period.

A4. The operating characteristics of the generation units remain unchanged during a simulation period. Further, each unit has uniform characteristics during the period.

A5. Each generator unit is independent of every other unit and of the system load.

A6. The impacts of the unit commitment decisions for the simulation period are incorporated into the specified loading list of the generation units arranged in the order of increasing marginal costs/prices.

A7. Only those generation units not on planned maintenance may be scheduled for generation in the given simulation period.

A8. The system load exhibits uniform characteristics during the simulation period.

A9. The transmission network has adequate capability to accommodate the economic operation of the units without imposing any constraints during the entire simulation period.

The subperiod is the smallest indecomposable unit of time and therefore determines the time resolution for the study. The subperiods allow the representation of the short term changes including variations in the demand and the availability of the supply resources used to meet the demand. The power system is assumed to be in steady-state during each subperiod of the simulation period. Phenomena of duration shorter than that of a subperiod cannot be represented and are ignored in the simulation. A simulation period consists of all of the subperiods over its duration. We assume the simulation period consists of a finite number of

subperiods, and we denote by H the number of subperiods. Then the set,

$$\mathcal{H} \triangleq \{h : h = 1, \ldots, H\} ,$$

denotes the collection of the indices of the subperiods in the simulation period. In Fig. 3.1, we illustrate the partitioning of the simulation period into subperiods.

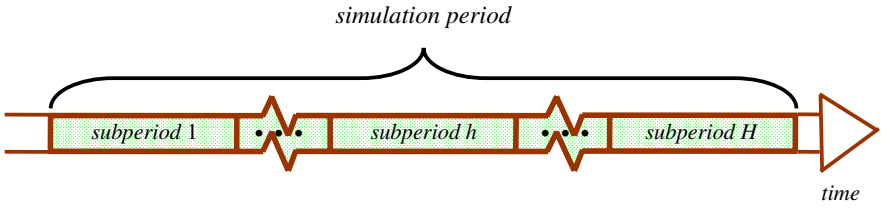

Figure 3.1: The partitioning of the simulation period into subperiods

We start with the modeling of the load for the simulation period. We model the load as the sum of all the individual demands and refer to the sum as the *system load*. Statistical regularity is obtained by summing over a large number of the individual random demands. The specification of the system load during the simulation period is required to evaluate the demand shape and quantity, and to determine the subset of units which need to be operational and their operating levels. The chronological load curve displays the value taken by the system load at each subperiod in the simulation period. The chronological load provides information on the total energy demand for the simulation period, the peak load value ℓ^p, the base load value ℓ^b, along with the temporal information, such as weekday load versus weekend load, and displays all the inter-temporal effects. We use the chronological load to construct the probabilistic representation of the load for the simulation period. We view the load as a random variable (rv), $\underset{\sim}{L}$, that takes the sample values of the chronological load with one sample for each of the H subperiods. To determine the distribution of $\underset{\sim}{L}$, we first construct the *load duration*

curve (LDC) by rearranging the chronological loads in the order of decreasing values starting at the peak load value and ending with the base load value. The reordering of the load values results in the loss of all the temporal information and the intertemporal effects. However, the LDC still retains information on the total energy demand, the peak load value and the base load. In Fig. 3.2, we illustrate the chronological load curve and reordered LDC for a typical week period with an hourly resolution.

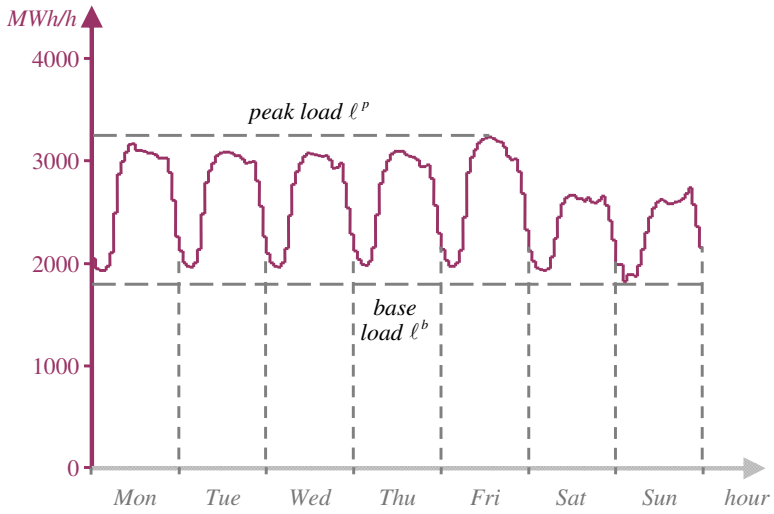

(a) chronological load curve

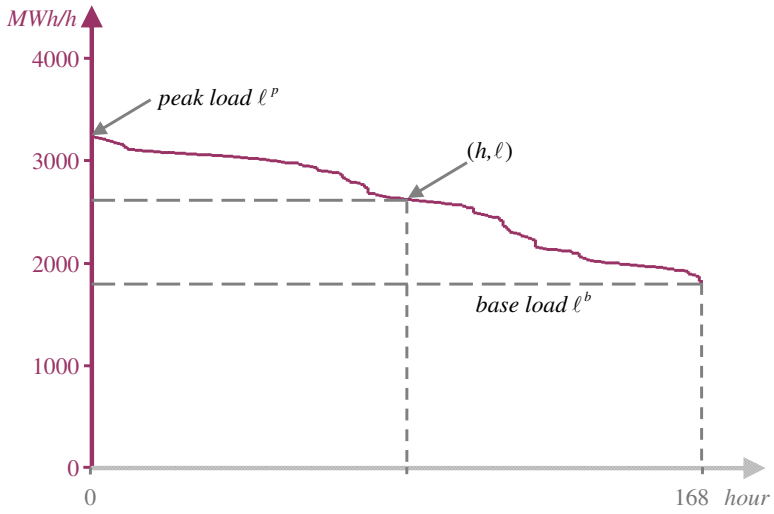

(b) load duration curve

Figure 3.2: Chronological load curve and LDC for a week

A point (h, ℓ) on the LDC may be interpreted as indicating that for h subperiods, the load exceeds ℓ. In other words, the point (h, ℓ) provides an indication that of the H subperiods in the simulation period, the event $\left\{\underset{\sim}{L} > \ell\right\}$ occurs over h subperiods. By normalizing the time, the fraction h/H may be viewed as an estimate of the probability of the event $\left\{\underset{\sim}{L} > \ell\right\}$. We use the probability interpretation to construct the distribution function of $\underset{\sim}{L}$. The normalization of the time axis results in the loads occurring in the interval $[0, 1]$. We flip and invert the LDC to obtain the so-called inverted LDC, which we denote by $\mathscr{L}(\cdot)$. The curve $\mathscr{L}(\cdot)$ is derived from the LDC by normalizing the horizontal axis of the LDC, inverting the curve and rotating through a 90° clockwise angle. Clearly, for a specified value ℓ of the load, the curve $\mathscr{L}(\cdot)$ provides the value of the probability that $\underset{\sim}{L} > \ell$ for the simulation period, i.e.,

$$\begin{aligned} \mathscr{L}(\ell) &= \mathbb{P}\left\{\underset{\sim}{L} > \ell\right\} \\ &= 1 - \mathbb{P}\left\{\underset{\sim}{L} \leq \ell\right\} \\ &= 1 - \mathbb{F}_{\underset{\sim}{L}}(\ell) \ . \end{aligned} \tag{3.1}$$

Indeed, the inverted LDC is the complement of the cumulative distribution function (cdf) of the rv $\underset{\sim}{L}$.

Next, we consider the modeling of the generation units in the resource mix. The probabilistic simulation approach requires the definition and the description of the entire set of supply-side resources used to meet the energy demand for the simulation period. The resources are described in terms of their individual characteristics, which include

- operational characteristics such as efficiency,
- availability in terms of planned maintenance outages (scheduling and dura-

tion) as well as forced outages (forced outage rate or FOR)

- constraints such as limitations on the energy or fuel

To simplify the explanation, we assume that each unit in the resource mix is controllable/dispatchable. We use the set $\mathcal{I}$ to represent the loading list of controllable generation units for the simulation period. The units out for planned maintenance are not included. Let I be the total number of controllable units. To ease the discussion, we present the case where each unit is loaded as a single block, so that $|\mathcal{I}| = I$. Each controllable unit has its output level set by the system operator, but the output is a function of the *available capacity* of the unit. The available capacity of a unit is the capacity that is used to provide service, taking into account random generator outages that may befall the unit. We model the available capacity of a unit $i \in \mathcal{I}$ by a discrete rv $\underset{\sim}{A}^i$ to represent the multi-states capacities with which the unit may be dispatched. The cdf of $\underset{\sim}{A}^i$, denoted by $\mathbb{F}_{\underset{\sim}{A}^i}(\cdot)$, may be determined from the historical operating data. For probabilistic simulation, we use the outage capacity rv of the unit i, which is given by

$$\underset{\sim}{Z}^i \triangleq c^i - \underset{\sim}{A}^i , \tag{3.2}$$

where, c^i is the capacity of the unit i.

The generation units are loaded in the order specified in the loading list constructed to reflect actual power system operations. The unit economics may be expressed in terms of marginal cost information or in terms of the prices for which the blocks of energy are offered for each unit. In this report, we use the price information to describe the unit economics, since true costs constitute private information and may not be available. The units with the lowest prices are loaded ahead of those with the higher prices to reflect the objective of efficient production costs.

The probabilistic simulation makes use of the notion of equivalent load. The equivalent load is viewed as the load that must be served by the units that are yet to be loaded. We define the equivalent load of the system after loading up to unit i to be

$$\underset{\sim}{L}^{\,i} \;=\; \underset{\sim}{L}^{\,i-1} + \underset{\sim}{Z}^{\,i}\,, \tag{3.3}$$

where, $\underset{\sim}{L}^{\,i-1}$ is the equivalent load after the first $i-1$ units have been loaded. Consequently, we have

$$\underset{\sim}{L}^{\,0} \;=\; \underset{\sim}{L}\,, \tag{3.4}$$

since $\underset{\sim}{L}^{\,0}$ denotes the equivalent load before loading the generation units and is therefore equal to the system load, $\underset{\sim}{L}$. We iteratively evaluate Equation (3.3) and compute $\mathscr{L}^{\,i}(\cdot)$ until all I units are loaded. The computation is carried out in terms of the inverted LDCs; we successively compute $\mathscr{L}^{\,i}(\cdot)$ as the complement of the cdf of the equivalent load rv $\underset{\sim}{L}^{\,i}$. We make use of the statistical independence assumption **A5** to apply convolution techniques to evaluate the cdf of $\underset{\sim}{L}^{\,i}$ using the Equation (3.3). We make use of $\mathscr{L}^{\,i-1}(\cdot)$ to compute the expected generation $\mathcal{E}^{\,i}$ and the expected generation costs $\mathcal{C}^{\,i}$ for the unit i [40]. The capacity factor of each unit i is evaluated as

$$CF^{\,i} \;=\; \frac{\mathcal{E}^{\,i}}{c^{\,i}\cdot H}\,, \tag{3.5}$$

where, the denominator signifies the maximum energy production of the unit i over the simulation period. We make use of the notion of equivalent load to evaluate reliability metrics such as the *loss of load probability* (LOLP) and *expected unserved energy* (EUE). The inverted LDC $\mathscr{L}^{\,I}(\cdot)$ corresponds to the equivalent

load rv $\underset{\sim}{L}^{I}$ after all the I units have been loaded and, consequently, provides the complement of the cdf of the load that remains unserved. Since we interpret the LOLP as the probability that the load remains unserved after all the units are loaded, we have

$$LOLP \;=\; \mathscr{L}^{I}\left(C^{I}\right)\;, \tag{3.6}$$

where

$$C^{I} \;=\; \sum_{i=1}^{I} c^{i}\;.$$

Similarly, we use $\mathscr{L}^{I}(\cdot)$ to compute the EUE $\mathcal{U}$,

$$\mathcal{U} \;=\; H\int_{C^{I}}^{\infty} \mathscr{L}^{I}(\ell)\,d\ell\;. \tag{3.7}$$

The probabilistic simulation emulates the energy production of each unit in the loading list. In actual production costing, the units may be loaded in blocks to reflect the economics of generation or the resource mix may contain limited energy plants and/or storage devices. The modeling and simulation approach for such systems is discussed in references [36], [40] and [41].

3.2 Extension of Probabilistic Simulation Approach for Systems with DRRs

The deployment of DRRs is a time-dependent phenomenon. In typical ISO/RTO jurisdictions, the prescriptive language of the market rules allows DRR participation only during certain hours of the day [3, 4]. Typical DRR deployment is associated with the critical peak hours of the weekdays, as discussed in Chapter 2.

The usual probabilistic simulation approach is useful for simulating system behavior in a time-abstracted manner; however, this approach is inadequate for the simulation of systems with DRRs. Primary reasons for this inadequacy are:

- the lack of temporal information in the load representation as expressed by the rv $\underset{\sim}{L}$
- the inability to incorporate the impacts of the transmission–constrained market outcomes

The principal challenge in extending the probabilistic simulation approach for the systems with DRRs is to mesh the time-abstracted framework of the probabilistic simulation with the time-dependent framework of the transmission-constrained markets which include DRRs as active participants. Several key "synchronization" steps are needed to develop the desired simulation engine. In this section, we present the initial step in this synchronization process. This entails the modifications to the probabilistic load representation to incorporate the temporal effects.

As explained in Chapter 2, the IGO runs K DAMs corresponding to the K subperiods for each day in the simulation period. The DRR capacity offered in each of the K DAMs may be different. We assume that the capacity offered by the DRRs in the market is known *a priori*, and exogenously specified on a subperiodic basis for each daily subperiod k, where $k = 1, 2, \ldots, K$ for a typical weekday and a typical weekend day. The diurnal representation of the DRR capacity offers needs to be directly related to the random load that must be met. However, the load, as expressed by $\underset{\sim}{L}$, does not provide any temporal information. To mesh the two models, we modify the load representation and obtain the load representation for each daily subperiod for a typical weekend and weekday.

We start with the chronological load data which gives the sample space for the load rv $\underset{\sim}{L}$ for the entire simulation period. The sample space for the load is

given by

$$\Omega \triangleq \{\ell_1, \ell_2, \ldots, \ell_H\} \ ,$$

where, the load values are arranged in the chronological order and ℓ_h indicates the value taken by the load in the subperiod h of the period. Thus, the sample space consists of load sample values observed during all H subperiods of the simulation period. Let D be the total number of days in the period, so that $D \cdot K = H$. The load values in the sample space Ω can be classified according to days so that we obtain D non-overlapping subsets, with the subset for each day d consisting of the K load values observed in the K daily subperiods. Conceptually, we may view the sample space as a matrix with D rows and K columns. The value of the load in the d^{th} row and k^{th} column, $\ell_{K\star(d-1)+k}$, indicates the value taken by the load in the subperiod k of the day d. Each column k corresponding to the daily subperiods $k = 1, 2, \ldots, K$ may be viewed as the sample space $\Omega_{(k)}$ of the rv corresponding to the daily subperiod k, denoted by $\underset{\sim}{L}_{(k)}$. The distribution of $\underset{\sim}{L}_{(k)}$ is the distribution of $\underset{\sim}{L}$ conditioned on the event that the load is observed during the k^{th} subperiod of the day and the distribution of $\underset{\sim}{L}_{(k)}$ may be estimated from the D load samples in column k which constitute the subset $\Omega_{(k)}$. We use the load samples in the column k to construct the LDC for each daily subperiod k; the LDC provides a complement of the cdf of $\underset{\sim}{L}_{(k)}$. The distributions of $\underset{\sim}{L}_{(k)}$ obtained from the LDCs for $k = 1, 2, \ldots, K$, which are in fact the conditional distributions of $\underset{\sim}{L}$, allow us to restate the probability of the event $\left\{\underset{\sim}{L} \leq \ell\right\}$ in terms of the conditional distributions, as shown here:

$$\begin{aligned} \mathbb{P}\left\{\underset{\sim}{L} \leq \ell\right\} \ &= \ \mathbb{P}\left\{\underset{\sim}{L} \leq \ell \ \ \textit{in all subperiods } h \textit{ in the period}\right\} \\ = \ \sum_{k=1}^{K} \mathbb{P}\left\{\underset{\sim}{L} \leq \ell \ , \ \textit{subperiod } h \textit{ is the } k^{\text{th}} \textit{ subperiod of the day}\right\} \end{aligned}$$

$$= \sum_{k=1}^{K} \mathbb{P}\left\{ \underset{\sim}{L} \leq \ell \mid \textit{subperiod } h \textit{ is the } k^{\text{th}} \textit{ subperiod of the day} \right\} \times$$
$$\mathbb{P}\left\{ \textit{subperiod } h \textit{ is the } k^{\text{th}} \textit{ subperiod of the day} \right\}$$
$$= \sum_{k=1}^{K} \mathbb{P}\left\{ \underset{\sim}{L}_{(k)} \leq \ell \right\} \cdot \frac{1}{K} \; . \tag{3.8}$$

In Equation (3.8), we make use of the fact that the distribution of $\underset{\sim}{L}$ conditioned on the event that the subperiod h is the k^{th} subperiod of the day is the distribution of the rv $\underset{\sim}{L}_{(k)}$ for $k = 1, 2, \ldots, K$ and that each daily subperiod k has equal probability of occurrence in the simulation period, given by $\frac{1}{K}$. In Fig. 3.3, we provide a graphical representation of the conditioning of the load samples and the construction of the distributions of the load rv's $\underset{\sim}{L}_{(k)}$s corresponding to the K subperiods of a typical day. The load conditioning scheme described here is sufficiently general to be applied to any chronological load data set. The resulting characterizations of the rv's $\underset{\sim}{L}_{(k)}$s provides a diurnal representation of the load for the K subperiods of a typical day.

Since the DRR capacity is specified for K subperiods of a typical weekday and a typical weekend, the diurnal load representation needs to be further extended so as to be compatible with the representation of the DRR capacities. We start with the assumption that the simulation period consists of $\dot{D}$ weekdays and $\ddot{D}$ weekend days, so that

$$\dot{D} \; + \; \ddot{D} \; = \; D \; .$$

The diurnal representation of the load was obtained by visualizing the sample space as a $D \times K$ matrix. Now, we extract the rows corresponding to the $\dot{D}$ weekdays from this $D \times K$ matrix of sample load values to construct a matrix with $\dot{D}$ rows and K columns. This $\dot{D} \times K$ matrix corresponds to a subset, $\dot{\Omega}$, of the sample space Ω. We view $\dot{\Omega}$ as the sample space of the load observed in the

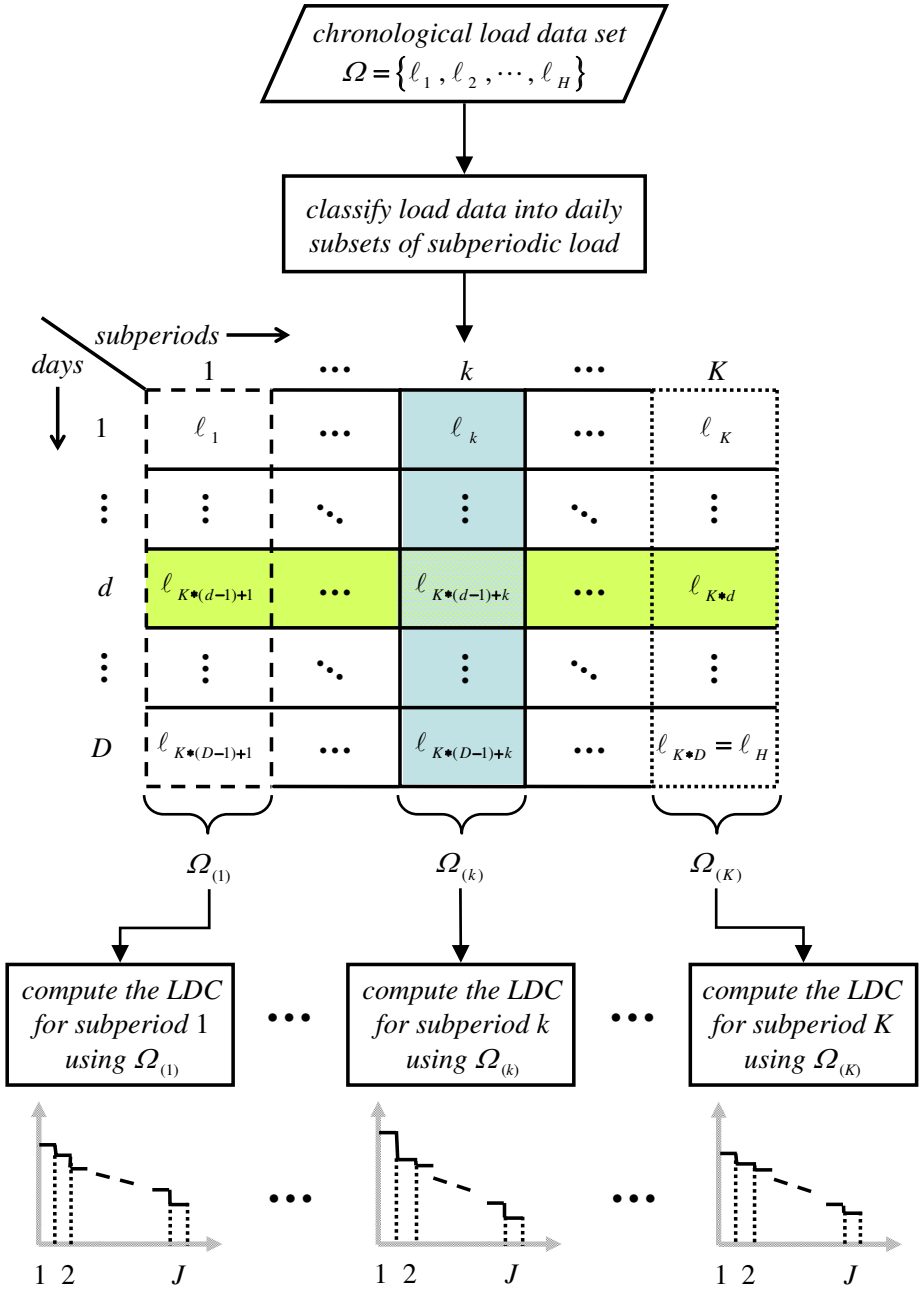

Figure 3.3: The load conditioning scheme to obtain the diurnal representation of the load

all weekday subperiods in the simulation period. We denote by the rv $\dot{\underset{\sim}{L}}$ the load for the weekday subperiods and use load samples from the subset $\dot{\Omega}$ to develop the distribution of the rv $\dot{\underset{\sim}{L}}$. Clearly, the distribution of the rv $\dot{\underset{\sim}{L}}$ is the distribution

of the load rv $\underset{\sim}{L}$ conditioned on the event that the load is observed in a weekday subperiod. Analogously, we may construct the sample space $\ddot{\Omega} \subset \Omega$ corresponding to the load observed in all the weekend subperiods in the simulation period and use $\ddot{\Omega}$ to develop the distribution of the load $\ddot{\underset{\sim}{L}}$ for the weekend subperiods. Again the distribution of the rv $\ddot{\underset{\sim}{L}}$ is the distribution of the load rv $\underset{\sim}{L}$ conditioned on the event that the load is observed in a weekend subperiod. We note that $\dot{\Omega}$ and $\ddot{\Omega}$ are non-overlapping subsets of the sample space Ω. This allows us to restate the cdf of $\underset{\sim}{L}$ in terms of the conditional distributions corresponding to the rv's $\dot{\underset{\sim}{L}}$ and $\ddot{\underset{\sim}{L}}$, as expressed below:

$$
\begin{aligned}
& \mathbb{P}\left\{\underset{\sim}{L} \le \ell\right\} \;=\; \mathbb{P}\left\{\underset{\sim}{L} \le \ell \;\; \textit{in all subperiods } h \textit{ in the period}\right\} \\
= \;& \mathbb{P}\left\{\underset{\sim}{L} \le \ell \;,\; \textit{subperiod } h \textit{ is a weekday subperiod}\right\} \;+ \\
& \mathbb{P}\left\{\underset{\sim}{L} \le \ell \;,\; \textit{subperiod } h \textit{ is a weekend subperiod}\right\} \\
= \;& \mathbb{P}\left\{\underset{\sim}{L} \le \ell \mid \textit{subperiod } h \textit{ is a weekday subperiod}\right\} \cdot \mathbb{P}\left\{\textit{weekdays}\right\} \;+ \\
& \mathbb{P}\left\{\underset{\sim}{L} \le \ell \mid \textit{subperiod } h \textit{ is a weekend subperiod}\right\} \cdot \mathbb{P}\left\{\textit{weekends}\right\} \\
= \;& \mathbb{P}\left\{\dot{\underset{\sim}{L}} \le \ell\right\} \cdot \frac{\dot{D}}{D} \;+\; \mathbb{P}\left\{\ddot{\underset{\sim}{L}} \le \ell\right\} \cdot \frac{\ddot{D}}{D} \;. \qquad (3.9)
\end{aligned}
$$

In Equation (3.9), we make use of the fact that the probability that a subperiod is a weekday (weekend) subperiod depends on the number of weekdays (weekend days). Next, we employ the load conditioning scheme of Fig. 3.3 on the weekday load sample space, $\dot{\Omega}$. Each column k of the $\dot{D} \times K$ weekday load matrix is viewed as the sample space of the rv $\dot{\underset{\sim}{L}}_{(k)}$, corresponding to the weekday subperiod k, for $k = 1, 2, \ldots, K$. In concept, the scheme illustrated in Fig. 3.3 is applied to the $\dot{D} \times K$ matrix of the weekday load sample space. Then, the cdf of the weekday

load rv $\dot{\underset{\sim}{L}}$ may be restated as

$$\mathbb{P}\left\{\dot{\underset{\sim}{L}} \leq \ell\right\} \;=\; \frac{1}{K}\sum_{k=1}^{K}\mathbb{P}\left\{\dot{\underset{\sim}{L}}_{(k)} \leq \ell\right\} \;. \tag{3.10}$$

Note that Equation (3.10) may be derived using the same logical development as the one employed to formulate Equation (3.8). Next, we perform the load conditioning on the weekend load set $\ddot{\Omega}$, to obtain the conditional distributions of the weekend subperiodic load, $\ddot{\underset{\sim}{L}}_{(k)}$ for $k = 1, 2, \ldots, K$, so that the cdf of the weekend load rv $\ddot{\underset{\sim}{L}}$ may be restated as

$$\mathbb{P}\left\{\ddot{\underset{\sim}{L}} \leq \ell\right\} \;=\; \frac{1}{K}\sum_{k=1}^{K}\mathbb{P}\left\{\ddot{\underset{\sim}{L}}_{(k)} \leq \ell\right\} \;. \tag{3.11}$$

Then, using Equations (3.10) and (3.11) in the Equation (3.9), we obtain the cdf of the load $\underset{\sim}{L}$ in terms of the cdf's of the weekday subperiodic loads, $\dot{\underset{\sim}{L}}_{(k)}$ s, and weekend subperiod loads, $\ddot{\underset{\sim}{L}}_{(k)}$ s,

$$\mathbb{F}_{\underset{\sim}{L}}(\ell) \;=\; \frac{\dot{D}}{D}\cdot\frac{1}{K}\sum_{k=1}^{K}\mathbb{P}\left\{\dot{\underset{\sim}{L}}_{(k)} \leq \ell\right\} \;+\; \frac{\ddot{D}}{D}\cdot\frac{1}{K}\sum_{k=1}^{K}\mathbb{P}\left\{\ddot{\underset{\sim}{L}}_{(k)} \leq \ell\right\} \;. \tag{3.12}$$

Consequently, the inverted LDC may be expressed as

$$\mathscr{L}(\ell) \;=\; 1 - \left[\frac{\dot{D}}{D}\cdot\frac{1}{K}\sum_{k=1}^{K}\mathbb{P}\left\{\dot{\underset{\sim}{L}}_{(k)} \leq \ell\right\} + \frac{\ddot{D}}{D}\cdot\frac{1}{K}\sum_{k=1}^{K}\mathbb{P}\left\{\ddot{\underset{\sim}{L}}_{(k)} \leq \ell\right\}\right] \;. \tag{3.13}$$

In Fig. 3.4, we illustrate the conceptual approach to obtain the representations of the load for the K subperiods for a typical weekday and K subperiods for a typical weekend day. We refer to this scheme as the subperiodic load conditioning scheme. The classification of the chronological load data and the resulting conditional distributions for weekday and weekend subperiods are compatible with

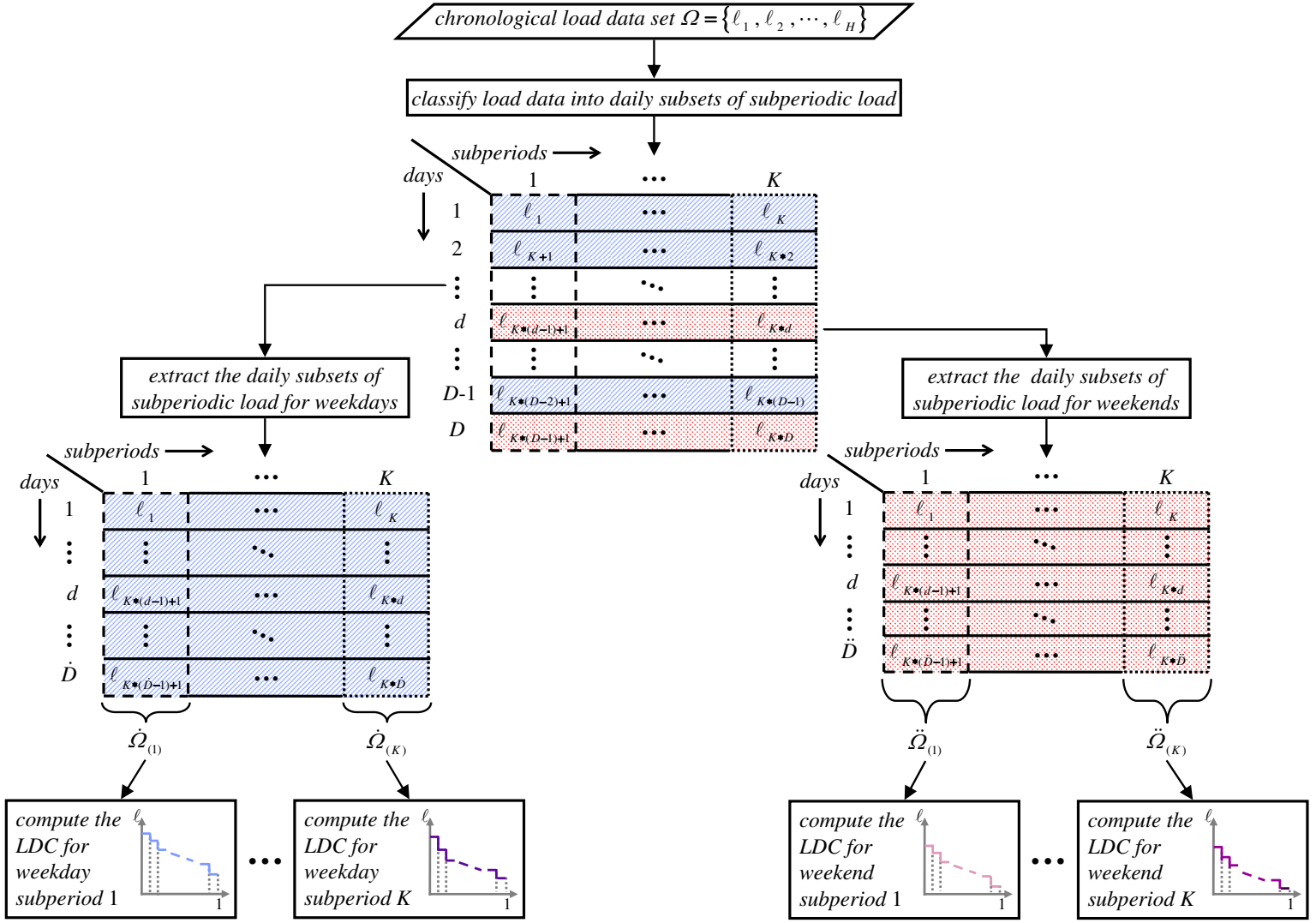

Figure 3.4: The subperiodic conditioning of the load samples to obtain the load rv's for weekday and weekend subperiods

the diurnal representation of the capacities offered by the DRRs for the typical weekday and weekend subperiods. We note that the assumption that available capacities of the generator units are independent of the subperiod, i.e., the assumption **A5** introduced in Section 3.1, holds true even for the generation units in the systems with DRRs. Assumption **A8** no longer holds. Consequently, we use the same model for the generation available capacity as the one presented in Section 3.1.

3.3 The Proposed Simulation Engine

The typical probabilistic simulation studies assume that all available capacity is dispatchable. However, this may not be true, especially in situations where the transmission constraints are binding, i.e., assumption **A9** no longer holds. In the competitive environment, the amount of capacity dispatched for a generator depends on the available generation capacity, the feasibility of the transaction with respect to the network constraints and the competitiveness of the generator in the DAM. Hence, it is important to consider both the resource availability represented by the probabilistic models, as well as the outcomes of the transmission-constrained markets to assess the variable effects for the power systems. The uncertainty associated with the load, the availability of the generation units for producing energy and the forced outages of the transmission lines effectively propagates to the outcomes of the transmission-constrained markets. In this section, we discuss the next step in the synchronization of the probabilistic simulation framework with the time-dependent market framework. The extended simulation approach integrating the two frameworks is used by the simulation engine to emulate the operations of the system and the market over a specified time period.

As explained in Chapter 2, we may conceptually represent the process for

the market clearing of the DAM by the problem formulation $\mathcal{M}(\mathcal{S}, \widehat{\mathcal{B}}, \hat{\mathcal{B}})$, where $\mathcal{S}$ denotes the set of supply-side sellers, $\widehat{\mathcal{B}}$ denotes the set of DRR players who participate in the DAM as sellers-cum-buyers and $\bar{\mathcal{B}}$ denotes the set of pure buyers. The problem $\mathcal{M}(\mathcal{S}, \widehat{\mathcal{B}}, \bar{\mathcal{B}})$ stated in Equation (2.25) represents the decision process of the IGO for integrated market and network operations. The DAM is settled on the basis of the solutions of $\mathcal{M}(\mathcal{S}, \widehat{\mathcal{B}}, \bar{\mathcal{B}})$, which determine the LMPs and the allocations to all the sellers and buyers based on the offers and bids submitted by the players.

The key thrust in the development of the extended simulation approach is to integrate the probabilistic representations of the load and the available generation capacity with the transmission-constrained market model. We simplify the modeling needs by assuming that the load demand of all the buyers is a pre-specified fraction of the system load. Further, we assume that the buyers submit *fixed* demand bids[1] – a fixed demand bid is a special case of the price sensitive bid in which the requested MWh quantity is submitted with no price information; such a bid indicates an unlimited willingness to pay for the electricity purchases to meet the fixed quantity bid. However, there are difficulties in determining the appropriate value of the benefits associated with the fixed demand buyers. We resolve this issue by using a high, constant, per MWh benefit value, γ, to evaluate the benefits associated with the fixed demand bids for the problem formulation $\mathcal{M}(\mathcal{S}, \widehat{\mathcal{B}}, \bar{\mathcal{B}})$.

Next, we assume, without loss of generality, that each generator unit $i \in \mathcal{I}$ corresponds to a single seller $s \in \mathcal{S}$. Then, the capacity offered by the unit i in the DAM for a subperiod h of the simulation period is a realization of the available generation capacity $\underset{\sim}{A}^{i}$, denoted by α^{i}. We assume that the offer function for

[1]This assumption is consistent with typical probabilistic simulation studies for reliability analysis and production costing.

the generator i is given by $\mathscr{C}^{\,i}(\cdot)$. The generation of the unit i depends on the outcomes of the DAM.

Now, the system demand and the availability of the generation for a specified subperiod h of the simulation period are viewed as rv's and these drive the bids and the offers submitted to the DAM. Hence, in concept, the bids and the offers submitted to the DAM are uncertain. Consequently, the outcomes of the DAM are uncertain and viewed as rv's. We use the following notation for rv's representing the outcomes of DAM for all the subperiods in the simulation period:

$\underset{\sim}{P}^{\,i}$ - energy sold by the unit i

$\underset{\sim}{P}^{\,\bar{b}}$ - demand of the pure buyer $\bar{b}$

$\underset{\sim}{P}^{\,\hat{b}}$ - demand of the DRR $\hat{b}$, without the demand curtailment

$\underset{\sim}{\hat{P}}^{\,\hat{b}}$ - demand curtailment by the DRR $\hat{b}$

$\underset{\sim}{\Lambda}_{\,n}$ - LMP at the node n

$\underset{\sim}{\mathcal{K}}$ - congestion rents

In Fig. 3.5, we conceptually illustrate the propagation of uncertainty from the inputs of the DAM to the outcomes of the DAM. It is evident that the procedure for characterizing the market outcome rv's. relies on transitions from the probability domain to the time domain and back from the time domain to the probability domain.

Since the buyer demands are fixed, the system load without the DRR curtailments is given by

$$\underset{\sim}{L} \;=\; \sum_{\bar{b}\,\in\,\bar{\mathcal{B}}} \underset{\sim}{P}^{\,\bar{b}} \;+\; \sum_{\hat{b}\,\in\,\hat{\mathcal{B}}} \underset{\sim}{P}^{\,\hat{b}}\;. \tag{3.14}$$

Whenever a curtailment offer by a DRR player is successful, the system load is reduced. Therefore, at any time, the generator units need to serve the load which remains after taking into account the DRR curtailments. We refer to this load as

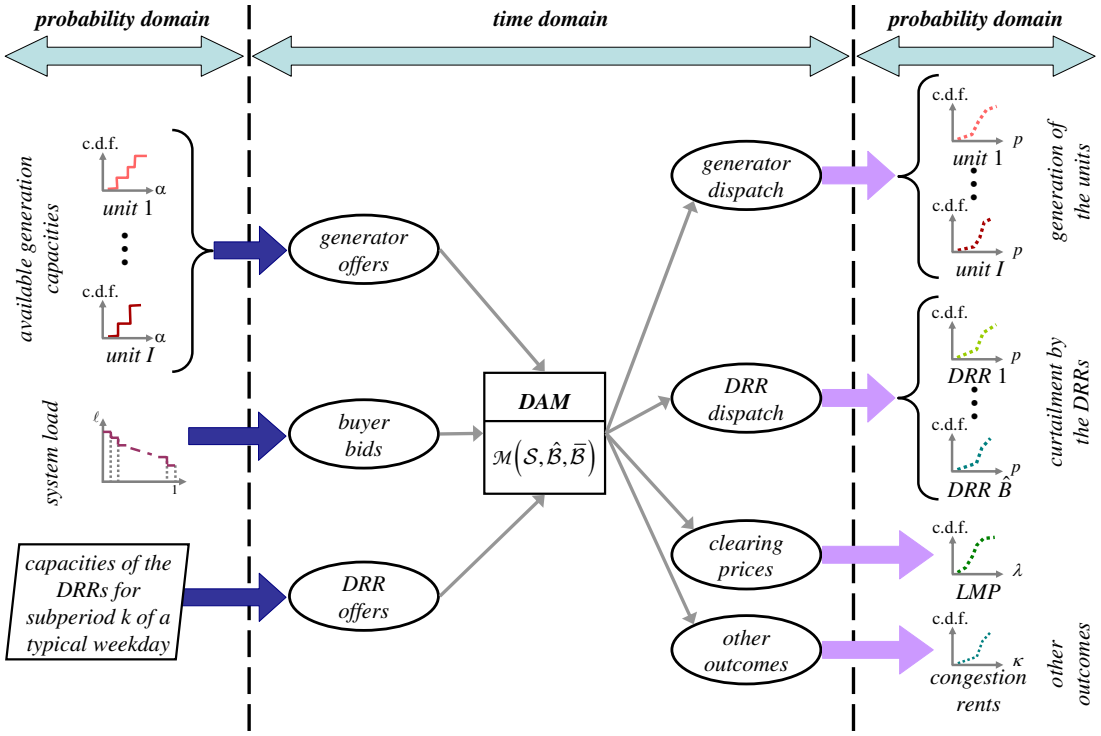

Figure 3.5: The propagation of uncertainty from the inputs of the transmission-constrained markets to the market outcomes

the "net" load; we model it by the rv $\underset{\sim}{L}^{g}$ and by definition, we have

$$\underset{\sim}{L}^{g} \;=\; \underset{\sim}{L} \;-\; \sum_{\hat{b}\,\in\,\hat{\mathcal{B}}} \underset{\sim}{\hat{P}}^{\hat{b}}\,, \tag{3.15}$$

where, the summation represents the total demand curtailment by the DRRs based on the outcomes of the DAM. A key requirement to run a production simulation with the DRRs is to probabilistically characterize the net load for the simulation period. As discussed in the previous section, we employ a diurnal subperiodic representation of the load and the DRR capacity for a typical day during the week and a typical day during the weekend. The actual curtailment by the DRRs is dependent on the outcomes of the DAM. Correspondingly, we define the following rv's:

$\dot{\underset{\sim}{P}}^{\hat{b}}_{(k)}$ - demand curtailment by DRR $\hat{b}$ during the k^{th} weekday subperiod

$\ddot{\underset{\sim}{P}}^{\hat{b}}_{(k)}$ - demand curtailment by DRR $\hat{b}$ during the k^{th} weekend subperiod

Then, we define the rv $\dot{\underset{\sim}{L}}^{g}_{(k)}$ to represent the net load for the subperiod k of a typical weekday so that

$$\dot{\underset{\sim}{L}}^{g}_{(k)} \;=\; \dot{\underset{\sim}{L}}_{(k)} \;-\; \sum_{\hat{b}\,\in\,\widehat{\mathcal{B}}} \dot{\underset{\sim}{P}}^{\hat{b}}_{(k)} \;, \tag{3.16}$$

where, $\dot{\underset{\sim}{L}}_{(k)}$ is the load demand for in the k^{th} weekday subperiod. Similarly, we define the rv $\ddot{\underset{\sim}{L}}^{g}_{(k)}$ to represent the net load for the subperiod k of a typical weekend so that

$$\ddot{\underset{\sim}{L}}^{g}_{(k)} \;=\; \ddot{\underset{\sim}{L}}_{(k)} \;-\; \sum_{\hat{b}\,\in\,\widehat{\mathcal{B}}} \ddot{\underset{\sim}{P}}^{\hat{b}}_{(k)} \;, \tag{3.17}$$

where, $\ddot{\underset{\sim}{L}}_{(k)}$ is the load demand for in the k^{th} weekend subperiod. Since the weekday subperiodic net loads, $\dot{\underset{\sim}{L}}^{g}_{(k)}$ s, and the weekend subperiodic net loads, $\ddot{\underset{\sim}{L}}^{g}_{(k)}$s, are conditional distributions of the net load rv $\underset{\sim}{L}^{g}$ for the simulation period, we use them to evaluate the cdf of $\underset{\sim}{L}^{g}$. We have

$$\begin{aligned}
&\mathbb{F}_{\underset{\sim}{L}^{g}}(\ell) \;=\; \mathbb{P}\left\{\underset{\sim}{L}^{g} \le \ell \;\; \textit{in all subperiods } h \textit{ in the period}\right\} \\
=\;& \mathbb{P}\left\{\underset{\sim}{L}^{g} \le \ell \;,\; \textit{subperiod } h \textit{ is a weekday subperiod}\right\} \;+ \\
&\mathbb{P}\left\{\underset{\sim}{L}^{g} \le \ell \;,\; \textit{subperiod } h \textit{ is a weekend subperiod}\right\} \\
=\;& \mathbb{P}\left\{\underset{\sim}{L}^{g} \le \ell \mid \textit{subperiod } h \textit{ is a weekday subperiod}\right\} \cdot \mathbb{P}\left\{\textit{weekdays}\right\} \;+ \\
&\mathbb{P}\left\{\underset{\sim}{L}^{g} \le \ell \mid \textit{subperiod } h \textit{ is a weekend subperiod}\right\} \cdot \mathbb{P}\left\{\textit{weekends}\right\} \\
=\;& \mathbb{P}\left\{\dot{\underset{\sim}{L}}^{g} \le \ell\right\} \cdot \frac{\dot{D}}{D} \;+\; \mathbb{P}\left\{\ddot{\underset{\sim}{L}}^{g} \le \ell\right\} \cdot \frac{\ddot{D}}{D} \;,
\end{aligned} \tag{3.18}$$

where, the rv $\dot{\underset{\sim}{L}}^{\,g}$ represents the net load in the weekday subperiods and the rv $\ddot{\underset{\sim}{L}}^{\,g}$ represents the net load in the weekend subperiods. We evaluate the cdf of $\dot{\underset{\sim}{L}}^{\,g}$ as follows:

$$\begin{aligned}
&\mathbb{P}\left\{\dot{\underset{\sim}{L}}^{\,g} \le \ell\right\} \;=\; \mathbb{P}\left\{\dot{\underset{\sim}{L}}^{\,g} \le \ell \;\; \textit{in all weekday subperiods } h \textit{ in the period}\right\} \\
=\;& \sum_{k\,=\,1}^{K} \mathbb{P}\left\{\dot{\underset{\sim}{L}}^{\,g} \le \ell \;,\; \textit{subperiod } h \textit{ is the } k^{\text{th}} \textit{ subperiod of a weekday}\right\} \\
=\;& \sum_{k\,=\,1}^{K} \mathbb{P}\left\{\dot{\underset{\sim}{L}}^{\,g} \le \ell \mid \textit{subperiod } h \textit{ is the } k^{\text{th}} \textit{ subperiod of a weekday}\right\} \times \\
&\qquad\qquad \mathbb{P}\left\{\textit{subperiod } h \textit{ is the } k^{\text{th}} \textit{ subperiod of a weekday}\right\} \\
=\;& \sum_{k\,=\,1}^{K} \mathbb{P}\left\{\dot{\underset{\sim}{L}}^{\,g}_{(k)} \le \ell\right\} \cdot \frac{1}{K} \;. \qquad (3.19)
\end{aligned}$$

Using similar reasoning, we evaluate the cdf of $\ddot{\underset{\sim}{L}}^{\,g}$,

$$\mathbb{P}\left\{\ddot{\underset{\sim}{L}}^{\,g} \le \ell\right\} \;=\; \sum_{k\,=\,1}^{K} \mathbb{P}\left\{\ddot{\underset{\sim}{L}}^{\,g}_{(k)} \le \ell\right\} \cdot \frac{1}{K} \;, \qquad (3.20)$$

so that Equation (3.18) is restated as

$$\mathbb{F}_{\,\underset{\sim}{L}^{\,g}}(\ell) \;=\; \frac{\dot{D}}{D} \cdot \frac{1}{K} \sum_{k\,=\,1}^{K} \mathbb{P}\left\{\dot{\underset{\sim}{L}}^{\,g}_{(k)} \le \ell\right\} \;+\; \frac{\ddot{D}}{D} \cdot \frac{1}{K} \sum_{k\,=\,1}^{K} \mathbb{P}\left\{\ddot{\underset{\sim}{L}}^{\,g}_{(k)} \le \ell\right\} \;. \qquad (3.21)$$

Thus, from Equation (3.21), it is evident that the cdf of the net load rv for the simulation period is a weighted average of the cdf's of the K weekday net load rv's and the K weekend net load rv's. Figure 3.6 illustrates the extended simulation approach to obtain the distribution of the net load for the simulation period by aggregating the conditional distributions of the net load rv's corresponding to the K weekday subperiods and K weekend subperiods.

The simulation approach based on aggregating the conditional distributions is sufficiently general and can be extended to characterize probabilistically all the

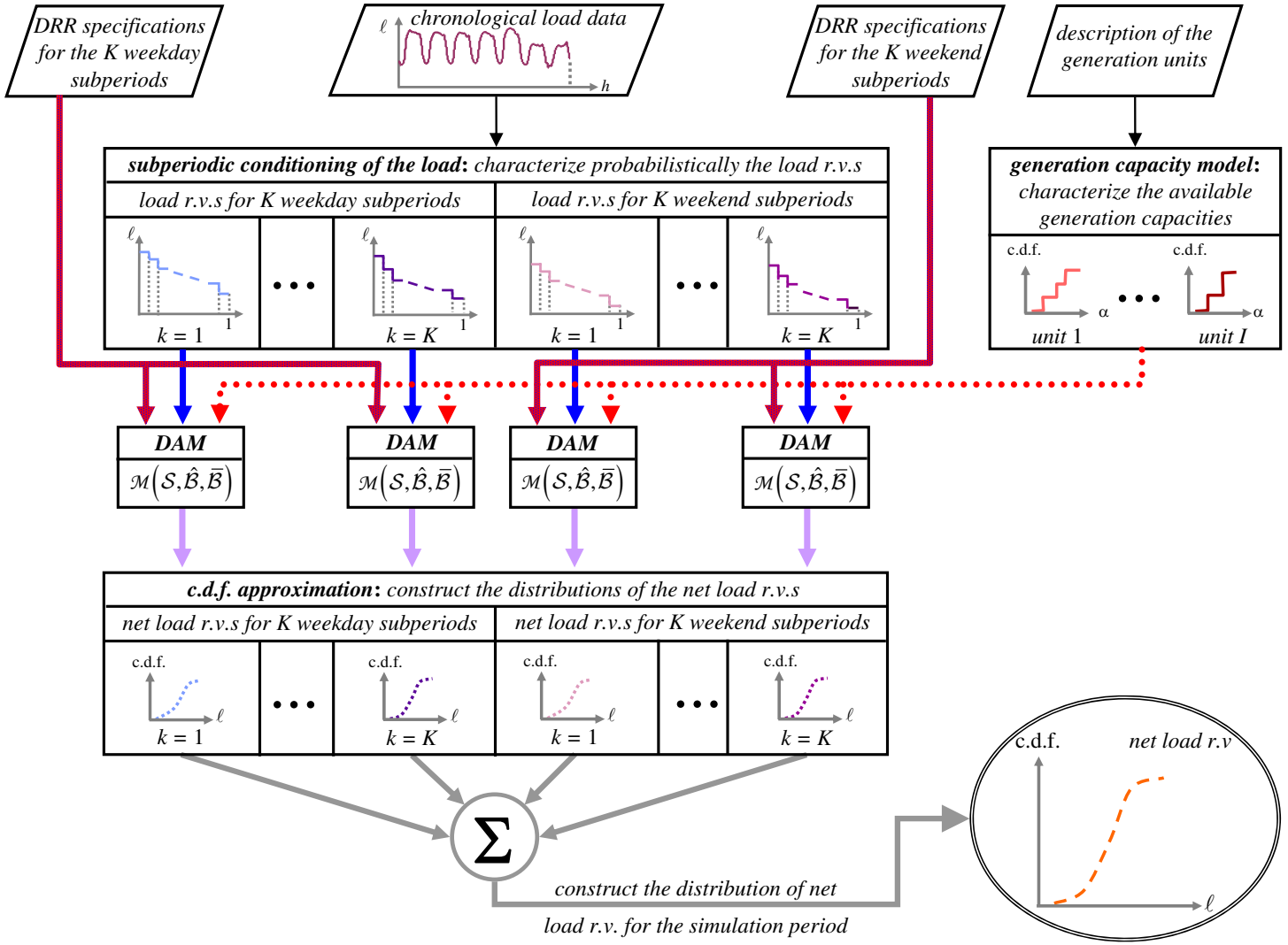

Figure 3.6: The extended approach for the simulation of the systems with DRRs over a specified simulation period

outcomes of the market so that the cdf of each market outcome is obtained as a weighted average of the cdf's of the corresponding K weekday market outcomes and the K weekend market outcomes. In particular, we apply the simulation approach to characterize the generation $\underset{\sim}{P}^{\,i}$ of each unit i, using the K rv's $\underset{\sim}{\dot{P}}^{\,i}_{(k)}$ s representing the generation of the unit for K weekday subperiods and the K rv's $\underset{\sim}{\ddot{P}}^{\,i}_{(k)}$ s representing the generation of the unit for K weekend subperiods. The expected generation and the capacity factor of the unit i are then evaluated as

$$\mathcal{E}^{\,i} \;=\; H \cdot \mathbb{E}\left\{\underset{\sim}{P}^{\,i}\right\} \;, \tag{3.22}$$

$$CF^{\,i} \;=\; \frac{\mathcal{E}^{\,i}}{c^{\,i} \cdot H} \;=\; \frac{\mathbb{E}\left\{\underset{\sim}{P}^{\,i}\right\}}{c^{\,i}} \;. \tag{3.23}$$

Since we focus on a competitive environment, we evaluate the revenues received by a generation unit instead of the costs for generation. We denote by the rv $\underset{\sim}{W}^{\,i}$ the revenue received by the unit i from the IGO in any subperiod of the simulation period; $\underset{\sim}{W}^{\,i}$ depends on the LMP of the node where i is located and the amount sale by the unit. Then the total revenues of the unit i for the simulation period are given by

$$\mathcal{W}^{\,i} \;=\; H \cdot \mathbb{E}\left\{\underset{\sim}{W}^{\,i}\right\} \;. \tag{3.24}$$

Analogously, we define $\underset{\sim}{W}^{\,\bar{b}}, \underset{\sim}{W}^{\,\hat{b}}, \mathcal{W}^{\,\bar{b}}, \mathcal{W}^{\,\hat{b}}$. The rv's corresponding to the other relevant economic metrics are listed below:

$\underset{\sim}{\Lambda}_{\,n}$	LMP at the node n
$\underset{\sim}{\mathcal{K}}$	congestion rents
$\underset{\sim}{W}^{\,\mathcal{I}}$	total revenues of the generators
$\underset{\sim}{W}^{\,\widehat{\mathcal{B}}}$	total payments from the DRR players
$\underset{\sim}{W}^{\,\bar{\mathcal{B}}}$	total payments from the pure buyers

We use the expected values as key metrics for the assessment of the economic variables of interest. The total congestion rents during the H subperiods of the simulation period are denoted by κ and given as

$$\mathcal{K} \;=\; H \cdot \mathbb{E}\left\{\underset{\sim}{\mathcal{K}}\right\} \;. \tag{3.25}$$

We use analogous expressions to evaluate the total supply-side revenues, $\mathcal{W}^{\mathcal{S}}$, the total payments from the DRR players, $\mathcal{W}^{\widehat{\mathcal{B}}}$, and the total payments from the pure buyers, $\mathcal{W}^{\bar{\mathcal{B}}}$. We make use of the net load rv to evaluate the reliability metrics, LOLP and EUE, as follows:

$$LOLP \;=\; \mathbb{P}\left\{\sum_{i\,\in\,\mathcal{I}} \underset{\sim}{P}^{\,i} < \underset{\sim}{L}^{\,g}\right\} \;, \tag{3.26}$$

$$\mathcal{U} \;=\; H \cdot \mathbb{E}\left\{\underset{\sim}{L}^{\,g} \;-\; \sum_{i\,\in\,\mathcal{I}} \underset{\sim}{P}^{\,i} \mid \underset{\sim}{L}^{\,g} > \sum_{i\,\in\,\mathcal{I}} \underset{\sim}{P}^{\,i}\right\} \cdot LOLP \;. \tag{3.27}$$

The simulation engine accommodates the extended probabilistic simulation approach and, hence, explicitly represents the uncertainty effects along with the impacts of the transmission-constrained markets. We may use the engine to emulate the operations of the electricity markets and the power system over a period for which the assumptions **A1**-**A7** introduced in Section 3.1 hold true. The application of the engine requires the specification of the system load and resource characteristics, the transmission network configuration, the market structure and the policies for the simulation period.

3.4 Summary

In this chapter, we reviewed the basics of the probabilistic simulation approach for the power systems with dispatchable generation units and extended the same for the systems which also include DRRs in the resource mix. The synchronization of the probabilistic simulation approach with the time dependent simulation of the markets with DRRs necessitated the modifications to probabilistic simulation techniques. We modified the load model so as to obtain representations that are compatible with the diurnal representation of the DRR capacities for a typical weekday and a weekend day. Next, the probabilistic simulation approach was adapted to accommodate the incorporation of market and network impacts. The resulting changes in the evaluation procedure of the variable effects were discussed. The extended probabilistic simulation approach is embodied by the simulation engine which constitutes one of the key building blocks in the development of the overall simulation methodology. The simulation engine may be used to realistically emulate the electricity production in the systems which have DRRs over specified periods. However, the application of the engine to simulate system behavior for longer-term periods requires careful consideration so that the assumptions for the extended simulation approach hold.

CHAPTER 4

THE PROPOSED SIMULATION METHODOLOGY AND ITS IMPLEMENTATION

The simulation engine described in Chapter 3 is not be applicable for simulating the longer-term periods which do not not satisfy the assumptions **A1**-**A7** introduced on pp. 45–46. Hence, we need to partition the multi-year study periods into shorter periods which may be simulated by the proposed engine. We devote this chapter to the development of the proposed simulation methodology for the longer-term study periods. The implementation of the proposed methodology for studies on large–scale systems needs the identification and the resolution of the computational tractability issues. We exploit the structural characteristics of power system models to reduce the computation required by the proposed methodology. We introduce appropriate mechanisms into the implementation embodying the proposed methodology so as to make it useable for simulation studies of large-scale power systems over longer-term periods.

The chapter has three sections. We describe in Section 4.1 the proposed methodology for simulating longer-term study periods. We discuss in Section 4.2 the techniques that take advantage of the characteristics the power system, the market operations and the load consumption patterns to reduce the computational tasks of the proposed simulation methodology. We present in Section 4.3 the implemented simulation methodology and describe its applications to different studies.

4.1 The Proposed Simulation Methodology

The simulation engine described in Chapter 3 may be applied to emulate the electricity system behavior over a period for which the assumptions **A1**-**A7** hold true. However, the assumptions may not hold for longer study periods; it is not reasonable to assume that the policy environment, the market structure, the resource mix, the transmission network and the seasonality effects remain unchanged during a multi-year study period. In order to use the simulation engine for a longer-term study period, we first partition the study period into shorter simulation periods which may be simulated by the engine. We describe the proposed methodology for simulating longer-term study periods in this section.

The study period is specified once the study horizon is set, depending on the scope, the nature and the objectives of the study. For a realistic emulation of the way the electricity system behavior, we need to take into account the changes in the transmission grid, the generation unit retirements/additions, planned maintenance outages and other modifications to the resource mix, changes to the market structure, the various policy initiatives as well as the seasonality effects that may impact system and market operations during the study period. Therefore, we partition the study period into T non-overlapping simulation periods and denote by

$$\mathscr{T} \triangleq \{t : t = 1, \ldots, T\} \ ,$$

the index set of the simulation periods. This partitioning of the study period is done so as to accommodate the less frequent changes in the system due to modifications in the resource mix, the transmission grid, the market structure and the policy environment. We define each simulation period so as to ensure that the assumptions **A1**-**A7** hold for that period. In effect, the resource mix, the transmission network, the market structure, the policy environment and the sea-

sonality effects remain unchanged within that period. Anytime a change occurs, we require the beginning of a new simulation period so that the change persists for the entire simulation period. In this way, we can represent all the changes that may occur during the study period.

Since the partitioning of the study period into simulation periods is dictated by the forecasted long-term events, the simulation periods may be of unequal duration. We express the duration of a simulation period in terms of the smallest indecomposable unit of time, i.e., the subperiod. We denote by $(H)_t$ the number of subperiods in a simulation period $t \in \mathscr{T}$. We summarize the study period partitioning process in Fig. 4.1. We note that the choice of the length of the

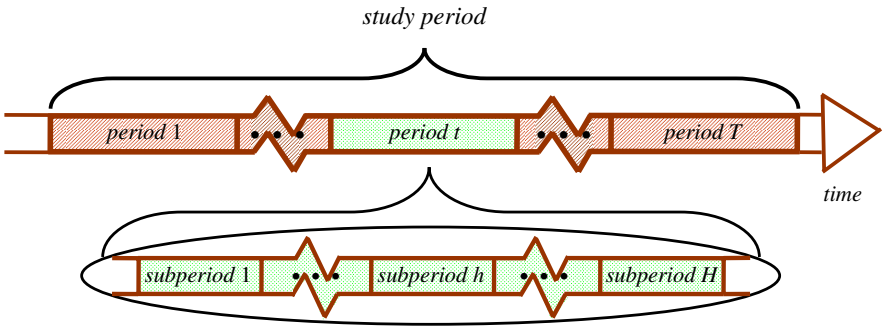

Figure 4.1: The time dimension for the simulation study

subperiod impacts the level of detail with which we represent short-term effects in the system operations. In actual operations, there are changes in the markets and system conditions brought about by the hourly electricity markets cleared in the day ahead and the balancing mechanisms that run on a nearly-real-time basis throughout each hour of the day. For the purposes of the simulation, the length of the subperiod is chosen to provide the level of detail required for the study. Phenomena of duration shorter than that of a subperiod cannot be represented and are ignored in the simulation.

Once the length of the subperiod is determined and the simulation periods are

defined, we use the simulation engine described in Section 3.3 to assess the variable effects for all the $(H)_t$ subperiods of each simulation period $t \in \mathscr{T}$. The variable effects for the simulation periods may then be aggregated to evaluate the variable effects for the study period. Clearly, the simulation engine is a key constituent of the proposed methodology. We now describe the other two components of the simulation methodology – the *scenario manager* (SM), which is used for defining the simulation periods, and the *assessment manager* (AM), which aggregates the simulation period assessments to quantify the variable effects over the study period.

The modeling and simulation of a power system for longer-term study periods requires a detailed representation, during the entire study period, of the system including the loads, the generation resources and the DRRs and the transmission grid, the market operations including the rules and the players and the policy environment. In this discussion, we implicitly assume that all the changes in the resource mix, the transmission grid, the DAM structure and the policy environment that occur during the study period are known *a priori* and exogenously specified as inputs, known as the *scenario specifications*. The definition of the simulation periods for the multi-year study is based on the scenario specifications. The definition process integrates all the scenario specifications to ensure that for each simulation period, the assumptions **A1**-**A7** hold. The pre-processing of the scenario specifications to determine the periods which are simulated by engine is performed the SM. The SM, in effect, defines T simulation periods and specifies the demand characteristics, the resource mix, the transmission network, the market structure and the policy environment for each of the T periods.

The system description for each simulation period serves as the input into the simulation engine. The engine emulates the electricity production for each simulation period $t \in \mathscr{T}$ as described in Chapter 3 and evaluates the variable effects for

that period. This entails the probabilistic characterization of the system load and the generator availabilities for each simulation period t. The realizations of the system load and the available generation capacity are then used to construct the probability distributions of the outcomes of the transmission-constrained DAM. The distributions of the DAM outcomes are used to evaluate the energy-related, financial and reliability metrics for the system as well as for individual players. We list in Table 4.1 the metrics obtained from the simulation of the period t. The

Table 4.1: Metrics used to quantify variable effects during a simulation period t

category		metric	notation
individual players	energy	generation of the unit i	$(\mathcal{E}^{i})_t$
		demand of the pure buyer $\bar{b}$	$(\mathcal{E}^{\bar{b}})_t$
		demand of the DRR $\hat{b}$	$(\mathcal{E}^{\hat{b}})_t$
		demand curtailment of the DRR $\hat{b}$	$(\hat{\mathcal{E}}^{\hat{b}})_t$
	financial	revenues of the generator i	$(\mathcal{W}^{i})_t$
		payments from the pure buyer $\bar{b}$	$(\mathcal{W}^{\bar{b}})_t$
		payments from the DRR $\hat{b}$	$(\mathcal{W}^{\hat{b}})_t$
system-wide	energy	total system load demand	$(\mathcal{E})_t$
		net system load demand	$(\mathcal{E}^{g})_t$
	financial	congestion rents	$(\mathcal{K})_t$
		total revenues of the generators	$(\mathcal{W}^{\mathcal{I}})_t$
		total payments from the pure buyers	$(\mathcal{W}^{\bar{\mathcal{B}}})_t$
		total payments from the DRRs	$(\mathcal{W}^{\hat{\mathcal{B}}})_t$
	reliability	loss of load probability	$(LOLP)_t$
		expected unserved energy	$(\mathcal{U})_t$

metrics resulting from the simulation of a specified period provide quantification of the variable effects of the system for that period.

The energy, financial and reliability metrics for each representative simulation

period are stored in the AM for further processing. The metrics for each simulation period $t \in \mathscr{T}$ are aggregated to assess the variable effects for the entire study period. For example, the total generation of the unit i for the entire study period may be evaluated as

$$(\mathcal{E}^i)_{\mathscr{T}} = \sum_{t \in \mathscr{T}} (\mathcal{E}^i)_t \,, \tag{4.1}$$

We use analogous expressions to evaluate other metrics in the AM.

The SM, the simulation engine and the AM are the three basic components of the proposed methodology. We use Fig. 4.2 to provide a conceptual illustration of the these three components and the interactions between them. Clearly, the

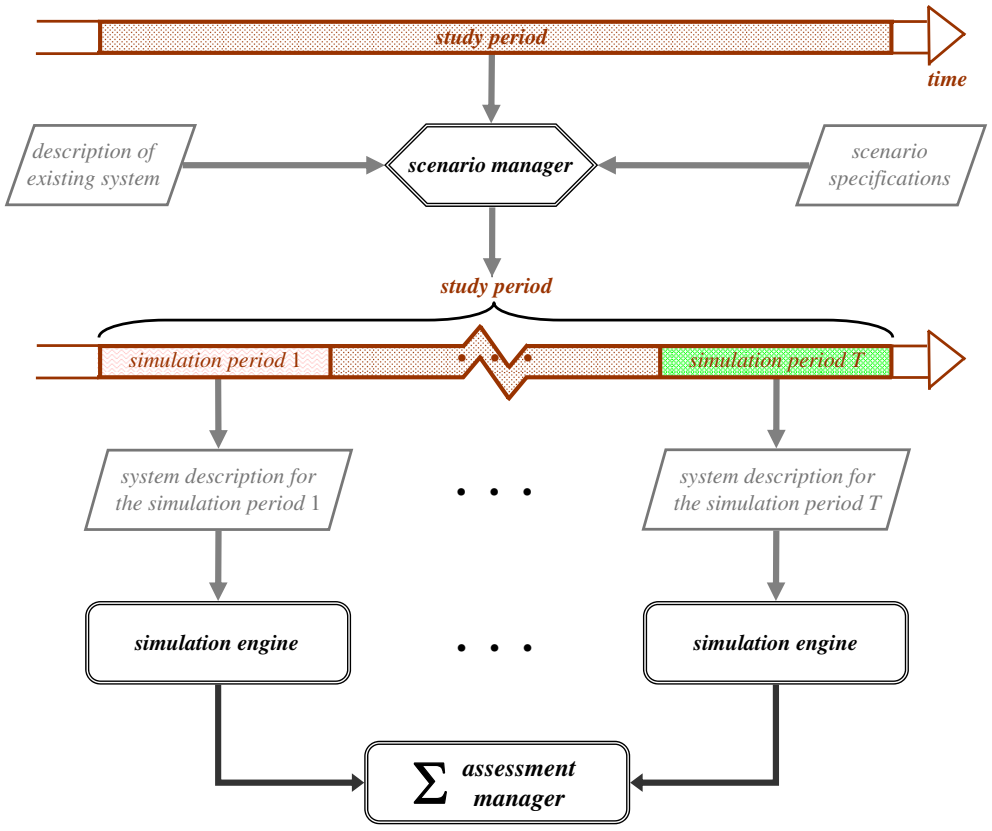

Figure 4.2: The proposed methodology for simulation of the system over longer-term study periods

simulation engine is the key driver in the application of the methodology. The SM and the AM act as pre- and post-processing units. The interactions between the three components of the methodology are through the information flows. The scenario specifications are provided to the SM so that the simulation periods are appropriately defined. The SM provides the system description for each simulation period $t \in \mathscr{T}$. This information flows to the engine and is used in the simulation of the power system for that period t. The simulation engine evaluates the energy, financial and reliability metrics for each simulation period t. This information flows to the AM for further analysis and is used to determine the variable effects for the entire study period.

We note three salient characteristics of the proposed methodology for simulating longer-term study periods:

- *Comprehensive representations*: The methodology accommodates detailed representations of the loads, the DRRs, the generators, the transmission grid, the competitive markets and the policies as well as the interactions between them during the entire study period. The scenario specifications can be effectively used to consider a broad range of possible future developments which may impact the operation of the power system and the electricity markets for the multi-year study period. The methodology takes into consideration the various sources of uncertainty such as the variability in the load demand, the availability of the generation units, the behavior of the market participants, the transmission congestion and the outcomes of the transmission-impacted DAMs. The explicit representation of the impacts of the different sources of uncertainty provides a realistic representation of the operations of the power system and the electricity markets for the study period. Hence, the methodology is designed to deal with all aspects of multi-year simulations comprehensively.

- *Modular and flexible implementation*: Structural modularity in the implementation allows the user to change the representation of one or more elements in the simulation without affecting the modeling of the other elements. For example, we can accommodate changes in a specified resource by modifying the generator capacity model without affecting any other resource or load models in the simulation engine. Also, the simulation methodology provides a choice to the user in terms of specifying the level of detail commensurate with the scope of the study. The choice of the subperiod depends on the level of detail. Hence, in addition to its application to long-term planning and analyses, the methodology may also be used for shorter-term operational studies with higher resolution and more level of detail. Moreover, the representation of the physical grid may be easily modified so as to accommodate, in sufficient detail, the system operational constraints for the short-term studies. The modularity and flexibility of the methodology make it useable for many different studies of interest to system operators and planners.

- *Versatility in the applications*: The methodology has the capability to comprehensively evaluate the different variable effects of the power system. The evaluation explicitly incorporates the network effects and thus captures the interactions of the existing and future resources with the transmission grid so that the impacts of resource additions/retirements on the transmission usage and possible congestion situations may be effectively assessed. The transmission usage patterns coupled with the market impacts provide a consistent basis to compare different resource alternatives or policies. Furthermore, the simulation methodology may be used to evaluate the metrics from the point of view of either an individual player or the entire system. As a

result, the methodology is usable by different decision makers such as independent investors, policy makers, ISOs or RTOs. In fact, the simulation results allow the decision makers to make better informed decisions.

The primary drawback of the proposed methodology is the very long computing time associated with its implementation. The simulation of the power system and electricity markets for each simulation period entails the approximation of the probability distributions of the outcomes of the transmission-constrained DAMs. Such approximation requires consideration of the various sources of uncertainty such as variability in load demand, availability of the generation resources, possible transmission congestion situations, behavior of the market participants and DAM outcomes. The computing needs of the simulation engine depend on the size of the power system and the level of detail which is needed for the study. Indeed, for large-scale system studies requiring a high level of detail, the simulation may constitute a highly time-consuming computation. Moreover, the computation time increases exponentially with the size of the system, making the methodology impractical for large-scale systems. Hence, the implementation of the proposed simulation methodology needs to consider the computing issues and address them suitably.

4.2 Computational Tractability Issues

The implementation of the proposed methodology for longer-term studies on large-scale power systems requires careful attention to address the the computational tractability issues. We fully exploit the structural properties of the power system and electricity markets to bring about reduction in the computation. In this section, we discuss the appropriate mechanisms which may be introduced in the simulation methodology to make it useable for studies on large-scale systems.

The length of the subperiod determines the time resolution of the study, thereby impacting the computing requirements. The subperiod is determined by the level of detail needed for the study. In fact, the length of the subperiod is chosen such that the variations in the system conditions within the subperiod are sufficiently small to allow us to ignore their impacts on the variable effects for the entire study period. The aim is to choose as long a subperiod as possible, while ensuring the effective representation of all the short-term changes over the study period with adequate level of detail. Along the same lines, we choose as few simulation periods as possible, while taking into account all the specified long-term changes during the study period.

We reduce the computational requirements by taking advantage of the nature of the load demand in power systems. For the purposes of making this discussion more concrete, we select the weeks in the study period as the simulation periods. The scheme, however, is sufficiently general to allow the adoption of any other choice of simulation periods and they need not be uniform in length. The choice of weekly simulation periods allows us to take advantage of the fact that due to seasonal nature of the load demand, representative weeks in a year may be used to model the load demand patterns during the entire year so as to avoid the need to perform all 52 weekly simulations. However, we note that although several weeks in a year may exhibit similar load consumption patterns, the set of generating units not on scheduled maintenance may differ across the weeks with the similar load patterns. Hence, we may need to increase the number of representative weeks for each year in the study period to take into account the impacts of the maintenance schedules and the seasonality effects. We denote by $\mathscr{T}'$ the subset of the indices of the representative weeks in the study period; clearly, $\mathscr{T}' \subset \mathscr{T}$. The electricity system needs to be simulated for each representative week $t \in \mathscr{T}'$ and the resulting assessments for the week t get weighted by the number of weeks, ν_t,

that have similar load and resource patterns. Since the number of representative weeks selected for a study year can be an order of magnitude smaller than 52, the judicious selection of the representative weeks brings about tangible reductions in the computing.

Another aspect of the study period simulation that may be modified to achieve computational tractability is the simulation of each selected representative week. The approximation of the distributions of the random transmission-impacted DAM outcomes requires substantial computation since we need to take into account all the possible combinations of the load, the available capacities of the generators, the transmission system configurations and the behavior of the market players. For example, if we adopt an hourly subperiod, then for a one week simulation period, we have at most 168 sample load values. Further, let us consider a system of 100 generators, with each generator having a 2-state representation of its available capacity. Assuming that the market players bid all the available generation capacity and all the transmission lines are available 100%, the total number of possible combinations that impact the DAM outcomes is, at most, $168 \cdot 2^{100}$. To construct the probability distributions of the DAM outcomes, we need to consider all the $168 \cdot 2^{100}$ possible combinations – a rather arduous task – without bringing in uncertainty due to the availability of the transmission and the behavior of the market participants. Clearly, the computational requirements grow exponentially with the size of the power system. Furthermore, the rv's characterizing the loads, the available generation capacities, the bids (offers) of players, the LMPs, the payments (revenues) of the players, the congestion rents, the net loads and the dispatched generation may not be independent. Hence, it is very difficult to obtain analytical expressions for the outcomes of the DAMs.

The incorporation of transmission considerations necessitates the use of the time-domain based DAM simulations, which requires the specification of the sys-

tem load, the available generation capacities and the transmission system configurations. As illustrated in the previous paragraph, an *exhaustive search* method which takes into account all the possible combinations of the DAM inputs is time consuming. Instead, we choose some representative samples of the inputs to the DAMs to reduce the computation involved and we use the corresponding outcomes of the DAM to construct the distributions of the rv's representing the DAM outcomes. A primary objective in the choice of the input samples is to faithfully represent the entire sample space of all the input rv's. To meet the stated objective, we apply the Latin hypercube technique – a robust and flexible sampling technique – developed in 1979 by McKay et al. [42]. The thrust of the Latin hypercube technique is to systematically sample across the multivariate distribution of the input rv's so as to choose representative samples that reflect the entire range of each rv being sampled. Each sample generated by this technique – referred to as the Latin hypercube sample (LHS) – is used to construct the distribution functions of the DAM outcomes.

Suppose we want to generate a total of M LHSs from a collection of R input rv's. The range each input rv r, for $r = 1, 2, \ldots, R$, is divided into M ranges with each having an equal probability of occurrence given by $\frac{1}{M}$. The consideration of M intervals for each of the R input rv's constitutes the partitioning of the R-dimensional sample space into M^R cells. We choose from the total M^R cells, a collection of M cells. The collection of the cells is chosen in such a way that each of the M ranges of each input rv r, $r = 1, 2, \ldots, R$, appears in one and only one of the selected M cells. Such a collection of M cells from the entire sample space of the inputs is then used to generate the M LHSs. We describe the basics of the Latin hypercube sampling technique in Appendix B.

The application and effectiveness of the Latin hypercube technique to power system simulation studies was investigated and led to the conclusion that the

technique is more effective than simple random sampling [43], [44]. The systematic sampling reduces dramatically the computation for the characterization of the rv's corresponding to the DAM outcomes. To illustrate this, we consider a sample size of 168 so that each LHS corresponds to one of the 168 load sample values. Since the Latin hypercube technique samples across the multivariate distribution of the load and the available generation capacities, the 168 LHSs corresponding to all the load values also provide realizations of the available generation capacities for the 100 generators. Then, we use these 168 combinations of the load and available generation to simulate the DAMs, and use the resulting 168 set of outcomes to approximate the distributions. We note that the reduction in the number of computations is significant – from $168 \cdot 2^{100}$ to 168. Often, it may be necessary to consider the impacts of forced outages on some of the largest generators in the system. Let us assume that we have 10 such generators among the collection of 100 generators. Even with this consideration, the number of possible input combinations is still significantly smaller – $168 \cdot 2^{10}$ – as compared to the total number of combinations. Thus, the use of LHSs to construct the approximate cdf's drastically improves the computational tractability.

The judicious selection of representative simulation periods and representative subperiodic input samples can drastically improve the computational tractability of the implementation of the proposed simulation methodology.

4.3 Implementational Aspects of the Simulation Methodology

The implementation of the simulation methodology uses the techniques for simulation period selection and Latin hypercube sampling to bring about computational tractability. In this section, we describe the implementation of the proposed sim-

ulation methodology.

The preprocessing tasks performed by the SM are modified to incorporate the representative simulation period selection process. The description of the system load and the maintenance schedule of the generation resources is used to select T' representative simulation periods from the T periods defined by the SM. The definition and selection process integrates all the input specifications and system description to ensure that for each selected representative simulation period, the assumptions **A1**-**A7** hold. The SM also defines the subperiod length to obtain the level of detail required for the simulation study. Then, for each representative simulation period, the SM specifies the demand characteristics, the resource mix, the transmission network, the market structure and the policy environment for all the subperiods in the simulation period.

The system description for each representative simulation period serves as the input into the probabilistic simulation engine. The engine emulates the electricity production for each representative period $t \in \mathscr{T}'$ as described in Chapter 3, with one modification – the engine uses the LHSs to approximate the distributions of the DAM outcomes. The procedure for simulating a period t involves the following steps:

(1) Characterize the distribution of the load rv's corresponding to the K weekday subperiods and K weekend subperiods based on the chronological load data.

(2) Characterize the distribution of the available generation capacities for the simulation period using the specifications of the resources and the historical operating data.

(3) Approximate the distributions of the DAM outcomes for the K weekday subperiods and K weekend subperiods. The substeps involved for a typical

weekday (weekend) subperiod k include the following:

(i) Generate LHSs comprising of the system load for the weekday (weekend) subperiod k and the available generation capacities.

(ii) Evaluate the market outcomes and the transmission usage for the offers and the bids corresponding to each LHS input using the transmission constrained electricity market model.

(iii) Construct the cdf's of the rv's representing the market outcomes for the weekday subperiod k using the corresponding outcomes of the DAM simulations based on the LHS inputs.

Repeat steps (i)-(iii) for all weekday (weekend) subperiods k, where $k = 1, 2, \ldots, K$.

(4) Construct the cdf of each market outcome rv for the entire simulation period as a weighted average of the distributions of the corresponding K weekday market outcome rv's and the K weekend market outcome rv's.

(5) Evaluate the expected generation and capacity factor of each unit, in addition to the reliability and financial metrics of interest using the rv's representing the market outcome for the simulation period.

The energy, financial and reliability metrics for each representative simulation period are stored in the *assessment manager* (AM) for further processing. The metrics for each representative period $t \in \mathscr{T}'$ are weighted by the number of simulation periods, ν_t, with similar load and resource characteristics. The weighted aggregation of the metrics corresponding to representative simulation periods is used to estimate the variable effects over the entire study period. For example, the total generation of the unit i for the entire study period may be approximated

as

$$(\mathcal{E}^{i})_{\mathscr{T}} \approx \sum_{t \in \mathscr{T}'} (\mathcal{E}^{i})_{t} \cdot \nu_{t} , \tag{4.2}$$

where, $\mathscr{T}' \subset \mathscr{T}$ and

$$\sum_{t \in \mathscr{T}'} \nu_{t} = T .$$

We use analogous expressions to evaluate other relevant metrics of interest in the AM.

The implementation of the proposed simulation methodology incorporates the mechanisms discussed in Section 4.2 so as to make it usable for applications of practical interest. The main advantage of the implemented simulation methodology is the capability to perform assessments for large-scale interconnected systems over multi-year study periods in a computationally tractable manner. The methodology uses advantageously the nature and the structure of the power system to reduce the computing requirements. Thus, the tool may be applied for the simulation of large-scale power systems for studies of practical interest.

The key areas for the application of the implementation of the proposed simulation methodology include the following:

- *Resource investment analysis*: identification of potential resource investment options, comparison between different resource alternatives, determination of the optimal timing of a resource investment, development of resource investment strategies while taking into account emissions' policies and renewable portfolio standards.

- *Transmission planning*: analysis of the impacts of transmission investments on the economics of the electricity supply, identification of transmission in-

vestment projects from the congestion signals obtained from the simulations, cost-benefit analysis of upgrades to the transmission grid.

- *Policy analysis*: assess the fiscal impacts of new policies regarding GHG emissions and/or cap-and-trade mechanisms, evaluation of the monetary impacts of emissions' policies on the market players, comparison between different policy initiatives based on the effectiveness of each.

We demonstrate the use of the simulation methodology for some representative application studies in Chapter 5.

4.4 Summary

In this chapter, we developed the simulation methodology for longer-term study periods. We presented the salient features of the proposed methodology and addressed the implementational aspects of the same. Specifically, we introduced mechanisms which fully exploit the structural properties of the power system and the electricity markets to reduce the computing requirements of the simulation. The incorporation of such mechanisms into the implementation of the proposed methodology makes it useable for different applications of practical interest.

The key advantage of the implemented simulation methodology is the computational tractability achieved through its careful design. The comprehensive and flexible modular design imparts versatility in its application to a wide range of power system studies. The application areas of the tool broadly include resource investment analysis, planning activities and policy analysis. In fact, the methodology allows the decision makers – be they independent investors or the IGO or policy makers – to make better informed decisions.

CHAPTER 5

APPLICATION STUDIES

We devote this chapter to the demonstration of a few representative applications of the simulation methodology developed in Chapter 4 to a large-scale test system. The studies described in this chapter quantify the range of benefits the integration of DRRs can provide to the system as well as to individual players. In all the studies, we explicitly represent various sources of uncertainty to ensure the realism of the results and the assessments. The simulations reported in this chapter are representative of the extensive studies performed and serve to demonstrate the application of the simulation methodology to studies of power system operations for planning and analyses. For the purpose of discussing the results, we limit the analysis to a one year simulation. The analysis of the year–long study period aids in the understanding of the application of the proposed methodology to the simulation studies and the key results and the essential insights obtained from the simulations.

This chapter contains six sections. In Section 5.1, we describe the large-scale test system. We discuss in Section 5.2 the nature of the simulations. We report in Section 5.3 the impacts of DRRs on the system. We investigate the payback effects and the increasing penetration of DRRs in the resource mix. We demonstrate in Section 5.4 the application of the methodology to evaluate the benefits of a DRR aggregation to an ESP. We describe in Section 5.5 additional examples of the application of the methodology to planning and policy analysis. We conclude in Section 5.6 with a summary of the findings and the key insights obtained from

the simulation studies.

5.1 The Test System

We use a test case system with a large network and many market participants to represent a hypothetical large-scale IGO network. We describe in this section the characteristics of the test system. We describe briefly the four main types of the physical components of the system – namely, the transmission grid, the loads, the DRRs and the supply-side resources. We also discuss the market structure.

The transmission network of the test system consists of 241 buses and 555 lines. Each bus is connected to at least one other bus in the network via a transmission line. Each line has a specified upper limit on the active power flow through that line.

We consider a summer peaking system – the load demand requirements in the summer months are significantly higher than those in the non-summer months. We use the load shapes from the Midwest ISO (MISO) system. The system load demand is the aggregated demand of all the loads in the system. The loads of individual entities are specified fractions of the system load demand. Further, the demand of the buyers is *fixed*, i.e., inelastic to the electricity prices. We discuss this further when we describe the market structure.

Some loads in the system have the capability of providing demand response services and hence act as DRRs. The total capacity of the DRRs in the system for each year in the study period is expressed as a fraction of the peak annual load demand of the system and is a key decision variable in the simulation studies. The DRRs are used by the IGO to meet the system demand requirements for the subperiods. The payback effects due to the load curtailments by a DRR $\hat{b}$ are specified in terms of the load recovery factor (LRF) $\chi^{\hat{b}}$ [11], [12]. The LRF $\chi^{\hat{b}}$

indicates the fraction of the curtailed consumption of the DRR $\hat{b}$ that is recovered during the specified load recovery subperiods. Further, we assume that the load recovery is uniform throughout the recovery period. We also assume that the DRRs are available for scheduling throughout the study period.

The supply-side resource mix for the existing system is described in Table 5.1.

Table 5.1: Supply-side resources

type of generation	capacity (GW)
base coal units	70
cycling units	21
peaking units	24
other units	20
total capacity	135

Each generation unit has pre-specified maintenance schedules, so the unit is out of service during that time period. Furthermore, each unit may be subjected random forced outages. The forced outage rates for the unit are known *a priori* and used to characterize the available generation capacity for each unit.

The IGO, the pure buyers, the DRRs and the generators are the key players in the DAM of the test system. The IGO meets the demand requirements of all the buyers using offers from generators as well as DRRs. We assume that the DRRs are eligible to offer demand curtailments during DAMs for the subperiods from 8 a.m. to 6 p.m. during each weekday. This assumption is consistent with the implementation of the day-ahead demand response programs in ISO-NE and PJM. Also, we assume that the load recovery is restricted to the off-peak (night) subperiods. Further, we assume that the buyers and sellers in the DAM are price takers. The buyer bids are fixed demand bids which specify the MWh/h quantity

without any price information. Such bids indicate an unlimited willingness to pay for the electricity purchases. We use a very high constant per MWh benefit value, $\gamma = 2000$, to determine the appropriate value of the benefits for these fixed demand bids. Also, we assume that the offer price of each seller remains unchanged during each simulation period. The marginal offer price of the supply-side seller s, β^s, is expressed in \$/MWh per hour while the marginal offer price of the DRR seller $\hat{b}$, $\beta^{\hat{b}}$, is expressed in \$/MW per hour. To accurately describe possible bidding patterns, we assume that the seller offer parameters β^s and $\beta^{\hat{b}}$ change due to the seasonal demand patterns – an increase (decrease) in demand causes an increase (decrease) in both the parameters.

We use this realistic-sized test system in all the case studies presented in this chapter. The size of the system provides the basis for extensive testing of the proposed methodology.

5.2 The Nature of the Simulations

The objective of the simulation studies is to provide comprehensive assessment of the benefits of DRRs to the system and to individual players. We discuss briefly the specific studies presented in this chapter.

The first set of studies investigates the system-wide impacts of DRRs. We use the metrics developed in Chapters 3 and 4 to quantify the variable effects for each scenario simulated. We use as a reference the scenario $\mathbb{R}$ with no DRRs in the system, and we use the variable effects from this scenario as benchmarks to assess the impacts of the DRRs on the system. To study the effects of DRR integration on the system, we simulate additional scenarios with varying DRR capacity in the resource mix as indicated below:

- scenario $\mathbb{D}_3$: resource mix has DRRs with total capacity of 3,500 MW,

approximately 3 % of annual peak load for the selected study period

- scenario $\mathbb{D}_5$: resource mix has DRRs with total capacity of 5,600 MW, approximately 5 % of peak load
- scenario $\mathbb{D}_7$: resource mix has DRRs with total capacity of 7,800 MW, approximately 7 % of peak load
- scenario $\mathbb{D}_{10}$: resource mix has DRRs with total capacity of 11,000 MW, approximately 10 % of peak load

The load payback effects are simulated by varying the load recovery factor, $\chi^{\hat{b}}$. For initial comparisons, we ignore the load payback so that $\chi^{\hat{b}} = 0$. To study the load recovery phenomenon, we vary $\chi^{\hat{b}}$ for a specified DRR scenario.

In case studies simulated to assess the benefits of DRR aggregation to individual players, we use as reference the scenario $\mathbb{D}_5$ with 5,600 MW of DRR capacity, so as to represent a system where the ESP as a DRR aggregator competes with other DRRs as well as generators in the DAMs. To compare the DRR integration with implementation of the conservation measures and the deployment of the AMI, we simulate two additional scenarios with reference scenario $\mathbb{R}$ resource mix:

- scenario $\mathbb{C}$: 2,500 MW of base load conserved
- scenario $\mathbb{A}$: 5,600 MW of load capacity equipped with AMI

We choose a year-long study period, as an illustrative example of how the simulation methodology may be implemented. The choice of one year duration allows us to incorporate the seasonal variations in the load demand and illustrate the nature of the results and the key insights. We choose the weekly periods and hourly subperiods for the simulation studies. The choice of one week allows the

assumption that the set of generation units participating in the DAM and not out for planned maintenance remains unchanged for the entire duration of the period. We choose the length of the subperiod as an hour, since most ISOs/RTOs have hourly DAMs.

We use the annual load data for the year 2006 from MISO [45]. The average hourly demand is 70,000 MWh/h, and the annual peak demand is 117,000 MWh/h. The analysis of the load in the study period indicates that the load patterns conform with the summer peaking nature of the system. Specifically, we note the higher demand levels during the summer months, July and August, and the large variations in the daily peak demand levels in the summer months. We illustrate in Fig. 5.1 the hourly system load for the entire study period. We select representative weekly load profiles for each of the four seasons in order to take into account the seasonality effects. Since the load profiles for each of the 13 winter weeks are similar, we choose one representative winter week load profile to model the load demand during winter. We use similar reasoning to choose the one representative autumn week load profile to represent the autumn load. However, the load for the spring and summer weeks cannot be modeled using a single load profile, because the weekly load profiles during spring and summer are markedly different. We observe that for the spring weeks, there are two distinct load profiles - a "low load" profile during the first 8 weeks and a "high load" profile during the next 5 weeks. So, we use two representative weekly load profiles for the spring in our studies. Similarly, for the summer weeks, we represent two distinct load profiles - "peak load" profile for 3 weeks and "average load" profile for 10 weeks.

We increase the number of representative weeks to take into consideration the maintenance schedules. We depict the impacts of planned maintenance outages on the generation capacity available for scheduling for each of the 52 weeks in Fig. 5.2. Most of the maintenance and repairs are carried out during the weeks of March

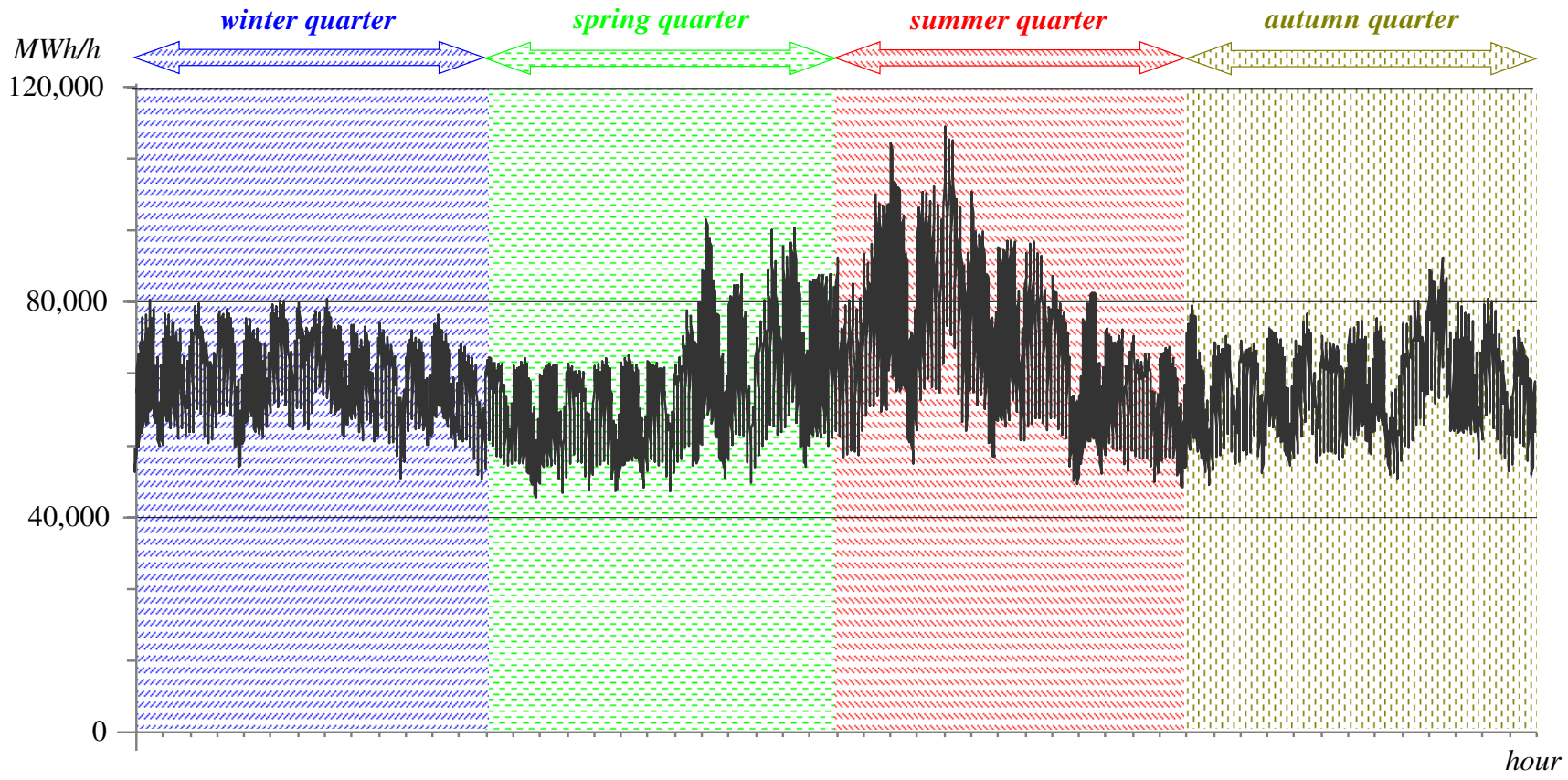

Figure 5.1: Hourly load for the study duration

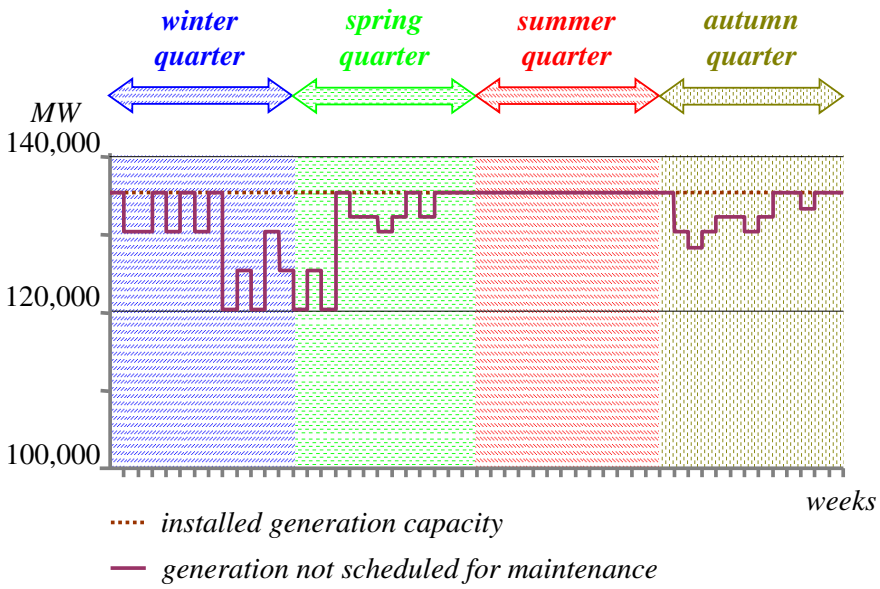

Figure 5.2: Total generation capacity available for scheduling during the study period

and April [46] and, consequently, the generation capacity available for the IGO operations is significantly reduced during these weeks, as seen from Fig. 5.2. In our simulations, we assume that all the units are available during summer weeks, since most generation owners do not schedule maintenance during the summer, when electricity prices tend to be higher. In total, we simulate the power system for 15 out of the 52 weeks in the study period.

We employ the Latin hypercube sampling technique to reduce the computing tasks in the simulation of each selected representative week. For comparative analysis, we choose a sample size between 30 and 150 because the focus of the simulations is to evaluate relative variable effects between different scenarios under consideration. If precise valuations of investment candidates are desired, we need more detailed representations and a higher sample size, between 80 and 200. For the simulation reported here, we select sample sizes between 50 and 100 and we use the LHSs to approximate the distributions of the market outcomes for each of the 15 selected representative weeks. This results in significant reductions in

the computing requirements.

5.3 System-Wide Impacts of DRRs

An attractive aspect of integrating DRRs into electricity systems is the reduction in the demand and the consequent decrease in electricity prices, thereby resulting in lower payments from all the consumers. Another appealing effect of DRR deployment is the effective utilization of the system, due to the reduction in the generation which lowers the GHG emissions and the possible transmission congestion relief. The simulations presented in this section serve to investigate these impacts in detail.

We start with the reference scenario without DRRs – scenario $\mathbb{R}$. The metrics of interest are the net load, the consumer payments, the congestion rents and the CO_2 emissions.[1] The hourly and aggregate annual values for the relevant metrics are tabulated in Table 5.2. Next, we simulate the DRR scenario $\mathbb{D}_5[\chi^{\hat{b}} = 0]$,

Table 5.2: System-wide metrics for scenario $\mathbb{R}$

metric	hourly values			annual
	average	max	min	value
net load demand (MWh)	$69,910$	$117,658$	$50,806$	610.73×10^6
consumer payments (million \$)	4.453	46.096	2.068	38.90×10^3
congestion rents (million \$)	0.068	2.486	0.008	591.88
CO_2 emissions ($\times 10^6$ kgC)	11.82318	22.378	7.038	103.29×10^3

with 5,600 MW of DRR capacity and no load payback associated with the DRR curtailments. The hourly and annual metrics for relevant metrics are presented in Table 5.3. The comparative analysis of the simulation results for the two scenarios

[1] We use the emissions factor, expressed in kgC/MWh, from the report [47] to estimate the expected CO_2 emissions for different generators.

Table 5.3: System-wide metrics for scenario $\mathbb{D}_5$ with $\chi^{\hat{b}} = 0$

metric	hourly values			annual
	average	max	min	value
net load demand (MWh)	68,831	112,720	50,806	601.31×10^6
consumer payments (million \$)	3.985	14.901	1.996	34.81×10^3
congestion rents (million \$)	0.044	0.176	0.009	387.45
CO_2 emissions ($\times 10^6$ kgC)	11.574	21.115	7.063	101.11×10^3

provide the necessary quantifications of the impacts of DRRs.

We start with the impacts on the net load. With DRRs available for scheduling, the IGO is able to meet the system demand requirements by dispatching the generation as well as by reducing the demand of the DRRs. As a result, the net demand for the whole system is lowered when the system load or the electricity prices are very high. We compare the net load demand for the study period in the 5 % DRR scenario against the reference scenario in Fig. 5.3. The figure provides a good illustration of the capability of the DRRs to reduce the load demand during the few critical hours in the study period – the reduction in the system load is observed in approximately 23% of the hours in the year. The reduction in the peak demand from 117,658 MWh/h to 112,720 MWh/h improves the capacity margin for the system by 3.65%. Further, the simulations provide insights into the seasonal patterns associated with the DRR deployment. The simulation results indicate that the DRRs are used more aggressively during the summer weeks when the electricity prices and the demand requirements are significantly higher, than in the non-summer weeks, when the electricity prices and the demand requirements are comparatively lower. This is better understood by comparing the net load demand for the peak summer week and the winter week for both the scenarios, as illustrated in Fig. 5.4. The reduction in the demand due to the

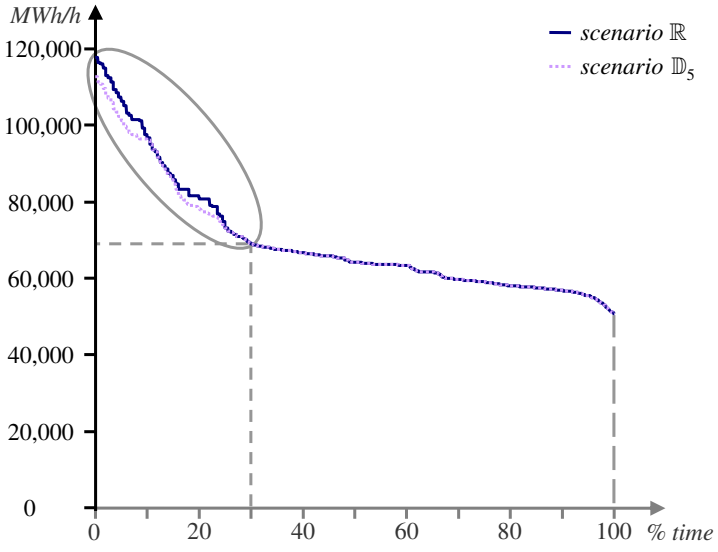

(a) annual LDC in the two scenarios

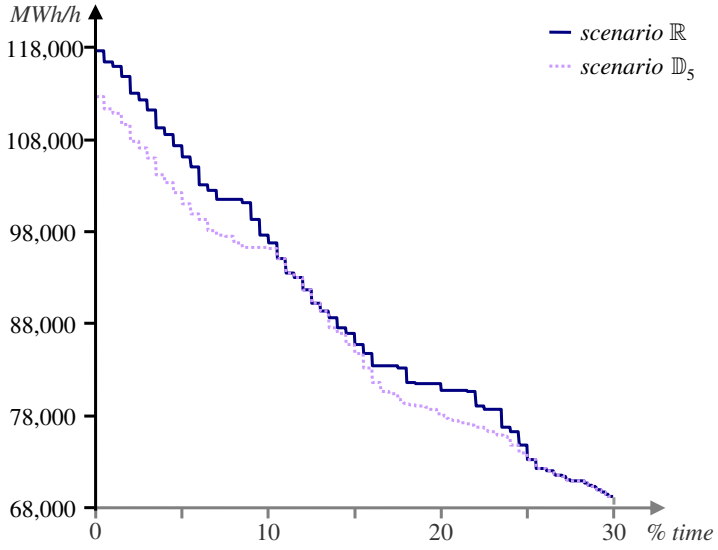

(b) blow-up of the circled region in (a)

Figure 5.3: Reduction in the net load demand due to DRR curtailments as seen using the LDCs for the study period

DRR curtailments is observed in approximately 35% of the summer week hours. However, the number of hours for which the demand is reduced during the winter week is less, approximately 20%. We also note that the amount of curtailment by the DRRs is higher during the summer. We hypothesize that the higher demand levels during the summer week lead to increased DRR deployment, as compared

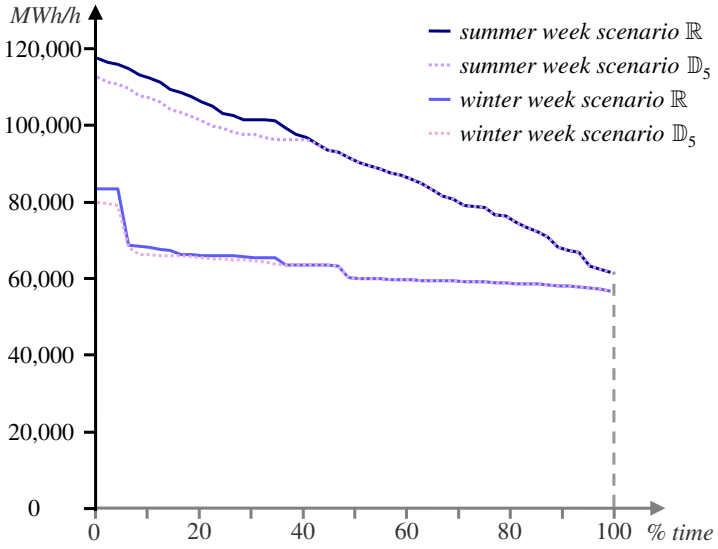

Figure 5.4: Seasonal variations in the DRR deployment as seen comparing the weekly LDCs for summer and non-summer months

to the non-summer weeks.

The reduction in the net load during the high load/high price hours for the year lowers LMPs for the system. DRR curtailments may also relieve transmission congestion which impacts the congestion rents. This results in an overall decrease in the total consumer payments received by the IGO. We observe that the curtailments due to DRRs significantly improve the transmission congestion, as witnessed by the reduction in the average and maximum congestion rents as compared with scenario ℝ. Also, the average consumer payments are lower in the DRR scenario as compared to the reference scenario. In particular, substantial savings may be accrued during the critical peak load hours when the demand is very high – this is evident by the reduction in the maximum consumer payments from \$46 million to \$15 million.

We summarize the impacts of the DRRs on the system by investigating the reduction in the annual energy consumption, energy consumption in the peak

hours,[2] peak load demand, total consumer payments, aggregate congestion rents and total CO_2 emissions for the scenario $\mathbb{D}_5[\chi^{\hat{b}} = 0]$ with respect to scenario $\mathbb{R}$. We present the results in Table 5.4. The simulation results indicate that even

Table 5.4: Reduction in the metrics of interest in scenario $\mathbb{D}_5$ with respect to scenario $\mathbb{R}$

aggregate annual metrics	reduction due to DRR deployment	
	decrease	% decrease
net load demand ($\times 10^6$ MWh)	9.42	1.54
peak load demand ($\times 10^6$ MWh)	1.93	3.10
peak load ($\times 10^3$ MW)	4.94	4.19
consumer payments (billion \$)	4.09	10.51
congestion rents (million \$)	204.43	34.54
CO_2 emissions ($\times 10^9$ kgC)	2.18	2.11

a small reduction in the energy consumption of about 1.5% can result in large savings in the consumer payments – of about 11% – and can drastically impact network congestion – as evident from the 35% reduction in the congestion rents. Also, the decrease in the energy consumption implies that the generation for the system is also reduced, and hence we find a proportional decrease in the CO_2 emissions.

To analyze the impacts of increasing DRR penetration, we simulate additional DRR scenarios – $\mathbb{D}_3$, $\mathbb{D}_7$ and $\mathbb{D}_{10}$ – ignoring the load recovery effects, so that $\chi^{\hat{b}} = 0$. As the DRR capacity in the resource mix increases, the demand curtailed during the peak load hours also increases. This results in further decrease in the total energy consumption over the year-long study period, and may cause proportional decrease in other metrics. We compute the reduction in the total energy consumption, energy consumption in the peak hours, the peak load,

[2]We estimate this using the energy consumption in the top 15% hours.

consumer payments, congestion rents and CO_2 emissions as compared to the reference scenario in order to assess the relative benefits of incorporating DRRs in the resource mix. We compute the % reduction in the relevant aggregate metrics for each of the scenarios with DRRs in the resource mix and present the results in Table 5.5. The table indicates that the increasing DRR penetration results in

Table 5.5: % decrease in the metrics for the different DRR scenarios with respect to scenario $\mathbb{R}$

scenario	$\mathbb{D}_3$	$\mathbb{D}_5$	$\mathbb{D}_7$	$\mathbb{D}_{10}$
net load demand	1.21	1.54	2.21	2.98
peak load demand	2.03	3.10	4.59	6.49
peak load	2.57	4.19	6.28	9.02
consumer payments	9.70	10.51	13.33	14.99
congestion rents	34.54	34.54	38.11	40.18
CO_2 emissions	1.81	2.11	3.17	4.11

higher savings in the metrics of interest. However, we note that the DRR scenarios discussed here assume that there is no payback associated with the DRR curtailments and hence the simulation results may overstate the benefits associated with DRR deployment.

As the penetration of the DRRs in the resource mix increases, it is not reasonable to assume that no load recovery will occur during the study period. In fact, if a large number of consumers opt to curtail load at critical peak hours, then this curtailed demand is bound to be recovered during the off-peak hours, increasing the load demand during these recovery hours. The higher off-peak demands increase the off-peak generation and may result in higher LMPs, leading to higher consumer payments. Such increases in the generation and consumer payments lower the benefits accrued from the lowering of the peak load demand.

For a thorough analysis of the DRR impacts, we investigate the payback effects. We repeat scenario $\mathbb{D}_5$ with $\chi^{\hat{b}} = 0.70$. We compare the annual LDC of scenario $\mathbb{D}_5$ $[\chi^{\hat{b}} = 0.70]$, with the $\mathbb{R}$-scenario without DRRs in Fig. 5.5. Similar to the

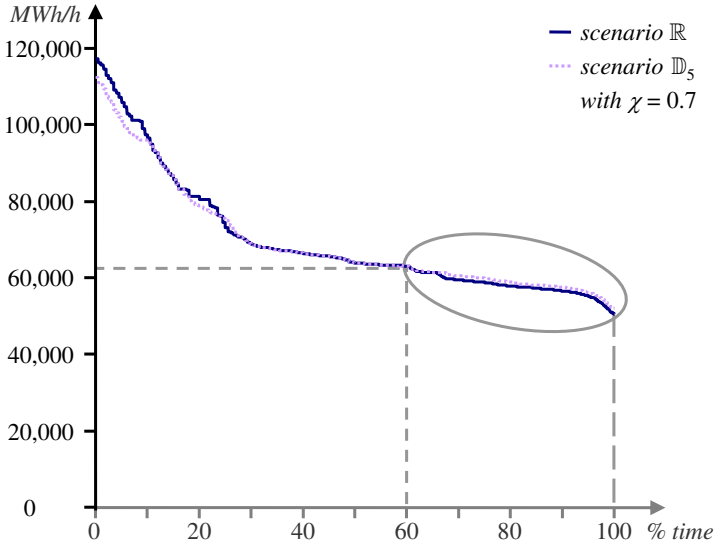

(a) annual LDC in the two scenarios

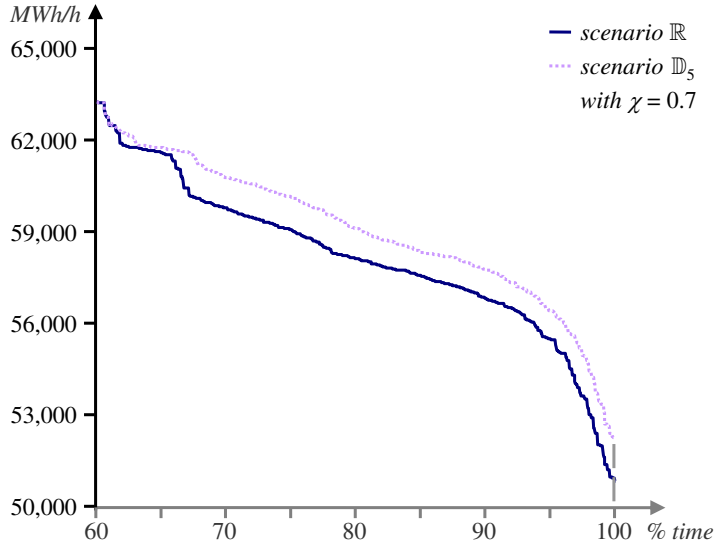

(b) blow-up of the circled region in (a)

Figure 5.5: Redistribution of the net loads due to load curtailments and recovery by DRRs as seen from the annual LDC

previous simulation of DRR scenario $\mathbb{D}_5$ with $\chi^{\hat{b}} = 0$, the deployment of DRRs reduces the net load in the peak load hours. But with payback effects incorporated,

the DRRs recover the load during the off-peak hours resulting in an increase in the off-peak load. This essentially results in the shifting of the demand from peak hours to off-peak hours. We illustrate this redistribution effect in Fig. 5.5.

We compute the hourly net demand, consumer payments, congestion rents and CO_2 emissions for the scenario $\mathbb{D}_5$ with $\chi^{\hat{b}} = 0$ and present the results in Table 5.6. The simulation results indicate that with 70% curtailed demand recovered during

Table 5.6: System-wide metrics for the scenario $\mathbb{D}_5$ with $\chi^{\hat{b}} = 0$

metric	hourly values			annual
	average	max	min	value
net load demand (MWh)	69,575	112,720	52,243	607.81×10^6
consumer payments (million \$)	4.066	14.901	2.076	35.52×10^3
congestion rents (million \$)	0.046	0.176	0.009	397.62
CO_2 emissions ($\times 10^6$ kgC)	10.866	21.115	7.439	102.54×10^3

the off-peak hours, the minimum and the average values of the relevant metrics increase as compared to scenario $\mathbb{D}_5$ without payback, but the the maximum values – associated with the peak load hours – remain the same. The increases in the off-peak hours result in higher values for the aggregate annual metrics as compared to the scenario $\mathbb{D}_5$ with $\chi^{\hat{b}} = 0$, but the metrics are still less than aggregate annual metrics for scenario $\mathbb{R}$.

Thus, the increased load consumption in the off-peak hours due to load recovery impacts the benefits associated with the DRR deployment. To further investigate impacts of load payback we compute the benefits for accrued due to the DRR curtailments for varying $\chi^{\hat{b}}$. We present the % reduction in the relevant metrics with respect to the metrics obtained from scenario $\mathbb{R}$ in Table 5.7. Note that we do not provide the benefits associated with the peak load hours in this table because they are the same for variations of the scenario $\mathbb{D}_5$ due to variation

Table 5.7: % reduction in the metrics of scenario $\mathbb{D}_5$ for varying $\chi^{\hat{b}}$

aggregate annual metrics	scenario $\mathbb{D}_5$ with			
	$\chi^{\hat{b}} = 0$	$\chi^{\hat{b}} = 0.5$	$\chi^{\hat{b}} = 0.7$	$\chi^{\hat{b}} = 1.0$
net load demand	1.54	0.78	0.48	0.02
consumer payments	10.51	9.24	8.69	7.87
congestion rents	34.54	33.25	32.82	31.50
CO_2 emissions	2.11	1.11	0.72	0.14

of $\chi^{\hat{b}}$. As $\chi^{\hat{b}}$ increases, a higher fraction of the demand curtailed during peak hours is recovered, which correspondingly increases the energy consumption. As a result, the benefits associated with the decrease in energy consumption and the lower CO_2 emissions are impacted. However, the reduction in the consumer payments and the congestion rents are relatively unaffected by the load recovery effects. Even with all of the curtailed load recovered, i.e., for $\chi^{\hat{b}} = 1.0$, the savings in the consumer payments and congestion rents with respect to the $\mathbb{R}$-scenario are as large as \$3 billion and \$186 million, respectively. We hypothesize that the shifting of the load demand from peak hours to off-peak hours results in more efficient utilization of the generation and transmission resources. Thus, DRRs improve the overall system utilization.

The simulation studies discussed in this section shed light on the impacts of the DRR aggregation on the system. The results clearly show that significant benefits may be achieved by incorporating DRRs in the resource mix. Some key insights include the following:

- DRR curtailments significantly improve the network congestion situation, as seen from the tangible decrease in the congestion rents.

- Even with the payback effects considered, the redistribution of the load from

peak to off-peak hours is advantageous since it results in substantial savings in the consumer payments and the congestion rents.

- The increasing penetration of DRRs causes further reduction in the peak loads thereby improving the capacity margin.

The improvement in the congestion and the capacity margin implies that there is a side-benefit associated with DRR curtailments – a possible deferral in the need for additional transmission and generation resources. We investigate these impacts in more detail in Section 5.5.

5.4 Application to Individual Player Studies

The simulation methodology may be used to assess the impacts of the DRRs on individual players. Since many utilities and energy service providers (ESPs) are rolling out demand response programs because of the associated benefits such as possible reduction in electricity payments and energy demands, we use the proposed methodology to analyze these benefits via simulations. We present the observation in this section.

We assume that an ESP at a particular node of the test system is considering the option of investing in DRR aggregation. The ESP, in effect, can participate in the market as a buyer of electricity as well as a seller of demand curtailment services. With ESP providing DRR services, the IGO has an additional resource to meet the demand requirements for the system. The simulation results from Section 5.3 indicate that the DRRs enrolled with the ESP under consideration are dispatched during the peak load hours when the electricity demand or prices are high. Thus, the ESP can benefit from avoiding consumption at high electricity prices. We use the proposed simulation methodology to thoroughly investigate

such benefits so as to provide sufficient information to the ESP to make the decision to invest in the DRR aggregation. We simulate the scenarios with and without DRR aggregation to compare the benefits accrued to the ESP by proceeding with the DRR aggregation project. We use as a reference here scenario $\mathbb{D}_5$ with 5,600 MW of the DRR capacity in the resource mix. As a result, the ESP, as a provider of DRR services, competes with other DRRs as well as generators when participating in the hourly DAMs. The ESP is obligated to reduce its demand by the specified amount for the hours in which the ESP offer in the DAM is successful. We investigate the impacts of the ESP participation in the power system operation as a DRR services provider.

We start with a comparison between scenario $\mathbb{D}_5$, without DRR aggregation at the ESP node and a DRR aggregation scenario with 100 MW DRR capacity at the ESP node. We ignore the payback effects for these simulations. The simulations provide the average values and the range for the hourly load demand, the LMP at the ESP node and the energy payments incurred by the ESP. We present the key statistics in Table 5.8. The simulation results clearly indicate the benefits

Table 5.8: Statistical information for the relevant metrics with and without 100 MW DRR aggregation

scenario	metric	average	range	
			max	min
scenario $\mathbb{D}_5$: without 100 *MW* DRR	net demand (MWh/h)	1,062	1,766	727
	LMP ($/MWh)	57.75	140.55	40.04
	energy payments ($/h)	66,307	255,353	29,125
scenario $\mathbb{D}_5$: with 100 *MW* DRR	net demand (MWh/h)	1,014	1,666	727
	LMP ($/MWh)	57.49	133.04	40.04
	energy payments ($/h)	62,697	226,286	29,875

accrued to the ESP by aggregating the loads with demand response capabilities. The high prices in the peak load hours result in the reduction of the net load of the ESP, due to the DRR curtailments. We use Fig. 5.6 to illustrate the reduction in the demand of the ESP during peak load conditions. We observe

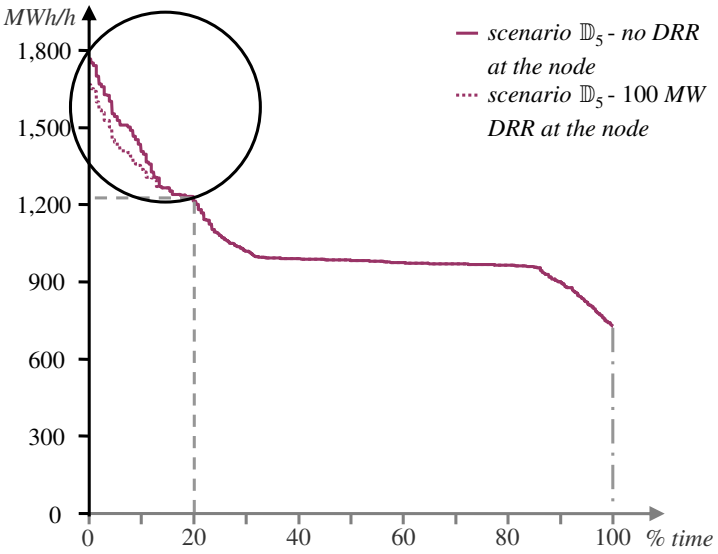

(a) annual LDCs of the ESP for the two scenarios

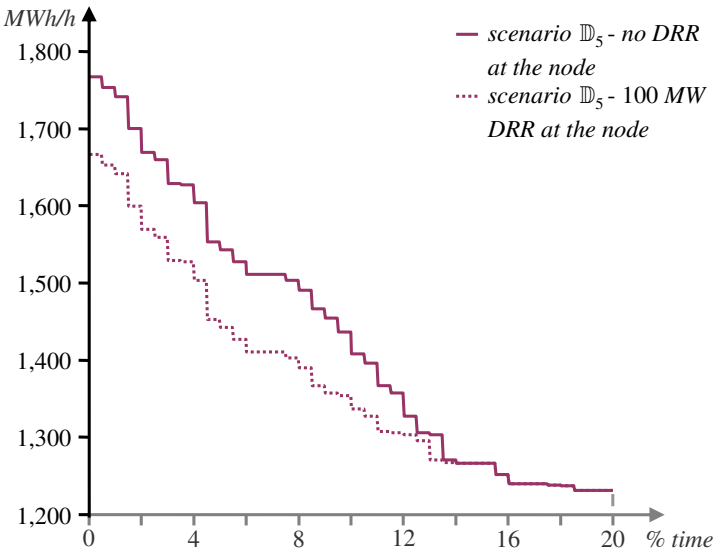

(b) blow-up of the circled region of (a)

Figure 5.6: Reduction in the load demand of an ESP via DRR aggregation

that the demand curtailment due to the effective use of DRRs is very high, over

70 MWh/h, for approximately 10% of all the hours in the year. However, the DRR aggregation as such is only dispatched for less than 15% of all the hours in the year because the prescriptive rules of the DAM allow the ESP to compete in the market for a limited set of hours. Nevertheless, even with such small reduction in the load demand of the ESP, the LMP of the node where the ESP is located is lowered. This is evident from the LMP duration curve presented in Fig. 5.7. The simulations quantify the benefits accrued to the ESP by lowering its demand requirements when the prices are high. Since the reduction in the demand of the ESP induces a reduction in the LMP of the node where the ESP is connected, the ESP buys its net demand requirements at a reduced price. In addition to these benefits, the ESP is compensated by the IGO for providing curtailment services, and hence the total payments that the ESP makes to the IGO are significantly lowered.

Since the simulation results establish that the ESP benefits from the DRR aggregation, the ESP may further employ the proposed methodology to choose an appropriate size of the DRR aggregation. We investigate the impacts of the aggregation size on the benefits accrued to the ESP by simulating scenarios with varying size of the DRR aggregation. We compute the total expected energy consumption and energy payments for different sizes of the DRR aggregation and present the same in Fig. 5.8. As the size of the DRR aggregation increases, we observe a reduction in the energy consumption and the energy payments incurred by the ESP. This implies that the effective use of the loads with demand response capability brings about large benefits associated with the load curtailments to the ESP. The magnitude of the reduction observed for the relevant metrics increases up to the aggregation size of 140 MW, after which there is negligible change in both the energy consumption and the energy payments. In effect, contrary to the popular belief that more demand response implies more benefits, the ESP

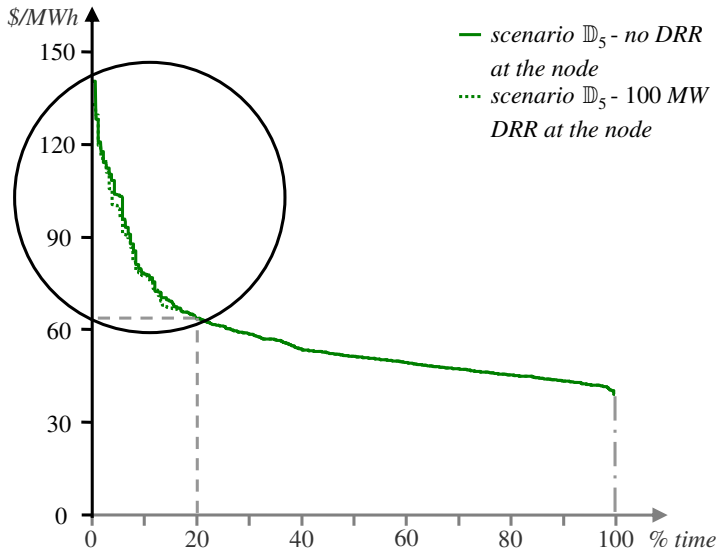

(a) annual LMP duration curve for the two scenarios

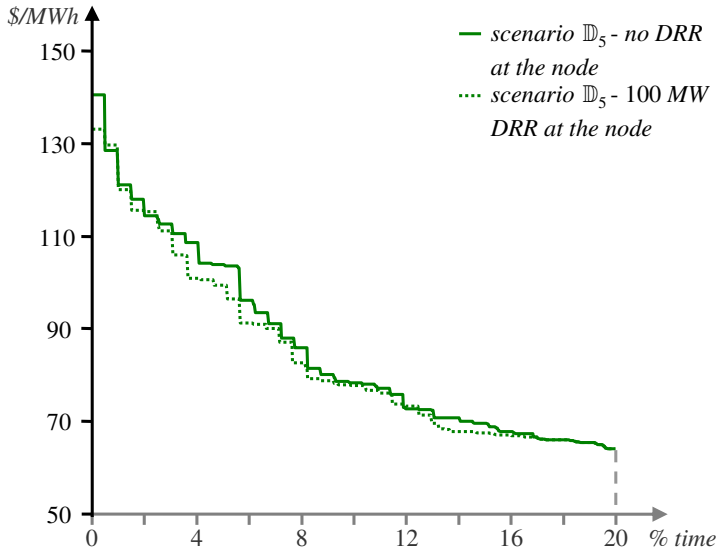

(b) blow-up of the circled region of (a)

Figure 5.7: Reduction in the LMP due to the DRR aggregation

cannot reap more benefits beyond an aggregation size of 140 MW. Hence, the ESP may choose 140 MW DRR aggregation. However, we note that increasing the aggregation size implies more consumers being enrolled with the ESP in the demand response program. In such cases, we need to carefully consider payback effects to quantify rigorously the benefits accrued to the ESP. Moreover, the ESP

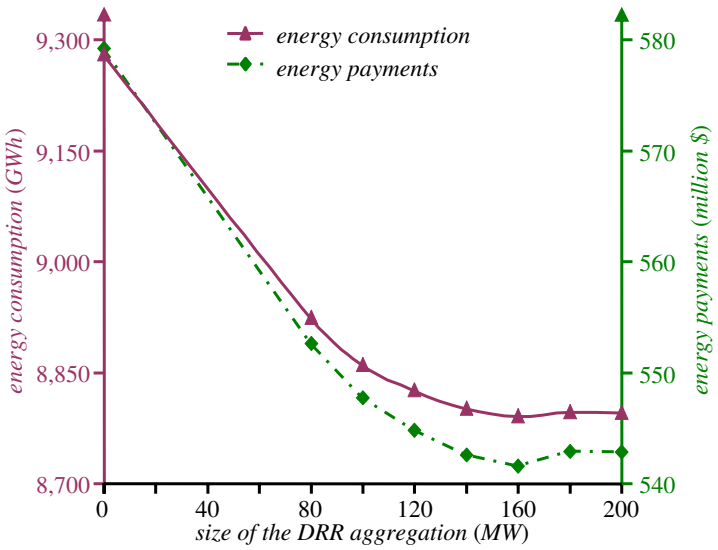

Figure 5.8: Impacts of the DRR aggregation size on the energy consumption and payments of the ESP

needs to also take into account the higher costs of control and metering equipment associated with the increasing aggregation size.

Before the ESP decides to implement a DRR aggregation of 140 MW, the ESP may want to consider the possible future developments in the subsequent year to successfully decide strategies for future growth of the DRR aggregation. We simulate the electricity system for the subsequent year using the same load patterns as the current year, but with a growth rate of 3%. We assume that all other parameters of the scenario $\mathbb{D}_5$ remain unchanged. We simulate multiple scenarios with increasing size of the DRR aggregation. We present the total expected consumption of the ESP and the energy payments for the varying sizes of DRR aggregation in Fig. 5.9. The results presented in Figs. 5.8 and 5.9 may be used to determine an appropriate size of the DRR aggregation for the current as well as the subsequent year.

The simulation studies presented in this section illustrate the applicability of the methodology to investment analyses performed by independent investors. The

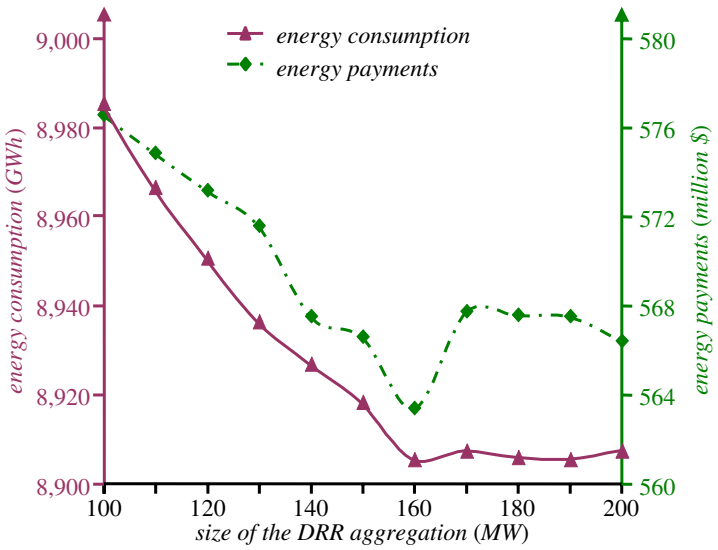

Figure 5.9: Impacts of the DRR aggregation size on the energy consumption and payments of the ESP in the subsequent year

simulation methodology imparts flexibility to the decision-maker, in this case – the ESP – to consider a wide range of future scenarios so as to ensure the economic viability of the candidate investment project and to make more informed decisions. The specific studies reported in this section highlight the benefits associated with the effective use of DRRs to aggregators such as ESPs and other load serving entities.

5.5 Applications in Planning and Analysis

The previous sections provide rigorous quantification of the impacts of DRRs on the system as well as on individual players. The substantial benefits associated with DRRs may result in a sizable DRR participation in the electricity industry. Thus, the DRRs and their impacts must be carefully represented in power system planning and analyses. In this section, we discuss the use the proposed simulation methodology to investigate the impacts of DRRs on the transmission and generation investments. We also present case studies which compare the DRR ag-

gregation benefits with two related demand-side activities – energy conservation measures and implementation of AMI.

The significant decrease in the congestion rents due to DRR deployments, as evident from simulations reported in Section 5.3, indicates a positive effect of the DRR curtailments on the network congestion. The decrease in the transmission congestion due to effective use of the DRRs may lower the need for investments in the transmission network. Hence, the interplay between the transmission congestion and DRR deployment needs to be appropriately investigated. For our investigations, we use scenario $\mathbb{R}$ and scenario $\mathbb{D}_5$ with $\chi^{\hat{b}} = 0$ reported in Section 5.3. These scenarios provide congestion signals for the dispatch of the generators without and with DRRs, respectively, for the existing transmission grid. We simulate scenarios $\mathbb{R}$ and $\mathbb{D}_5$ for an additional two cases in which we consider upgrades in the capacities of 3 and 5 transmission lines from the existing system so that the total transfer capability of the system is improved. The choice of the candidate lines for upgrades in the two additional case studies is based on the reference case simulation on the existing system.[3] We simulate the two cases, with 3 and 5 line upgrades in the existing system, with increased line flow limit for the selected lines. We compare congestion rents for the two scenarios – with and without DRRs – for each of the two cases with the improved transmission system. We present the congestion rents for the existing system and the two cases with transmission upgrades in Fig. 5.10.

First, we observe that an improvement in the transfer capability of the transmission grid results in a decrease in the congestion rents for both the sets of scenarios – with and without DRRs. However, the reduction in the congestion

[3]We analyze the congestion rents and the LMP differences in the $\mathbb{R}$-scenario simulation on the existing system to choose candidate pair of nodes for which the LMP difference is very high. For each selected node pair, we upgrade that line in the path between the nodes which determines the transfer capability between the node pair.

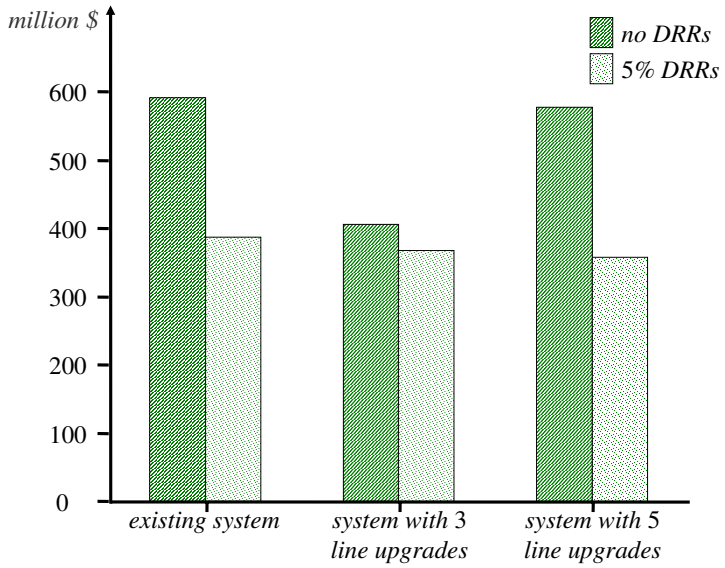

Figure 5.10: Congestion rents for the scenarios with and without DRRs for cases with transmission line upgrades

rents is more drastic for the scenarios without DRRs, as compared to the scenarios with DRRs. Second, a comparison between the relative decrease from scenario $\mathbb{R}$ to scenario $\mathbb{D}_5$ for each of the three system cases indicates that the improvements in the transfer capability reduce the DRR benefits associated with the decrease in the congestion rents. Third, we note the most significant observation from these case studies – the lowest congestion rents in scenario $\mathbb{R}$ without DRRs – \$406 million for the case with 3 line upgrades on the existing transmission grid – are higher than the congestion rents in scenario $\mathbb{D}_5$ with DRRs, \$387 million, on the existing transmission system. Thus, effective utilization of the DRRs leads to more reduction in the congestion rents than undertaking the capital intensive projects such as transmission line upgrades. This finding also implies that the DRR integration into power system operations may defer the need for additional transmission.

Next, we investigate the impacts of DRRs on the need for additional generation. The reduction in the peak load demand, as revealed from the scenario $\mathbb{R}$ and

scenario $\mathbb{D}_5$ simulations reported in Section 5.3, improves the capacity margin by 3.65%. The reduced peak demand requirements result in less utilization of the peaking units and may impact the need for additional peaking units. To analyze such impacts, we simulate the power system operations for the subsequent year, assuming 3% growth in the demand and with no modifications in the resource mix. We compute the hourly dispatched generation for each of the two scenarios and compare it with the original demand requirements of the system. The simulation studies indicate that there is a shortage of available generation for 2% of the peak hours in the scenario $\mathbb{R}$ without DRRs, which results in mandatory curtailment in the load demand at a few nodes. However, in scenario $\mathbb{D}_5$ with DRRs, the voluntary curtailments by the DRR players at peak hours result in a reduction in the peak load demand and there is no shortage as such of available generation. We compare relevant planning metrics for the two scenarios in Table 5.9.

Table 5.9: Comparison between relevant metrics for the subsequent year

aggregate annual metrics	scenarios	
	$\mathbb{R}$	$\mathbb{D}_5$
expected net demand ($\times 10^6$ MWh)	617.45	610.93
expected peak demand ($\times 10^6$ MWh)	40.39	39.18
expected unserved energy (MWh)	95,950	0
maximum mandatory curtailment (MWh/h)	876	0
peak net load (MW)	119,418	114,206
capacity margin (%)	11.54	15.40

We present the annual LDC and the duration curves for the dispatched generation for the two scenarios in Fig. 5.11. The generation dispatch with DRRs is lower because the demand requirements get modified due to DRR curtailments.

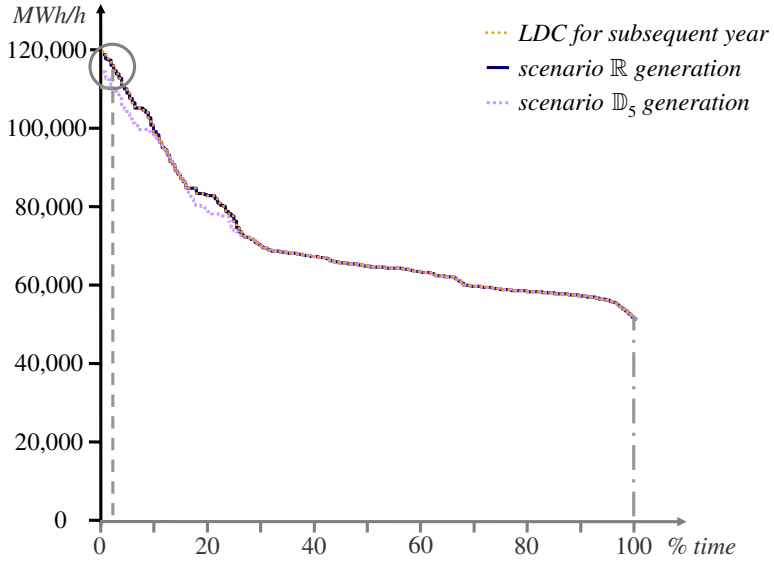

(a) duration curves for the dispatched generation for the subsequent year

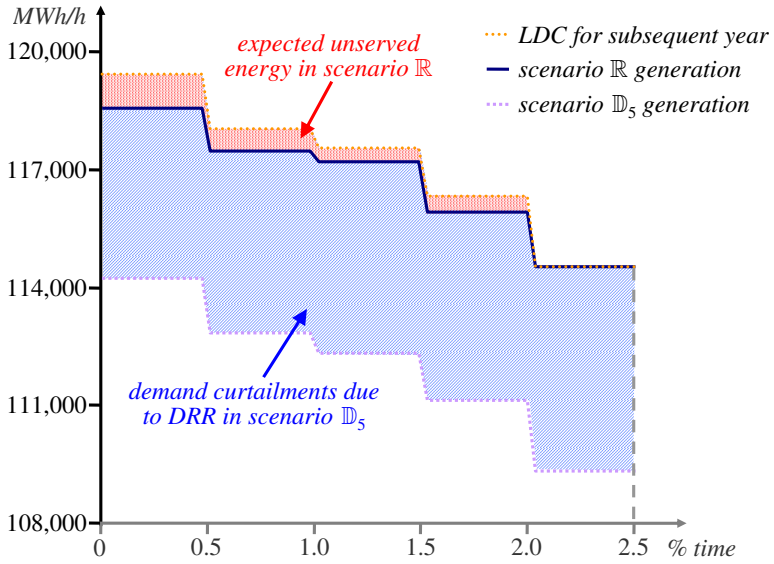

(b) blow-up of the circled region in (a)

Figure 5.11: Comparison between the dispatched generation in scenarios $\mathbb{R}$ and $\mathbb{D}_5$ for the subsequent years

However, for the scenario without DRRs, the forecasted demand requirements are to be met only with the available generation. The illustration in Fig. 5.11(b) clearly indicates the shortage of the dispatched generation in the 2% of all the hours in scenario $\mathbb{R}$. We note that to prevent this generation shortage, an ad-

ditional peaking generation of approximately 900 MW is needed. However, with the effective use of DRRs this need for new generation is indeed deferred. Thus, DRR deployments impact the supply-side additions.

Next, we investigate the application of the methodology to analyze the impacts of other demand-side activities. We first focus on the energy conservation measures. Suppose a new energy conservation policy calls for a reduction in the base load demand of the system by $2,500$ MW. Since the base load reduction results in around-the-clock savings in the energy consumption, we can easily compute the savings in the net energy demand, as follows:

$$\begin{aligned} \textit{reduction in the net demand} &= 2,500 \text{ MW } \times (168 \cdot 52) \text{ hours} \\ &= 21,840,000 \text{ MWh} \end{aligned}$$

From the reference scenario with out DRRs, scenario $\mathbb{R}$, we compute the average cost of electricity as \$ 63.69 per MWh. Hence, we may be tempted to evaluate the reduction in the total consumer payments as follows:

$$\begin{aligned} \textit{reduction in consumer payments} &= 21,840,000 \text{ MWh } \times 63.69 \text{ \$/MWh} \\ &= \text{\$ } 1,391,082,803 \end{aligned}$$

But this computation ignores the network and market effects. To appropriately assess the benefits, we simulate scenario $\mathbb{C}$ with the conservation policy implemented. We evaluate the hourly dispatched load for the scenario $\mathbb{C}$ simulation and compare the same with scenario $\mathbb{R}$. We compare the LDC for both the scenarios in Fig. 5.12.

With implementation of the base load reduction, we observe a downward shift in the LDC. Due to load reduction at all the hours, including the peak hours,

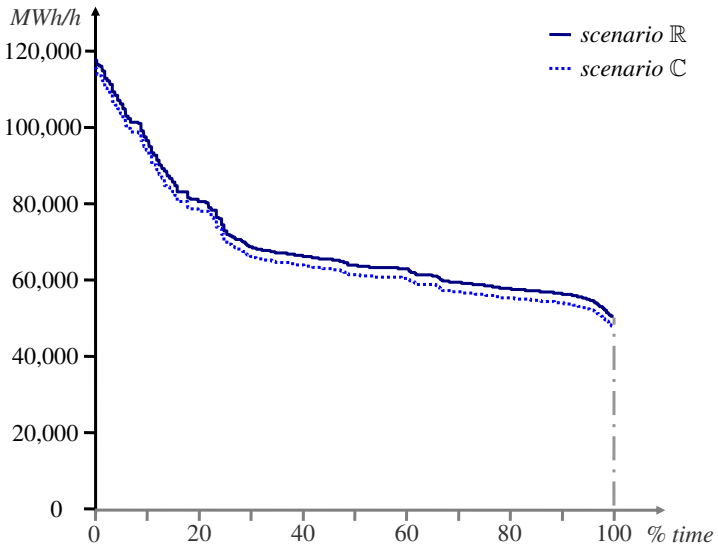

Figure 5.12: Impacts of conservation measures on the annual LDC

the consumer payments at the peak hours are reduced in scenario $\mathbb{C}$ as compared to scenario $\mathbb{R}$. We compute the aggregate annual metrics for scenario $\mathbb{C}$ and compare it with scenario $\mathbb{R}$ in Table 5.10. The base load reduction results in

Table 5.10: System-wide metrics for scenario $\mathbb{C}$

metrics	annual value	reduction with respect to scenario $\mathbb{R}$	
		decrease	% decrease
net energy demand ($\times 10^6$ MWh)	588.89	21.84	3.57
consumer payments (billion \$)	34.29	4.61	11.87
congestion rents (million \$)	379.96	211.92	35.80
CO_2 emissions ($\times 10^9$ kgC)	98.15	5.14	4.98

overall reduction in all the metrics of interest as compared to the $\mathbb{R}$-scenario. First, we observe that the savings in the consumer payments are over \$4 billion. The simple calculation approach, which indicates this reduction to be of the order of just over \$1 billion, does indeed underestimate the benefits of load conservation.

Second, we note that the reductions in the consumer payments and the congestion rents resulting from energy conservation measures are not very much different from those due to DRR curtailments. However, the saving in the total net energy demand and CO_2 emissions are more for scenario $\mathbb{C}$ as compared to scenario $\mathbb{D}_5$ due to the around-the-clock nature of the load conservation program as against the restrictive nature of DRR curtailments.

We now focus on the use of the AMI infrastructure. The incorporation of advanced metering techniques imparts flexibility to the end-use consumers to avoid consumption when the electricity prices are high and to shift their peak-hour demands to the hours when the electricity prices are low. The overall impact of the integration of the AMI results in a redistribution of the load. The impacts on the load shape due to AMI are similar to the case where DRR curtailments induce load payback effects in the off-peak hours. However, unlike the situation with DRRs, the load of the consumers with AMI is no longer a system resource, since such loads are controlled by the consumers themselves and not by the IGO. The consumers manage their load consumption according to their preferences and willingness to pay. Consequently, such loads do not receive any compensation from the IGO for avoiding consumption during the high price hours. To investigate the impacts of the AMI integration into the power grid, we simulate the scenario $\mathbb{A}$ with a few loads having the AMI installed.[4] The total capacity of the load equipped with AMI is 5,600 MW.

We specify the nodes where consumers with advanced meters are located and define for each consumer the threshold beyond which the consumers switch off their demands. The total demand curtailed is recovered during the hours when the electricity prices are below the specified thresholds. We assume that the

[4]In fact, we assume that the loads which possessed demand response capabilities in scenario $\mathbb{D}_5$ are equipped with AMI, and are no longer being used as DRRs. This assumption provides a consistent basis for comparison between the AMI and DRR scenarios.

load recovery is uniform throughout all the recovery hours. We compare the scenario $\mathbb{A}$ simulation with scenario $\mathbb{R}$ of Section 5.3 to evaluate the impacts of AMI integration. We illustrate the LDCs for scenarios $\mathbb{R}$ and $\mathbb{A}$ in Fig. 5.13. The demand curtailments during peak hours and demand recovery during the

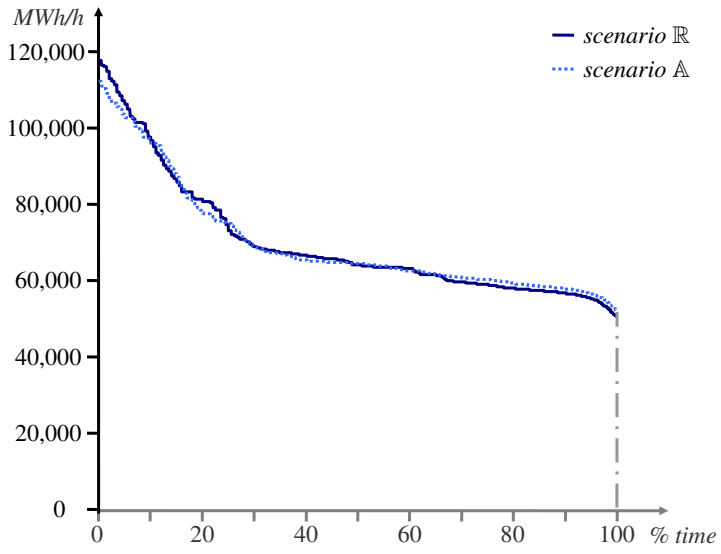

Figure 5.13: Impacts of AMI deployment on the annual LDC

off-peak hours redistribute the load, in much the same way as that due to DRR deployments with payback. The load shifting is triggered by the LMPs and the willingness to pay of each consumer with AMI. Since the consumers with AMI recover all their load, the area under both the LDCs is the same, i.e., the total energy consumption for both the scenarios is the same. The load reduction at the peak hours decreases the peak-hour consumer payments.

We compute the aggregate annual metrics for scenario $\mathbb{A}$ and compare it with the scenario $\mathbb{R}$ in Table 5.11. Since all the curtailed demand is recovered, the net energy demands for both the scenarios are similar.[5] This translates into similar CO_2 emissions in both cases. However, the utilization of the units differs for the

[5]The slight variation in the annual energy demand observed from the simulation results is due to the sampling and the LHS-based approximation techniques.

Table 5.11: System-wide metrics for scenario $\mathbb{A}$

metrics	annual value	reduction with respect to scenario $\mathbb{R}$	
		decrease	% decrease
net energy demand ($\times 10^6$ MWh)	610.29	0.07	0.44
consumer payments (billion \$)	35.88	7.76	3.02
congestion rents (million \$)	411.26	30.52	180.62
CO_2 emissions ($\times 10^9$ kgC)	103.07	0.21	0.22

two scenarios because of the load redistribution effects. The scenario $\mathbb{A}$ utilizes the generation units more efficiently. We compare the reduction in the consumer payments and the congestion rents for scenario $\mathbb{A}$ and scenario $\mathbb{D}_5$ with $\chi^{\hat{b}} = 1.0$. The comparison indicates that the impacts of the AMI integration into the power system are similar to the impacts of DRR curtailments with payback effects taken into account. The primary difference between the two scenarios is that with AMI, the load control lies with the consumers, whereas with DRRs, the load is controlled by the IGO.

The application studies reported in this section demonstrate the capability of the proposed simulation methodology to answer many different *what-if* questions. The versatile nature of the proposed methodology makes it usable for different power system planning and analysis studies. The specific studies reported here provide several key insights:

- The reduction in the congestion rents due to the DRR curtailments is more than the reduction due to transmission upgrades. Hence, DRRs provide cheaper means to reduce transmission congestion as compared to incurring heavy investments in transmission upgrades.

- The deployment of DRRs helps avoid *loss of load* situations that may arise

due to the unavailability of generation capacity. DRR curtailments bring about a tangible reduction in the total loading of the generation units, thereby impacting the need for additional generation.

- The load conservation measures are more effective in reducing CO_2 emissions and the total loading of the generators as compared to the DRR curtailments.

- The nature of the net cleared demand due to implementation of the AMI and the associated variable effects are similar to the corresponding variable effects of the scenario with DRR integration and load recovery effects.

The simulation studies and results illustrate how the proposed methodology provides the means to quantify a wide range of benefits associated with the DRR integration and other related demand-side activities.

5.6 Concluding Remarks

In this chapter, we present many different applications of the simulation methodology developed in Chapter 4 for power system studies. We conclude the chapter with a recap of the key insights obtained from the simulations.

We start off with the analysis of the system-wide impacts of DRRs. The curtailment due to DRRs reduces the load during the peak hours in the study period. The reduced demand results in a more effective utilization of the existing system resources, including the transmission grid. The DRR curtailments result in a substantial decrease in the consumer payments and the congestion rents. Increasing DRR penetration in the system requires careful analysis of the payback effects. A thorough study of the load recovery phenomena indicates that even with all the curtailed demand recovered, the load redistribution due to the DRRs results

in substantial reduction in the congestion rents and the consumer payments.

We provide illustrative examples of the application of the proposed simulation methodology to individual player studies. We use the methodology to assess the benefits accrued to an ESP by investing in a DRR aggregation. The ESP may use the methodology to simulate many possible future scenarios so as evaluate economic feasibility of the DRR aggregation and determine investment and growth strategies for the future.

We use the simulation methodology to investigate the interplay between transmission and generation investments and DRR deployment. Study results indicate that effective use of DRRs does indeed defer the need for additional transmission and generation resources. We demonstrate the application of the tool for assessing the impacts of energy conservation and AMI integration. We observe similarities in the system variable effects due to the implementation of AMI and the deployment of the DRRs.

The simulations reported in this chapter demonstrate the wide range of questions which may be answered using the proposed methodology. The simulation results provide comprehensive quantifications of the impacts of DRRs on the system as a whole as well as on individual players.

CHAPTER 6

CONCLUSIONS

In this chapter, we summarize the work presented in this report. We also discuss the directions for future research that can be developed using the progress reported in this work.

6.1 Summary

In this report, we focus on the impacts of DRRs on the variable effects of systems. We study such impacts over longer-term periods. We present the modeling required to develop the simulation methodology for the evaluation of DRR impacts over longer-term study periods. The proposed methodology accommodates detailed representations of the competitive markets which provide a platform for the DRRs to compete with the supply-side resources and the transmission considerations which impact the dispatch decisions of the IGO. A salient characteristic of the proposed methodology is the explicit representation of the various sources of uncertainty including the variability in the load demand, the availability of the generation units, the behavior of the market participants, the transmission congestion and the outcomes of the transmission-constrained markets. Moreover, the methodology is constructed so as to take into consideration the long-term changes to the system such as generator unit additions/retirements, transmission upgrades/additions and policy changes which may occur during the study period and which impact the operations of the IGO. We provide the implementational

steps to ensure computational tractability. The implementation of the methodology takes advantage of the nature and the structure of the power systems and the electricity markets to bring about tangible reductions in the computing.

An important tool used in the proposed methodology is the model of the transmission-constrained electricity market mechanism with DRR players. We model the decision making problem for the IGO to determine the dispatch of the generators and the DRRs in such a way as to ensure the feasibility of the schedules with respect to the transmission constraints. The analysis of the IGO's problem determines the outcomes of the market and provides quantification of the variable effects of the system. In particular, the problem solution determines the most economic dispatch of the generators and the DRRs so as to met the demand requirements of all the demand-side buyers and maintain the supply-demand balance. The solution also provides the LMPs which determine the revenues (payments) for all the sellers (buyers). We use this market model with DRRs extensively in the simulation methodology development.

We present in this report the construction of a simulation engine which may be used to emulate the electricity production of the systems with integrated DRRs. We construct the engine in such a way as to take into consideration the various sources of uncertainty as well as the impacts of transmission constraints and competitive market outcomes. The principal challenge in the engine construction is to effectively integrate the time-dependent nature of transmission-constrained markets into the probabilistic simulation of the system for longer-term periods. We overcome this challenge by developing an extended probabilistic simulation approach which accommodates temporal effects associated with the systems with DRRs. The extended probabilistic simulation approach is developed through suitable modifications to the probabilistic representation of the load and the extensive use of the transmission-constrained market model to approximate the cdf's of the

market outcomes. The simulation engine constitutes one of the contributions of this report and becomes a key building block in the development of the overall simulation methodology.

In order to use the simulation engine in the proposed simulation methodology, we partition the long-term study period into shorter periods which may be simulated by the engine. The simulation periods are defined in such a way that the requirements and the assumptions of the extended probabilistic simulation approach are met. In particular, the resource mix, the transmission grid, the policy environment and the seasonality effects remain unchanged during each simulation period. We use innovative schemes and mechanisms to achieve the computational tractability in the implementation of the proposed methodology. The judicious selection of the representative simulation periods and the use of Latin hypercube sampling technique bring about significant reductions in the computing.

We demonstrate the application of the proposed methodology to a few representative studies on a large-scale test system. The simulation studies reported provide, in their breadth, ample illustration of the capabilities of the proposed methodology to determine practical solutions to a wide range of problems in the areas of power system planning and analysis. The reported simulation results are representative of the range of benefits the integration of DRRs in the system can provide. DRR aggregations can act as controllable resources that "shave off" the peak load demands, resulting in a more efficient utilization of the installed generators and transmission assets. We are able to quantify the significant reductions in the total energy consumption, the consumer payments, the CO_2 emissions and the congestion rents due to deployment of the DRRs. In particular, as the penetration of DRRs becomes more significant, tangible reductions in the peak load consumption can be achieved. In fact, the peak-shaving capabilities of the DRRs impact the utilization of peaking units and also defer the need for addi-

tional peaking generation. Furthermore, the simulation results indicate that in certain situations, it is cheaper and more beneficial to deploy DRRs and reduce transmission congestion than undertake capital-intensive transmission upgrades.

The proposed simulation methodology provides a comprehensive quantification of the benefits of DRRs to the system as well as to individual players. The reported simulation results better our understanding of the impacts of the DRRs and serve to further the state of the art.

6.2 Directions for Future Work

The proposed methodology provides a good starting point for the development of quantitative tools that hitherto did not exist. There are numerous natural/logical extensions that may be introduced to enhance the capabilities of the proposed methodology. We discuss, in this section, the potential modifications/extensions to the current models and methodology.

We use a simplified representation of the market players' behavior, in the sense that we assume "price-taking" behavior for all market players. However, there are several questions which remain unanswered due to this assumption. For example, we are not able to determine how the behavior of the supply-side sellers is affected in the light of DRR curtailment offers. Similarly, we are not able to take into account profit-maximizing behavior for the DRR players, wherein they bid for demand and offer load curtailments so as to maximize their overall profits. The interactions between the supply-side and the demand-side in the light of profit-maximizing and strategic behavior of the players can provide meaningful insights to shape policies and regulatory guidelines for the market operations. Such behavioral considerations need to be carefully investigated and modeled. The extension of the models used in the proposed methodology for such analysis

is a good topic for future research.

Another topic of intense interest is the addition of new transmission lines for the reliable integration of renewable generation into the power system. The methodology used in the report is applicable to systems with controllable resources such as thermal generators and DRRs. The extension of the models to incorporate renewable generation technologies such as wind and solar generation requires the careful consideration of the intermittency effects associated with the renewable technologies. The simulation engine is equipped to accommodate the uncertainty associated with the demand and generator availability. Suitable modifications need to be made to incorporate the variability in the output of the wind and solar generation; such changes may necessitate the use of higher levels of detail. The challenge is to efficiently handle the added computational requirements. Another issue to address is the prediction of the wind/solar patterns over longer-term study periods.

We have so far limited the scope of our discussions to energy markets. However, DRRs are extensively used to provide operating reserves. Hence there is a need to include additional electricity markets of the ancillary service type in the proposed methodology for a more comprehensive evaluation of the services provided by DRRs. To meet this need, we require the incorporation of the models for ancillary service markets in addition to the representation of the energy commodity markets. In this way, the interrelationships between the energy and the ancillary service markets are explicitly represented. The efforts to represent the additional markets are important developments to improve the abilities of the methodology to capture the interrelationships between the markets.

In terms of risk management, we may extend the models to incorporate the financial transmission rights (FTR) markets as well as the forward contract auctions. The FTR markets are, essentially, orthogonal to the energy markets and

provide the means to the FTR holders to get reimbursement for the congestion costs incurred to implement the transactions schedule in the energy markets. The pattern of the FTR holdings may impact the bidding behavior of the market players and hence necessitates additional modeling. Similarly, the forward contracts serve as hedging tools used by the market participants to insure themselves against the uncertainty of the energy market outcomes. The inclusion of forward contract obligations entails modification to the IGO's dispatch problem. The extension of the methodology to include ancillary services and risk management tools is a major undertaking. Such a development could, however, enhance the usefulness of the extended methodology.

The suggested topics in this section provide a few fruitful directions for future research in extending the proposed methodology so as to incorporate additional capabilities for more comprehensive assessments of the variable effects of systems with DRRs.

APPENDIX A

ACRONYMS AND NOTATION

A.1 Acronyms

DRR	Demand response resource
DSM	Demand-side management
IGO	Independent grid operator
ISO	Independent system operator
RTO	Regional transmission operator
ESP	Energy service provider
FERC	Federal Energy Regulatory Commission
DAM	Day-ahead market
LMP	Locational marginal price
MCP	Market clearing price
OPF	Optimal power flow
LDC	Load duration curve
cdf	cumulative distribution function
rv	random variable
AM	Assessment manager
SM	Scenario manager
LRF	Load recovery factor
AMI	Advanced metering infrastructure

A.2 Notation

The following are the key aspects of the notation used:

- all variables are in italics
- all vectors and matrices are in **bold** and underlined
- all optimal solutions are contained inside the notation $[\,\cdot\,]^*$
- all rv's have tilde $\tilde{}$ under them
- all market-related indices are in superscripts
- all network-related indices are in subscripts
- all time-related indices are subscripts of the round brackets $(\cdot)$ enclosing the variable

The list of indices is

s : seller

$\hat{b}$: DRR player

$\bar{b}$: pure buyer

n : node

j : line

i : generator unit

h : subperiod

t : simulation period

k : daily subperiod

d : day

The indices come from the following sets:

$\mathcal{S} = \{s \,:\, s = 1, 2, \ldots, S\}$: set of supply-side sellers

$\widehat{\mathcal{B}} = \left\{\hat{b} \,:\, \hat{b} = 1, 2, \ldots, \hat{B}\right\}$: set of DRR players

$\bar{\mathcal{B}} = \{\bar{b} : \bar{b} = 1, 2, \ldots, \bar{B}\}$: set of pure buyers

$\mathcal{N} = \{n : n = 0, 1, \ldots, N\}$: set of buses

$\mathcal{J} = \{j : j = 1, 2, \ldots, J\}$: set of lines

$\mathcal{I} = \{i : i = 1, 2, \ldots, I\}$: set of generator units

$\mathcal{H} = \{h : h = 1, 2, \ldots, H\}$: set of hours in period t

$\mathscr{T} = \{t : t = 1, 2, \ldots, T\}$: set of simulations periods in the study period

$\{k : k = 1, 2, \ldots, K\}$: set of subperiods in a day

$\{d : d = 1, 2, \ldots, D\}$: set of days in period t

The network parameters for a single subperiod are

$\underline{\hat{\boldsymbol{A}}}$: augmented branch-to-node incidence matrix

$\underline{\boldsymbol{A}}$: branch-to-node incidence matrix

$\underline{\hat{\boldsymbol{B}}}$: augmented nodal susceptance matrix

$\underline{\boldsymbol{B}}$: nodal susceptance matrix

$\underline{\boldsymbol{B}}_d$: diagonal branch susceptance matrix

f_j^{max} : maximum power flow through line j

The market offer/bid functions for a single subperiodic DAM are

$\mathscr{C}^s(\cdot)$: integral of the marginal offer function of seller s

$\mathscr{B}^{\bar{b}}(\cdot)$: integral of the marginal bid function of buyer $\bar{b}$

$\mathscr{C}^{\hat{b}}(\cdot)$: integral of the marginal offer function of DRR $\hat{b}$ as a seller

$\mathscr{B}^{\hat{b}}(\cdot)$: integral of the marginal bid function of DRR $\hat{b}$ as a buyer

The decision variables of IGO's market clearing problem for a single DAM are

p^s : electricity sold by seller s

$p^{\bar{b}}$: electricity purchased by buyer $\bar{b}$

$p^{\hat{b}}$: electricity purchased by DRR $\hat{b}$ as a buyer

$\hat{p}^{\hat{b}}$: load curtailment sold by DRR $\hat{b}$ as a seller

p_n^g : total electricity sold at node n

p_n^d : total electricity purchased at node n

$\hat{p}_n^d$: total load curtailment sold at node n

f_j : real power flow through line j

θ_n : voltage phase angle at node n

λ_n : LMP at node n

All electricity commodities are expressed as MWh/h while the load curtailment is expressed as MW/h. All prices are in \$/h.

The rv's used in the analysis of a single simulation period are

$\underset{\sim}{L}$: system load

$\underset{\sim}{A}^i$: available generation capacity of generator i

$\underset{\sim}{P}^i$: electricity sold by generator i

$\underset{\sim}{P}^{\bar{b}}$: electricity purchased by pure buyer $\bar{b}$

$\underset{\sim}{P}^{\hat{b}}$: electricity purchased by DRR $\hat{b}$ as a buyer

$\underset{\sim}{\hat{P}}^{\hat{b}}$: load curtailment sold by DRR $\hat{b}$ as a seller

$\underset{\sim}{\Lambda}_n$: LMP at the node n

$\underset{\sim}{W}^i$: revenues of generator i

$\underset{\sim}{W}^{\bar{b}}$: payments from pure buyer $\bar{b}$

$\underset{\sim}{W}^{\hat{b}}$: payments from DRR player $\hat{b}$

$\underset{\sim}{\mathcal{K}}$: congestion rents collected by IGO

$\underset{\sim}{L}^g$: system net load met using generator offers

We denote the realizations of these rv's by ℓ, α^i, p^s, $p^{\bar{b}}$, $p^{\hat{b}}$, $\hat{p}^{\hat{b}}$, λ_n, w^i, $w^{\bar{b}}$, $w^{\hat{b}}$, κ and ℓ^g respectively.

The metrics from the individual player's point of view for a single simulation period include the following:

$\mathcal{E}^i$: generation of unit i

$\mathcal{E}^{\bar{b}}$: demand of pure buyer $\bar{b}$

$\mathcal{E}^{\hat{b}}$: demand of DRR $\hat{b}$

$\hat{\mathcal{E}}^{\hat{b}}$: load demand curtailment of DRR $\hat{b}$

$\mathcal{W}^{i}$: revenues of unit i

$\mathcal{W}^{\bar{b}}$: payments from pure buyer $\bar{b}$

$\mathcal{W}^{\hat{b}}$: payments from DRR $\hat{b}$

The metrics from the system's point of view for a single simulation period include the following:

$\mathcal{E}$: total system load demand

$\mathcal{E}^{g}$: net system load demand

$\mathcal{W}^{\mathcal{I}}$: revenues of the generators

$\mathcal{W}^{\hat{\mathcal{B}}}$: payments from pure buyers

$\mathcal{W}^{\widehat{\mathcal{B}}}$: payments from DRRs

$\mathcal{K}$: congestion rents

$LOLP$: loss of load probability

$\mathcal{U}$: expected unserved energy

APPENDIX B

LATIN HYPERCUBE SAMPLING

The Latin hypercube sampling technique is widely employed for generating input samples for Monte Carlo simulations. The use of Latin hypercube sampling reduces the number of input samples to be picked. We describe here the general procedure for obtaining a Latin hypercube sample (LHS) of size M from $\underset{\sim}{\boldsymbol{X}} = \left(\underset{\sim}{X}_1, \ldots, \underset{\sim}{X}_I\right)$, where $\underset{\sim}{\boldsymbol{X}}$ has independently distributed components. Stein [48] discusses the implementation of LHS when $\underset{\sim}{\boldsymbol{X}}$ has dependent components, but we will not consider the dependent case here.

The concept for the sampling is as follows. Suppose we want to pick $\underline{x}_1, \ldots, \underline{x}_M$ samples, which together constitute the LHS. Note that each sample is given as $\underline{x}_m = (x_{m1}, \ldots, x_{mI})$, where x_{mi} is a sample from the i^{th} input variable $\underset{\sim}{X}_i$. To construct the LHS, the domain of each input variable $\underset{\sim}{X}_i$ is divided into M equal probability intervals. Each interval is represented in the LHS. The set of all possible Cartesian products of these intervals constitutes a partitioning of the I-dimensional sample space into M^I *cells*. A set of M cells is chosen from the M^I populations of cells in such a way that the projections of the centers of each of the cells onto each axis are uniformly spread across the axis; then a point is chosen at random in each selected cell.

The analytical explanation of the construction of the LHS is as follows: assume that for each $i = 1, \ldots, I$, the cdf of $\underset{\sim}{X}_i$, denoted by $F_{\underset{\sim}{X}_i}(\cdot)$, is known. We divide the i^{th} axis into M parts. Each of the parts have equal probability given by $\dfrac{1}{M}$

under $F_{\underset{\sim}{X}_i}(\cdot)$. The division points for the i^{th} axis are

$$F_{\underset{\sim}{X}_i}^{-1}\left(\frac{1}{n}\right), \ldots, F_{\underset{\sim}{X}_i}^{-1}\left(\frac{n-1}{n}\right)$$

To choose M of the cells so created, we create an $M \times I$ matrix $\underline{\boldsymbol{\Pi}}\,(\pi_{mi})$ having I columns which are different randomly selected permutations of $\{1, 2, \ldots, M\}$. Then, the i^{th} component of the m^{th} sample vector $\underline{x}_m$ is given by

$$x_{mi} = F_{\underset{\sim}{X}_i}^{-1}\left(\frac{1}{n}\left(\pi_{mi} - 1 + u_{mi}\right)\right)$$

where the $\{u_{mi}\}$ are independent and uniformly distributed deviates from the distribution $\sim U[0,1]$ for $m = 1, \ldots, M$ and $i = 1, \ldots, I$. To summarize, the m^{th} row of $\underline{\boldsymbol{\Pi}}$ identifies the cells from which components of $\underline{x}_m$ are sampled, while the corresponding uniform deviates determine the location of the sample components x_{mi} in the sampled cells.

Suppose we have two uniform rv's, $\underset{\sim}{X}_1$ and $\underset{\sim}{X}_2$, having distribution $\sim [0,1]$ as input variables and we want to construct an LHS of size 3. The sample space $[0,1] \times [0,1]$ into $3 \times 3 = 9$ cells. We need to choose 3 cells out of these 9 cells from which the input samples are chosen. In order to do this, we create a 3×2 matrix, $\underline{\boldsymbol{\Pi}}$. Figure B.1 illustrates the selection of cells for the sample space corresponding to two different $\underline{\boldsymbol{\Pi}}$'s. Any one set of cells may be selected and the samples are constructed by randomly choosing the samples $\underline{x}_m = (x_{m1}, x_{m2})$ within the cells.

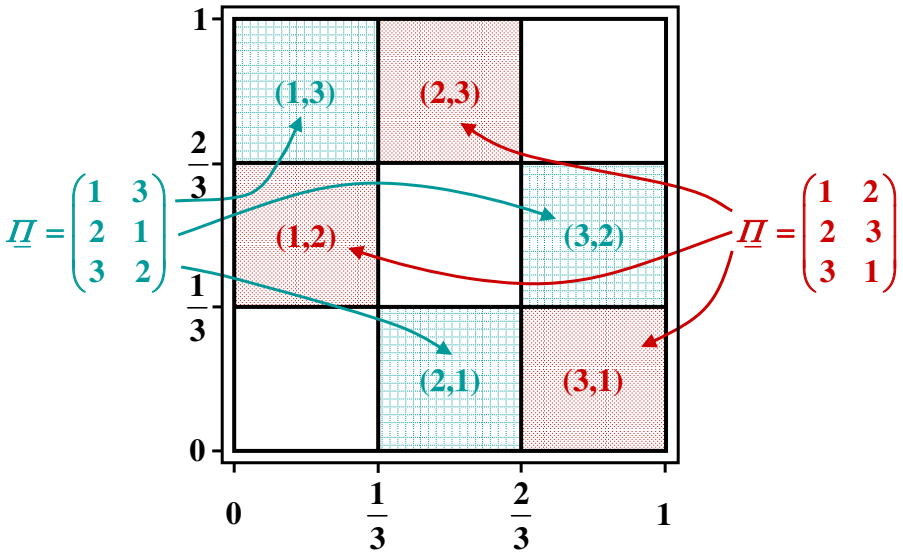

Figure B.1: Selection of cells in LHS

For example, supppose we choose the $\underline{\underline{\boldsymbol{\Pi}}}$ such that

$$\underline{\underline{\boldsymbol{\Pi}}} = \begin{pmatrix} 1 & 3 \\ 2 & 1 \\ 3 & 2 \end{pmatrix}.$$

Now, the first sample $\underline{x}_1 = (x_{11}, x_{12})$ is chosen such that the cdf of $\underset{\sim}{X}_1$ at the value x_{11} lies in the range $\left[0, \frac{1}{3}\right]$ while the cdf of $\underset{\sim}{X}_2$ at the value x_{12} lies in the range $\left[\frac{2}{3}, 1\right]$. Similarly, the second sample is chosen such that the cdf's of $\underset{\sim}{X}_1$ and $\underset{\sim}{X}_2$ evaluated at the sample points lie in the ranges $\left[\frac{1}{3}, \frac{2}{3}\right]$ and $\left[0, \frac{1}{3}\right]$, respectively, while the range of the cdf's for the third sample is given by $\left[\frac{2}{3}, 1\right]$ and $\left[\frac{1}{3}, \frac{2}{3}\right]$, respectively.

Reference [49] proves that the samples chosen using Latin hypercube sampling better represent the entire sample space of the inputs as compared to the samples chosen using simple random techniques.

REFERENCES

[1] C. Gellings, "The concept of demand-side management for electric utilities," *Proceedings of the IEEE*, vol. 73, no. 10, pp. 1468–1470, October 1985.

[2] NYISO Staff, *Day-Ahead Demand Response Program Manual*, July 2003. [Online]. Available: http://www.nyiso.com/public/webdocs/products/demand_response/day_ahead/dadrp_mnl.pdf

[3] PJM Member Training Department, *PJM Demand Side Response*, September 2008. [Online]. Available: http://www.pjm.com/~/media/training/core-curriculum/ip-dsr/20080930-pjm-demand-side-response-4.ashx

[4] ISO-NE Staff, *ISO New England Load Response Manual*, July 2003. [Online]. Available: http://www.iso-ne.com/rules_proceds/isone_mnls/index.html

[5] Boston Globe Business Team, "Four utilities sign contracts with EnerNOC," March 24, 2009. [Online]. Available: http://www.boston.com/business/ticker/2009/03/four_utilities.html

[6] J. S. John, "Comverge's home demand response: Pagers first, then smart meters," July 31, 2009. [Online]. Available: http://www.greentechmedia.com/articles/read/comverges-home-demand-response-pagers-first-then-smart-meters/

[7] "Energy Policy Act of 2005," August 8, 2005. [Online]. Available: www.epa.gov/oust/fedlaws/publ_109-058.pdf

[8] "Energy Independence and Security Act of 2007," December 19, 2007. [Online]. Available: http://www.govtrack.us/congress/billtext.xpd?bill=h110-6

[9] FERC Staff, "Assessment of demand response and advanced metering," Federal Energy Regulatory Commission, Tech. Rep., December 2008. [Online]. Available: http://www.ferc.gov/legal/staff-reports/12-08-demand-response.pdf

[10] Federal Energy Regulatory Commission, "Wholesale competition in regions with organized electric markets," Washington DC, July 16, 2009, Docket No: RM07-19-001, Order No. 719-A.

[11] G. Strbac, E. Farmer, and B. Cory, "Framework for the incorporation of demand-side in a competitive electricity market," *IEE Proceedings - Generation, Transmission and Distribution*, vol. 143, no. 3, pp. 232–237, May 1996.

[12] A. Borghetti, G. Gross, and C. A. Nucci, "Auctions with explicit demand-side bidding in competitive electricity markets," in *The Next Generation of Electric Power Unit Commitment Models*, B. F. Hobbs, M. H. Rothkopf, R. P. O'Neill, and H. po Chao, Eds. Norwell, MA: Kluwer Academic Publishers, 2001, vol. 36, pp. 53–74.

[13] R. Walawalkar, S. Blumsack, J. Apt, and S. Fernands, "Analyzing PJM's economic demand response program," in *2008 IEEE Power and Energy Society General Meeting - Conversion and Delivery of Electrical Energy in the 21st Century*, July 2008, pp. 1–9.

[14] C.-L. Su and D. Kirschen, "Quantifying the effect of demand response on electricity markets," *IEEE Transactions on Power Systems*, vol. 24, no. 3, pp. 1199–1207, August 2009.

[15] "A national assessment of demand response potential," Federal Energy Regulatory Commission, Tech. Rep., June 2009, prepared by The Brattle Group, Freeman, Sullivan & Co. and Global Energy Partners, LLC. [Online]. Available: http://www.ferc.gov/legal/staff-reports/06-09-demand-response.pdf

[16] L. Ruff, "Least-cost planning and demand-side management: Six common fallacies and one simple truth," *Public Utilities Fortnightly*, vol. 121, no. 8, pp. 19–26, April 28, 1988.

[17] C. Gellings and W. Smith, "Integrating demand-side management into utility planning," *Proceedings of the IEEE*, vol. 77, no. 6, pp. 908–918, June 1989.

[18] S. Borenstein, "The trouble with electricity markets: Understanding California's restructuring disaster," *The Journal of Economic Perspectives*, vol. 16, no. 1, pp. 191–211, 2002.

[19] E. Hirst, "Price-responsive demand in wholesale markets: Why is so little happening?" *The Electricity Journal*, vol. 14, no. 4, pp. 25–37, May 2001.

[20] A. Faruqui and S. S. George, "The value of dynamic pricing in mass markets," *The Electricity Journal*, vol. 15, no. 6, pp. 45–55, June 2002.

[21] R. H. Patrick and F. H. Wolak, "Real-time pricing and demand side participation in restructured electricity markets," in *Electricity Pricing in Transition*, A. Faruqui and K. Eakin, Eds. Norwell, MA: Kluwer Academic Publishers, 2002, vol. 42, p. 345.

[22] A. Faruqui and M. Mauldin, "The barriers to real-time pricing: Separating fact from fiction," *Public Utilities Fortnightly*, vol. 140, no. 13, pp. 30–40, July 15, 2002.

[23] K. Costello, "An observation on real-time pricing: Why practice lags theory," *The Electricity Journal*, vol. 17, no. 1, pp. 21–25, January 2004.

[24] L. Ruff, "Economic principles of demand response in electricity," Tech. Rep., October 2002, prepared for Edison Electric Institute, Washington, D.C.

[25] S. Borenstein, M. Jaske, and A. Rosenfeld, "Dynamic pricing, advanced metering and demand response in electricity markets," Center for the Study of Energy Markets, Tech. Rep. CSEM WP 105, October 2002. [Online]. Available: http://www.ucei.berkeley.edu/PDF/csemwp105.pdf

[26] M. L. Goldberg and G. K. Agnew, "Protocol development for demand-response calculations: Findings and recommendations," KEMA-Xenergy, Tech. Rep. 400-02-017F, February 2003, prepared for California Energy Commission. [Online]. Available: http://www.energy.ca.gov/reports/2003-03-10_400-02-017F.PDF

[27] K. Coughlin, M. A. Piette, C. Goldman, and S. Kiliccote, "Statistical analysis of baseline load models for non-residential buildings," *Energy and Buildings*, vol. 41, no. 4, pp. 374–381, April 2009.

[28] J. Bushnell, B. F. Hobbs, and F. A. Wolak, "When it comes to demand response, is FERC its own worst enemy?" Center for the Study of Energy Markets, Tech. Rep. CSEM WP 191, August 2009. [Online]. Available: http://www.ucei.berkeley.edu/PDF/csemwp191.pdf

[29] U. S. Department of Energy, "Benefits of demand response in electricity markets and recommendations for achieving them," February 2006. [Online]. Available: http://www.oe.energy.gov/DocumentsandMedia/congress_1252d.pdf

[30] G. C. Heffner and C. A. Goldman, "Demand responsive programs - An emerging resource for competitive electricity markets?" Lawrence Berkeley National Laboratory, Berkeley, CA, Tech. Rep. LBNL-48374, June 2001. [Online]. Available: http://repositories.cdlib.org/lbnl/LBNL-48374

[31] P. Cappers, C. Goldman, and D. Kathan, "Demand response in U.S. electricity markets: Empirical evidence," *Energy*, in press, corrected proof, 2009.

[32] H. S. Oh and R. Thomas, "Demand-side bidding agents: Modeling and simulation," *IEEE Transactions on Power Systems*, vol. 23, no. 3, pp. 1050–1056, August 2008.

[33] D. Menniti, F. Costanzo, N. Scordino, and N. Sorrentino, "Purchase-bidding strategies of an energy coalition with demand-response capabilities," *IEEE Transactions on Power Systems*, vol. 24, no. 3, pp. 1241–1255, August 2009.

[34] A. Faruqui, R. Hledik, S. Newell, and H. Pfeifenberger, "The power of 5 percent," *The Electricity Journal*, vol. 20, no. 8, pp. 68–77, October 2007.

[35] F. C. Schweppe, M. C. Caramanis, R. D. Tabors, and R. E. Bohn, *Spot Pricing of Electricity*. Norwell, MA: Kluwer Academic Publishers, 1988.

[36] A. J. Wood and B. F. Wollenberg, *Power Generation, Operation and Control*, 2nd ed. New York, NY: John Wiley and Sons, Inc., 1996.

[37] S. Stoft, *Power System Economics: Designing Markets for Electricity*. New York, NY: Wiley-IEEE Press, 2002.

[38] P. I. Caro-Ochoa, "Evaluation of transmission congestion impacts on electricity markets," M.S. thesis, Department of Electrical and Computer Engineering, University of Illinois at Urbana-Champaign, 2003.

[39] M. Liu, "A framework for congestion management analysis," Ph.D. dissertation, Department of Electrical and Computer Engineering, University of Illinois at Urbana-Champaign, 2005.

[40] G. Gross, *Class notes for ECE 588 - Electricity Resource Planning*, 2008. [Online]. Available: http://courses.ece.illinois.edu/ece588/

[41] R. Sullivan, *Power System Planning*. New York, NY: McGraw Hill International Book Company, 1977.

[42] M. McKay, R. Beckman, and W. Conover, "Comparison of three methods for selecting values of input variables in the analysis of output from a computer code," *Technometrics*, vol. 21, no. 1, pp. 239–245, 1979.

[43] P. Jirutitijaroen and C. Singh, "Comparison of simulation methods for power system reliability indexes and their distributions," *IEEE Transactions on Power Systems*, vol. 23, no. 2, pp. 486–493, May 2008.

[44] H. Yu, C. Chung, K. Wong, H. Lee, and J. Zhang, "Probabilistic load flow evaluation with hybrid Latin hypercube sampling and Cholesky decomposition," *IEEE Transactions on Power Systems*, vol. 24, no. 2, pp. 661–667, May 2009.

[45] Archived data in the Market Reports Section on the Midwest ISO website, July 2008. [Online]. Available: http://www.midwestiso.org/publish/Folder/7be606_10b7aacd66e_-7da30a48324a?rev=6

[46] A. Conejo, R. Garcia-Bertrand, and M. Diaz-Salazar, "Generation maintenance scheduling in restructured power systems," *IEEE Transactions on Power Systems*, vol. 20, no. 2, pp. 984–992, 2005.

[47] S. Meyers, C. Marnay, K. Schumacher, and J. Sathaye, "Estimating carbon emissions avoided by electricity generation and efficiency projects: A standardized method," Lawrence Berkeley National Laboratory, Berkeley, CA, Tech. Rep. LBNL-46063, July 2000. [Online]. Available: http://eetd.lbl.gov/ea/ems/reports/46063.pdf

[48] M. Stein, "Large sample properties of simulations using latin hypercube sampling," *Technometrics*, vol. 29, no. 2, pp. 143–151, 1987.

[49] T. J. Santner, B. J. Williams, and W. I. Notz, *The Design and Analysis of Computer Experiments*, 1st ed. New York, NY: Springer, July 2003.